EXPRESSION AND NEUTRALIZATION CAPACITY OF SINGLE DOMAIN HIV ANTIBODY FRAGMENTS

Agnieszka Szydlik

A dissertation submitted to the Faculty of Health Sciences, University of the Witwatersrand, Johannesburg, in fulfilment of the requirements for the degree of Master of Science in Medicine in the specialty of Virology.

Signed on 08 June 2018 in Johannesburg.

Declaration

I, **Agnieszka Szydlik** declare that this dissertation is my own, unaided work. It is being submitted for the Degree of Master of Science in Medicine in the specialty of Virology at the University of the Witwatersrand, Johannesburg. It has not been submitted before for any degree or examination at any other University.

Agnieszka Szydlik

Agnieszka Szydlik

08 day of June 2018

Summary

The discovery of broad and potent neutralizing HIV antibodies (bNAbs) has opened up new opportunities of passive immunization for HIV-1 prevention. In this study, we have engineered CAP256-VRC26.25, a V1V2 bNAb that neutralizes 70% of clade C viruses, as a single domain antibody (sdAb). These small antigen binding entities are derived from naturally occurring heavy chain only antibodies present in members of the dromedary families, and are characterized by the absence of a light chain, long complementarity-determining regions (CDR) heavy (H) chain 3 and high stability. Since CAP256.25 contains a highly charged and protruding CDR-H3 that binds mainly through its heavy chain, we hypothesized that it may function well as an sdAb.

Multiple camelization approaches to engineer CAP256.25 as a sdAb were tested in *silico* utilising structural modelling software. Parameters such as germline sequence homology, hydrophobicity and solubility, folding energy, torsion angles and native conformation of CAP256.25 in complex with its binding epitope were major factors considered during the modelling process. Four CAP256.25 sdAb derivatives were generated from parental antibody, the mut_0 or a wild type (WT), which was used as a base line for downstream optimization. CAP256.25 mut_4 in which residues involved in LC interactions were replaced with residues strongly conserved in camel sdAbs, which minimize hydrophobic interface of the sdAb. Mut_8 variant, which included four additional substitutions to increase solubility and mut_9 contained a single additional mutation at the base of CDR-H3 to improve the energetic landscape of sdAb. All genes were synthesized and sub-cloned into a mammalian expression vector and recombinant proteins expressed in HEK293T cell line, and purified by Immobilized Metal Ion Affinity Chromatography (IMAC) and Fast Protein Liquid Chromatography (FPLC). CAP256.25_mut0 expression was below the detectable level and whilst mut_4 expressed at low levels, it showed no neutralization activity. CAP256.25 sdAb mut_8 and mut_9 expressed at significantly lower levels compared to m36, a previously described sdAb used a positive control. Nevertheless CAP256.25mut_8 sdAb showed neutralization capability although it lost significant potency in comparison to the parental antibody, yet still within the therapeutic window of the VRC01 bNAb. Importantly, CAP256.25 sdAb was unable to neutralize the K169E mutant confirming that it retained specificity for the V2 epitope.

These data suggest that camelization of human antibodies is possible although further engineering is required to increase expression and improve stability. As such, sdAb engineering could be an encouraging step for the generation of small antigen binding fragments for future therapeutic purposes including topical delivery at mucosal surfaces, to interrupt or block sexual transmission of HIV.

Acknowledgements

"All growth is a leap in the dark, a spontaneous unpremeditated act without the benefit of experience". H. Miller

The work presented in this thesis was a big leap into unknown and would not have been accomplished without the guidance and endless support of many people, therefore, I wish to extend my sincere appreciation and gratitude to all who made this possible.

First and foremost, I can't thank enough my supervisor, Professor Lynn Morris for introducing me to the very exciting field of HIV research. I wish to express my deepest gratitude for her invaluable comments and engagement throughout the learning process, dedicated help, advice, inspiration, encouragement and continuous support.

Special words of thanks are reserved for my co-supervisor, Professor Penny Moore for her thoughts, support, and encouragement, for having her office door always open, whenever I ran into a trouble or was on the verge of losing my sanity.

I'm very grateful for all the help and support received from all of my colleagues at Prof. Morris laboratory, and especially Dr. Bronwen Lambson, Dr. Nigel Makoah, Miss Valerie Bekker and Dr. C. Kurt Wibmer, whose involvement and assistance in this project was invaluable. I would also like to acknowledge the examiners of this thesis, as I am very grateful for your time, input and insightful comments. I would also like to express a very special words of gratitude to NICD and PRF for financial assistance.

Finally, I want to express my deepest appreciation for my mom and for my partner, for providing me with limitless support throughout the process of researching and writing. This journey would not have been possible without you and for this, I'm eternally grateful. Thank you.

Aga Szydlik

Table of Contents

List of Figures

List of Tables

List of Abbreviations

Ad5	Adenovirus serotype 5
AMP	Antibody Mediated Protection
ART	Anti-retroviral therapy
AIDS	Acquired Immunodeficiency Syndrome
bNAbs	Broadly neutralizing antibodies
CAPRISA	Centre for the AIDS Programme of Research in South Africa
CD4bs	Cluster of differentiation 4 binding site
CDR	Complementarity Determining Region
CH	Constant heavy
CL	Constant light
CO_2	Carbon dioxide
CoP	Correlates of Protection
CRF	Circulating Recombinant Form
CV	Column volume
dNTP	Deoxynucleotide triphosphate
DMEM	Dulbecco's Modified Eagle Media
DNA	Deoxyribonucleic acid
EDTA	Ethylenediaminetetraacetic acid
Env	Envelope gene
EtOH	Ethanol
eOD	Engineered Outer Domain
Fab	Fragment antigen-binding

FBS	Foetal bovine serum
Fc	Fragment crystalline
FPLC	Fast Protein Liquid Chromatography
Fv	Fragment variable
gp120, gp41	Envelope subunits, glycoprotein 120kDa and 41kDa
HEK	Human embryonic kidney
HCAbs	Heavy-chain antibodies
HIV	Human Immunodeficiency Virus
HV	Hyper variable
IC_{50}	50% inhibitory concentration
IgG	Immunoglobulin G
IGVH	Immunoglobulin variable region heavy chain
IGVHH	Immunoglobulin variable region heavy chain (*Camelidae*)
IMAC	Immobilized metal ion affinity chromatography
LB	Luria-Bertani media
LRA	Latency reversing agents
mAbs	Monoclonal antibodies
MCS	Multiple cloning site
mut	Mutant
MPER	Membrane Proximal External Region
MLV	Murine Leukaemia Virus
MSM	Men who have sex with men
nAbs	Neutralizing antibodies
NHP	Nonhuman primates
OD	Outer domain

PCR	Polymerase chain reaction
PI	Primary infecting virus
PeP	Post-exposure prophylaxis
PrEP	Pre-exposure prophylaxis
rAAV	recombinant Adeno-Associated Viral
RLU	Relative light unit
RNA	Ribonucleic Acid
RT	Room temperature
sdAb	Single Domain Antibody
SEC	Size exclusion chromatography
SDS-PAGE	Sodium Dodecyl Sulphate-Polyacrylamide gel electrophoresis
SHIV	Chimeric SIV/HIV virus
SIV	Simian Immunodeficiency Virus
SU	Superinfecting virus
T_m	Melting temperature
URF	Unique recombinant forms
VH	Variable heavy
VHH	Variable heavy (*Camelidae*)
VIP	Vectored Immunoprophylaxis
V1V2	Variable region 1-2
WT	Wild type

Chapter 1 : Literature Review

1.1. Origin of HIV

Human Immunodeficiency Virus (HIV) entered the human host following a zoonotic spill over incident, which most likely originated in south eastern Cameroon around the 1930s (Chakrabarti *et al.*, 1987; De Leys *et al.*, 1990). Analysis of phylogenetic trees indicates that HIV-1 is closely related to chimpanzee simian immunodeficiency virus (SIVcpz) and HIV-2 to SIV found in sooty mangabey monkeys (Gao *et al.*, 1992). The HIV was first isolated in 1983 and by mid 80s multiple strains of the virus were circulating in human populations across the globe, shortly after HIV-1 and its close relative HIV-2 were named as a causative agents of Acquired Immunodeficiency Syndrome (AIDS) (Barré-Sinoussi *et al.*, 1983). HIV-1 is divided into four lineages based on genetic similarity and geographical association: group 'M' (main), 'N' (non-M/non-O), 'O' (outlier) and 'P' (putative/pending), each one characterized by an independent origin and prevalence (Sharp and Hahn, 2010). Viruses belonging to groups N and P are the least frequent in human populations, affecting 20 (group N) and 2 (group P) individuals worldwide, respectively, and although the origins of group P point to Cameroon, its reservoir remains unknown (D'arc *et al.*, 2015). Group M exhibits the most successful host adaptation, dominating the global pandemic and causing approximately 95% of HIV infections worldwide, while the remaining groups are restricted to individuals of West African origin (De Leys *et al.*, 1990; *HIV strains and types | AVERT*, 2017). Group M is further appended into nine phylogenetic subtypes (clades), which are defined with letters (A to K), and sub-subtypes, which are defined with numbers (Buonaguro, Tornesello and Buonaguro, 2007). Inter-subtype recombinant viruses infecting three or more non-epidemiologically related people, are classified as a circulating recombinant form (CRF). When multiple HIV-1 subtypes co-circulate with CRFs and freely exchange genetic material they generate unique recombinant forms (URF) (*HIV Sequence Database*, 2017). Rapid diversification of the virus within a host generates quasispecies, which are composed of similar-yet-different variants, contributing to highly diverse global virus population (Sharp and Hahn, 2010). Global geographical dissemination of HIV-1 subtypes and various CRFs is directly linked to efficiency of transmission and disease progression, reflecting high levels of viral diversity and molecular complexity of the HIV-1 epidemiology (Taylor *et al.*, 2008).

HIV-1 subtype A and D is prevalent in East Africa, whereas B in the Americas, Western Europe and Australasia, representing 12% of global HIV infections, where CRF subtypes are becoming more prevalent (*HIV strains and types | AVERT*, 2017). Subtype C predominates in southern Africa, the horn of Africa and India, accounting for nearly 50% of all global HIV-1 infections (UNAIDS, 2017). In 2016, more than 30% of all new infections reported in the sub-Saharan territory occurred in South Africa, making it the biggest HIV epidemic in the world (UNAIDS, 2017).

1.2. HIV/AIDS Pandemic

The first cases of AIDS were discovered in the early 1980s in the United States, marked by escalation of unusually uncommon opportunistic infections such as pneumonia, caused by a general immune deficiency (CDC, 2011). Since then HIV has spread throughout the world and remains the most deadly and infectious pathogen in the history of humankind. Globally, there are more than 36.7 million people infected with HIV, and more than 1.8 million new cases are reported each year (UNAIDS, 2017). South Africa bears the largest burden in the world with over 7.1 million cases, and over 200,000 annual deaths from ailments associated with AIDS, which continues to be the primary source of death among women of child bearing age, and the second leading cause of death for adolescent women in Africa (UNAIDS, 2017). In 2016, the number of new infections in South Africa was 270,000 and the prevalence in women aged 15-49 was 21.17%. Incidence was four times lower for males in the same age bracket (*Statistics South Africa*, 2017). The increased prevalence of HIV in 2017 is largely the result of the combined effect of new infections, and a successfully expanded ART treatment programme offering coverage to over 3.3 million people, which has improved survival among people living with HIV (*Statistics South Africa*, 2017). Although over the years, scientists have made extraordinary advances in understanding atomic structure and pathogenesis of HIV, new infections have not declined significantly in spite of scaled-up HIV testing, behavioural interventions, medical male circumcision, antiretroviral treatment and use of pre-exposure prophylaxis (PrEP).

1.3. Use of ART for treatment and prevention

Anti-Retroviral Therapy (ART) has had a major impact on the HIV epidemic reducing mortality and morbidity and extending the lives of people with HIV. In 2004, South Africa initiated the rollout of ART free of charge and today South Africa has the largest ART programme in the world. In 2016, approximately 3.9 million people received ART, steadily advancing the increase in life expectancy and rapidly lowering levels of mother-to-child HIV transmission rates (Department of Health, 2016). Although, HIV prevalence in the general population is high, affecting an estimated 7 million people (Figure 1.1A), that number is comprised from the sum of new infections and increased survival among people living with HIV, a result of a successful ART treatment programme (South Africa | UNAIDS, 2017). Massive increases in the use of ARTs for treatment and prevention has led to a nationwide drop in new infections (Figure 1.1B).

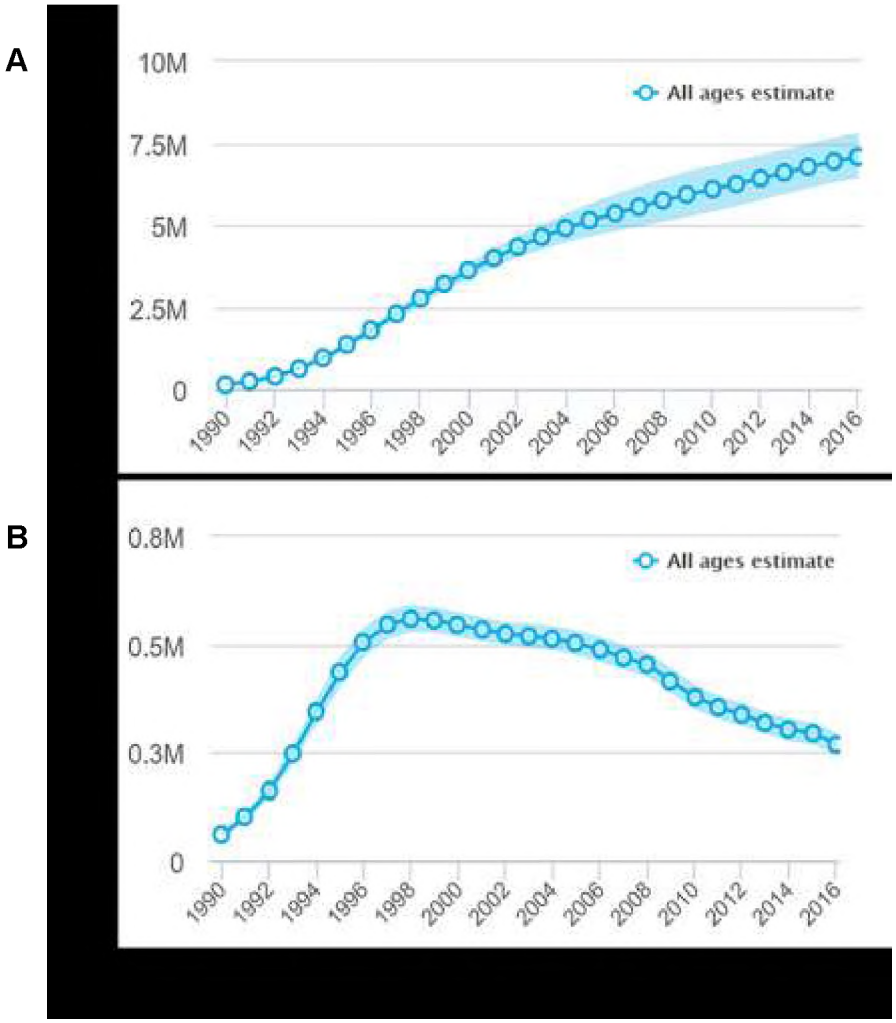

Figure 1.1 Impact of ART on HIV prevalence and incidence in South Africa. (A) People living with HIV (all ages estimate) **(B)** HIV incidence per 1000 population (all ages estimate) over time (South Africa | UNAIDS, 2017).

However, despite their success, ARTs are not a long-term solution to the AIDS pandemic, as lifelong ART treatment contributes to chronic immune dysfunction, toxicity, drug resistance, and accelerated non-AIDS disease burden. South Africa became the first country on the continent to approve the use of Truvada as PrEP for HIV prevention, targeting individuals at high-risk for infection, such as sex workers, men who have sex with men, intravenous drug users and adolescent women (UNAIDS, 2016). Clinical studies have confirmed the efficacy of PrEP as the risk of HIV was lowered by up to 90% when taken regularly (WHO, 2015). To eliminate the burden of a daily pill an ongoing trial is testing the safety and efficacy of a long-lasting, injectable cabotegravir as PrEP in high risk populations (Margolis *et al.*, 2017; Pottage, 2017). Today, daily oral PrEP is the only prevention that women can use to reduce risk of HIV infection that does not require a partner's consent. Currently, there is no commercially available microbicide although an ongoing clinical efficacy trial of vaginal rings showed modest levels of protection. The dapivirine ring provides a sustained release of antiretroviral drugs over a 4 week period correlated with a 31% decreased risk of HIV-1 infection among women at risk (Nel *et al.*, 2016). Microbicides, such as ART infused sponges, gels, creams or vaginal rings empower women by providing long-acting protection against HIV infection. Newer microbicidal approaches include the use of broadly neutralizing antibodies (bNAbs), which can potentially neutralize free virus at the pre-entry stage acting much earlier than antivirals.

1.4. Active immunization

Historically, vaccination and the induction of functional antibodies is the most successful way of dealing with viral diseases. However, the development of vaccines against HIV-1 has been challenging largely because of rapid rate of viral evolution and the ability of the virus to integrate into human DNA. Induction of bNAbs able to target diverse HIV strains by immunization and providing significant level of protection against HIV-1 infection, has been unsuccessful so far, in part because of the restricted immune detection of conserved regions of the trimer (Mascola and Haynes, 2013). Thus far, only one out of six vaccine trials has shown some level of success, with factors such as immunogen design, route of virus transmission, and diversity of circulating HIV-1 strains potentially contributing to poor outcomes of the trials, see Table 1.1 (Rerks-Ngarm *et al.*, 2009; Tomaras and Plotkin, 2017). The first two trials (Vax003 and 004),

were designed to induce and evaluate antibody responses, using a single immunogen, from two different clades in two different risk populations. However, no efficacy was demonstrated in either trial. Two subsequent trials (HVTN502 and 503) were designed to induce T cell responses using adenovirus serotype 5 (Ad5) vector combined with clade B Env genes (*gag, nef, pol*). The HVTN505 vaccine trial was designed to primarily induce cellular immunity, and involved DNA-based vaccine constructed to first prime the immune system, followed by an Ad5 vector-based boost vaccine (Hammer *et al.*, 2013). The only successful vaccine efficacy trial, RV144, used a prime/boost regimen capable of eliciting responses to the HIV-1 envelope with 31% efficacy (Rerks-Ngarm, 2009). The analysis of RV144 trial correlates of protection (CoP) generated the hypothesis that V1V2 binding antibodies can potentially lead to protection from HIV-1 acquisition (Haynes *et al.*, 2012). The HIV-1 viruses causing "breakthrough" infections in vaccine and placebo recipients were sequenced and characterized (sieve analysis) to provide CoP and valuable insights into vaccine efficacy, immunogen design and mechanism of viral evasion of vaccine-induced immune pressure (Edlefsen *et al.*, 2013).

Table 1.1 Summary table for HIV-1 vaccine efficacy trials.

Vaccine Regimen	Location/ Risk Population	Overall Vaccine Efficacy	Increased Risk of Infection	Immune Correlates of Decreased Vaccine Efficacy[2]	Immune Correlates of Decreased HIV Risk	Immune Correlates of Immune Control Post Infection
VAX003 (Phase III) Protein/ Alum (CRF01_AE/Clade B Env) (52)	Thailand/ Injection Drug Users	No Efficacy	No	No	No (52)	No
VAX004 (Phase III) Protein/ Alum (Clade B Envs)(53)	USA/ MSM/ High Risk Women	No Efficacy	No	No	**Yes** ADCVI, CD4 Blocking, Tier 1 NAb	*n/d*
STEP HVTN502 (Phase IIb) Ad5 Vector (Clade B Gag/Pol Nef) (54)	North and South America, Australia, Caribbean/MSM and High Risk Heterosexual Men and Women	No Efficacy (Efficacy futility determined at first interim analysis after full enrollment)	**Yes**	*n/d*	No	**Yes** T cell breadth /magnitude, Lower VL

Vaccine Regimen	Location/ Risk Population	Overall Vaccine Efficacy	Increased Risk of Infection	Immune Correlates of Decreased Vaccine Efficacy[2]	Immune Correlates of Decreased HIV Risk	Immune Correlates of Immune Control Post Infection
Phambili HVTN503 (Phase IIb) Ad5 Vector (Clade B Gag/Pol Nef) (57)	South Africa/ Heterosexual men and women	No Efficacy[1]	*n/d*	*n/d*	*n/d*	*n/d*
RV144 (Phase III) ALVAC vector (Clade B Gag/Pro + CRF01_ A/E Env)+ Protein/Alum (CRF01_A E/B	Thailand/ Community[2]	**31.2% Efficacy**	No	**Yes** Plasma Env IgA (75, 77)	**Yes** V1V2 IgG, Linear V2, V1V2 IgG3, Interactions (ADCC, Avidity, Tier I NAb, IgA), CD4+ T cell Polyfunction, Cytokines(75,	*n/d*

Notes: The HIV-1 vaccine efficacy studies are listed alongside their corresponding outcomes for efficacy, immune correlates of risk, and associations of vaccine efficacy. Positive outcomes for vaccine efficacy are shaded in blue and negative outcomes are shaded in grey. Men who have sex with Men (MSM); transgender (TG) ; antibody-dependent (ADCVI), cell-mediated virus inhibition; neutralizing antibodies that target easy to neutralize viruses (Tier 1 Nab) (Tomaras and Plotkin, 2017).

Key: [1] Vaccinations discontinued, unblinded early based on HVTN505 result. [2] No increased risk of infection compared to the placebo group. [3]No significant virus sieve that correlated with acquisition. [4]An atypical genetic sieve in the V2 region was identified but also did not correlate with acquisition.

The latest efficacy trial, HVTN 702, is based on the RV144 regimen but tailored to target HIV-1 subtype C, most prevalent in sub-Sahara Africa and began in November 2016 with results expected by the end of 2020. Since neutralizing antibodies are correlates of protection against infection (Pegu *et al.*, 2017) multiple efforts are ongoing to develop immunogens, designed to induce bNAbs in non-human primates (NHP). Engineering of stable and soluble, native-like HIV-1 Env trimers as immunogens, which are able to elicit bNAb response has been challenging because of the quaternary nature of most immunogenic sites of vulnerability, such as the V1/V2 trimer apex and the gp120-gp41 interface (Medina-Ramírez, Sanders and Sattentau, 2017). Stabilization of the HIV-1 Env trimer using the BG505 isolate in a “native-like”

confirmation was achieved by linking gp120 to gp41 (SOS gp140) by a disulfide bond and mutating Isoleucine to Proline (I559P) to improve trimerization (Sanders *et al.*, 2002). Immunogenicity studies in rabbits and NHP demonstrated that BG505 SOSIP.664 trimers were able to elicit neutralizing antibodies, and although some of the responses can be classified as strong, inducing tier 2 antibodies, all responses were autologous in nature, i.e. directed only against parental Env used in immunization (Sanders *et al.*, 2015). Germline targeting immunogens represents another approach to eliciting bNAbs. In this case, gp120 outer domain was engineered (eOD) to engage with naïve B cell precursors and elicit antibody responses, however, with mixed results, as the eOD elicited antibodies thus far showed binding but not neutralization (Sanders *et al.*, 2002; Jardine *et al.*, 2016).

1.5. Passive immunization

The isolation of many broad and potent monoclonal bNAbs from chronically infected individuals has provided an opportunity to explore passive vaccination for HIV-1 prevention. Passive immunity involves the transfer of protective antibodies to a non-immune person, i.e. transfer of maternal antibodies to the foetus, or through infusion of high levels of antibodies against a specific pathogen in antiserum or immunotherapy (Graham and Ambrosino, 2015). Pre-clinical data from non-human primates (NHP) supports the hypothesis that passive infusion with bNAbs confers sterilizing protection against infection with simian-human immunodeficiency virus (SHIV) (Moldt *et al.*, 2012). This hypothesis is presently being assessed in the Antibody Mediated Protection (AMP) trial, which is testing for the first time whether passive bNAb infusion confers immunity against HIV-1 infection in humans (*AMP Study*, 2015). This trial is using VRC01, a broadly neutralizing antibody targeting the CD4 binding site (CD4bs), and the antibody is given as an intravenous infusion every 2 months for almost 2 years.

1.6. Vectored immunization

Vectored Immunoprophylaxis (VIP) has recently emerged as an alternative to traditional vaccination approaches. In this method, transgenes encoding the desired antibody are delivered to tissues, resulting in secretion and systemic expression of

biologically active antibodies without the need for immunization (Brady *et al.*, 2017)VIP approaches using the recombinant adeno-associated virus (rAAV) vectors constitute the best studied gene therapy vector for use in human.

Adeno-associated virus (AAV) vectors have demonstrated an excellent safety profile (Mueller and Flotte, 2008) and a long-term protection against HIV-1 infection was achieved using this approach following intramuscular injection of the vector (Balazs *et al.*, 2012). BNAbs delivered by vector-mediated gene transfer in humanised mice provided complete protection against HIV infection following repetitive vaginal challenges with a heterosexually transmitted founder strain of the virus (Balazs *et al.*, 2014). Effective protection against SIV or SHIV infection has also been demonstrated in non-human primates (Johnson *et al.*, 2009; Gardner *et al.*, 2015; Saunders *et al.*, 2015; Julg, Sok, *et al.*, 2017) and two phase I clinical trials (www.clinicaltrials.gov, no date) are currently underway to assess the safety and efficacy of AAV-mediated gene transfer of bNAbs as part of a VIP approach (AAV1-PG9: NCT01937455; AAV8-VRC07: NCT03374202).

The VIP approach boasts many potential benefits as it bypasses dependence on humoral immunity and requires only a single dose for sustained expression of mature bNAbs (Brady *et al.*, 2017). However, more data from clinical trials are needed to confirm the efficacy and the long term safety of VIP. A major concern in the application of VIP is the pre-existence of cellular and humoral immunity to the capsid protein of the AAV vector and the feasibility for a large scale distribution (Johnson and Schnepp, 2014). AAV vectors could be used in future as tools to produce efficient and sustained antibody - based immunity to prevent HIV infection.

1.7. Antibody structure

Antibodies (Abs) are an essential component of the human immune system, where they are rapidly secreted by B cells into the circulation upon invasion by foreign substances (antigens). Their high affinity and specificity also make antibodies invaluable tools both in therapy and in research. Antibodies are classified according to structure and function and are subdivided into five classes (isotypes) of immunoglobulins (IgA, IgD, IgE, IgG, and IgM), IgG is the most abundant class in human serum (Vidarsson *et al.*, 2014). All immunoglobulins are similar in structure, but

differ in their functionality and mechanism of binding (Vidarsson *et al.*, 2014). Antibody structure has been determined by X-ray crystallography and its schematic is shown in Figure 1.2. In general an antibody comprises of four polypeptide chains: two identical heavy (H) chains and two identical light (L) chains, HC and LC segments are connected with an inter-chain disulfide bond forming a "Y" shaped molecule (Vidarsson *et al.*, 2014).

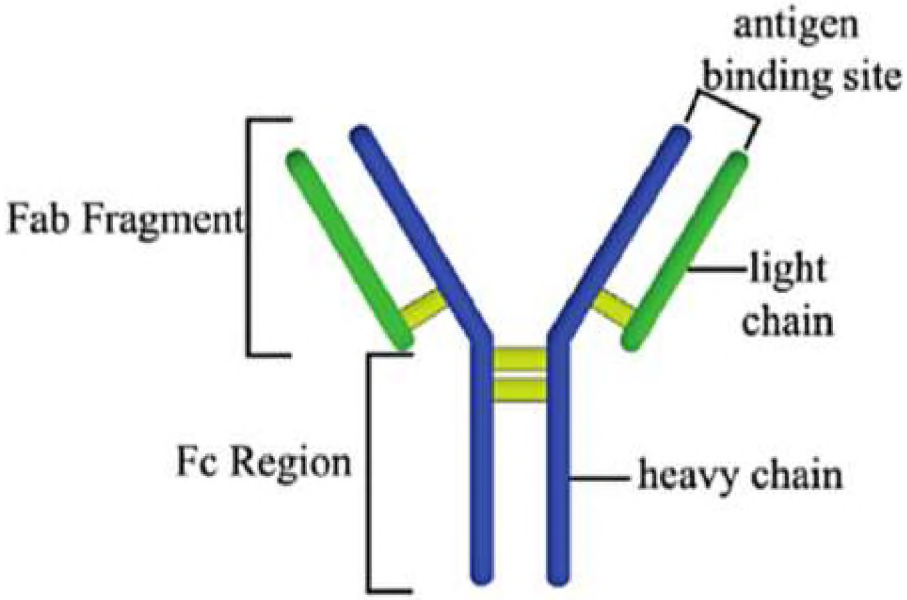

Figure 1.2 Illustration of antibody molecule. Heavy chain segments are indicated in blue and light chain portions in green. Disulfide bonds are represented with yellow lines (Kapur, 2012).

Located at the ends of the light and heavy chains is the variable region, which gives the antibody the specificity for binding its antigen. Located on the lower region is the Fc (fragment crystalline) portion of the antibody (Janeway CA *et al.*, 2001). The variable region of the molecule is further subdivided into three hyper variable (HV) regions per antibody chain and four framework (FR) regions intersecting the HV regions (Vidarsson *et al.*, 2014). Protruding parts of HV regions which are able to make a direct contact with the antigenic determinants are denoted as complementarity determining regions (CDRs). The FR regions form a scaffold to display the CDRs in the correct orientation to ensure contact with an antigen (Vidarsson *et al.*, 2014). Three light chain CDRs (L1, L2, and L3) and the first two heavy chain CDRs (H1 and H2) are

canonical in structure. The CDR-H3 high variety in length and amino acid sequence often plays a critical role in mediating antigen recognition (Gabrielli *et al.*, 2009).

1.8. Structure of the HIV-1 Envelope

The surface envelope glycoprotein (Env) encapsulates the viral genome, and is a critical component in interactions between the virion and host (Burrell, Howard and Murphy, 2017). The HIV spike is the only viral part which is presented on the virion exterior and is the major target of neutralizing antibodies. It consists of three identical receptor-binding subunits of gp120 non-covalently associated with three transmembrane fusion active gp41 subunits (Pancera *et al.*, 2014). The gp120 segment is subdivided into three individual domains: the inner and outer domain (OD) containing the CD4 binding site and reflecting gp120 orientation on the trimer and the bridging sheet (Kwong *et al.*, 2000; Rathore *et al.*, 2017). The gp120 OD contains a considerable number of conserved epitopes that are shielded by heavy levels of glycosylation, which is critical for the correct folding of the gp120 protein and virus infectivity (Kwong *et al.*, 2000). In contrast to the conserved core, gp120 loops are extremely diverse in sequence and structure, and are known to contain immunodominant epitopes comprised of multiple sequences, even within the same infected individual (Kwong *et al.*, 2000). In addition to sequence variability, gp120 loops are also the important determinants of resistance to antibody neutralization as they form dense glycan shields, sequestering relevant epitopes on the trimeric HIV-1 envelope (Kwong *et al.*, 2000). The gp41 glycoprotein anchors the complex in the membrane initiating fusion and the gp120 mediates virus entry into the host cell by binding sequentially to two surface receptors: CD4 and CXC-chemokine receptor 4 (CXCR4) or CC-chemokine receptor 5 (CCR5) to initiate the membrane fusion attaching the virus to the cell plasma membrane (Kwong *et al.*, 1998). The receptor-binding surfaces on gp120 are highly conformational in nature and comprise the CD4 binding site (CD4bs), CD4-inducible site and V3 chemokine receptor loop (Zolla-Pazner and Cardozo, 2010). The CD4bs is well conserved among species, despite large antigenic variation between HIV-1 strains making it a very attractive vaccine target, while the CD4-induced region is displayed only after gp120 engagement with the CD4 receptor (Zhou *et al.*, 2007; Pancera *et al.*, 2014). The V3 loop is highly variable in sequence, except for clade C viruses, and although it is critical for virus

functionality (deletion abrogates virus infectivity) antibodies specific for the V3 region are able to neutralize the most sensitive viral strains. In contrast, the V2 region is not critical for infectivity, but is, essential to Env trimer formation and epitope masking (Zolla-Pazner and Cardozo, 2010). HIV Env in its closed state is shown in Figure 1.3.

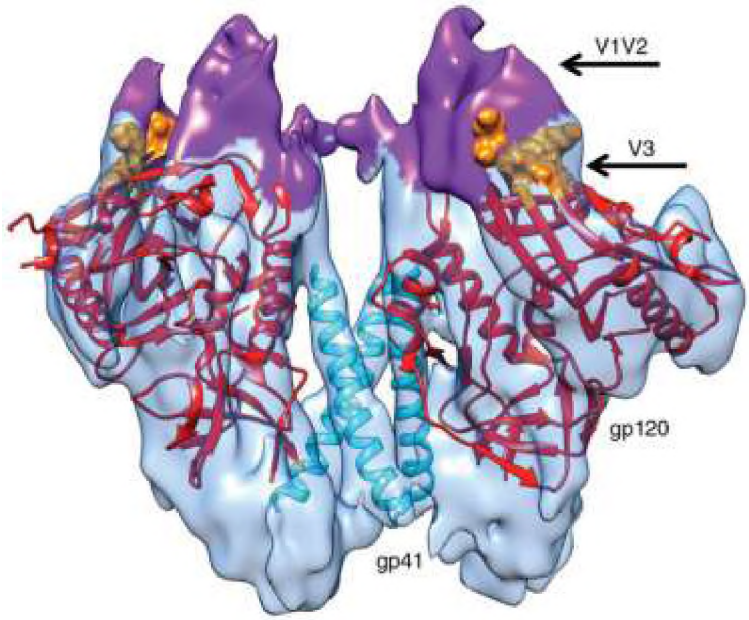

Figure 1.3 Structure of HIV-1 Env (PDB: 3HMG39). V1V2 region is coloured purple and indicated with arrow, V3 region is indicated with arrow and orange colour. HIV-1 Env is illustrated in its closed state (Bartesaghi *et al.*, 2013).

1.9. Broadly neutralizing antibodies (bNAbs)

Neutralizing antibodies targeting the HIV Env develop within few weeks post infection, however, they are specific only for the autologous strain and are ineffective against heterologous viruses (Moore, Gray and Morris, 2009). Recent studies have identified clinical and viral components associated with the evolution of cross-reactive neutralizing antibody responses in the course of natural HIV-1 acquisition (Doria-Rose *et al.*, 2009; Stamatatos *et al.*, 2009; E. S. Gray *et al.*, 2011). Broadly neutralizing antibodies (bNAbs) develop in about 15–30% patients in a few years post infection, and they are able to neutralize 80–90% of viruses by recognizing conserved epitopes present on the HIV-1 Env (Stamatatos *et al.*, 2009; Moore, Williamson and Morris, 2015). Multiple viral evasion mechanisms, such as the high mutation rate of the envelope spike, glycan shielding and epitope occlusion puts pressure on the host and lead to the development of bNAbs with unusual structural characteristics, such as

polyreactivity for non-HIV-1 antigens, long or short CDR-H3s and a high degree of somatic hypermutation (Burton and Mascola, 2015).

BNAbs target five major neutralization epitopes on the HIV envelope and they include the CD4bs, V3/Asn332 supersite, V1/V2 quaternary site, MPER, and quaternary epitopes bridging gp120 with gp41 (Wibmer, Moore and Morris, 2015). The location of major bNAb epitopes and antibodies that target them are shown in Figure 1.4.

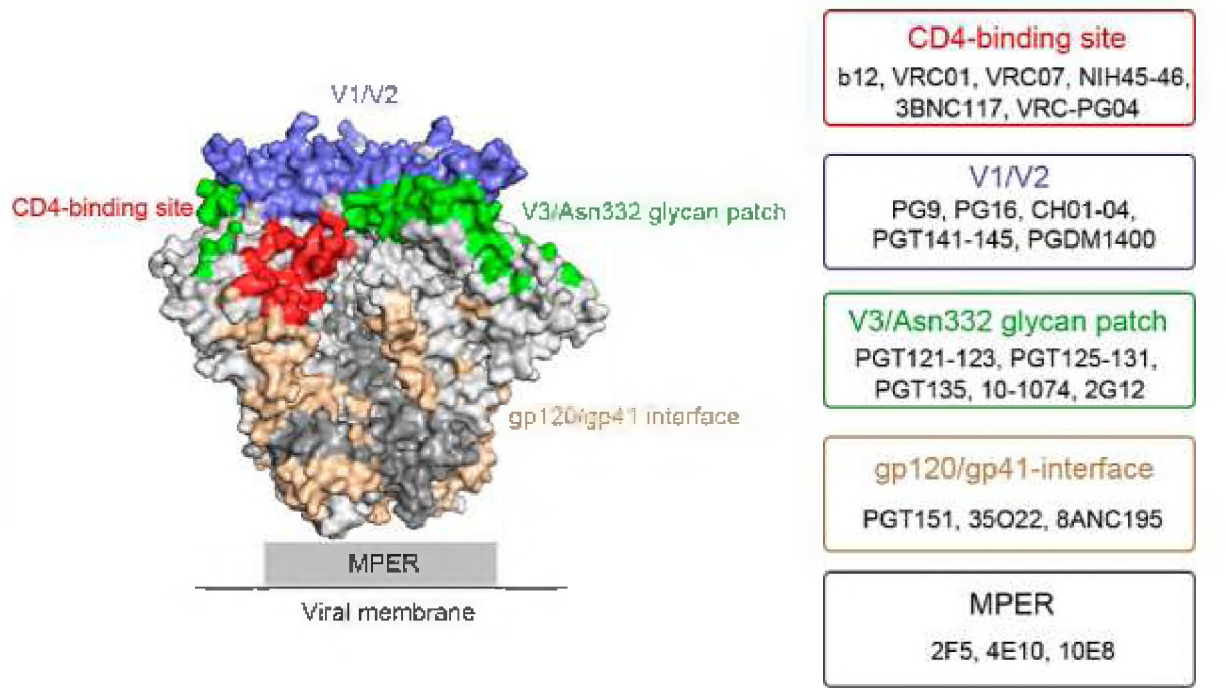

Figure 1.4 Surface representation of Env spike BG505 SOSIP.664 (PDB: 4TVP). Viral epitopes targeted by major bNAbs are indicated in distinct colours: CD4bs (red), V1/V2 (blue), V3/Asn332 glycan patch (green), gp120/gp41-interface (wheat) and MPER is illustrated with the grey rectangle. The bNAbs are subdivided in accordance to their specificity against the sites of vulnerability of HIV Env, and are shown on the left side of a trimer (Zhang *et al.*, 2016).

The CD4bs is enclosed by the glycan-shielded silent face and the flexible inner domain in a recessed manner on the viral spike (Zhou *et al.*, 2007). CD4bs epitopes are described as cryptic, because the coreceptor-binding site, which is not well accessible on the native virion surface shifts its conformation and becomes unmasked after CD4 binding (Kwong *et al.*, 1998). Although various CD4bs antibodies were isolated from different individuals only some are classified as a ‘‘VRC01-class’’ antibodies, and are characterized by remarkable breadth and potency, similar usage of their immunoglobulin heavy chain variable gene (VH1–2) and mode of antigen recognition

(Burton and Mascola, 2015; Zhou *et al.*, 2015). VRC01 like antibodies bind the "closed" confirmation of the trimer by mimicking CD4 ligand – receptor interactions (Pantophlet and Burton, 2006; Li *et al.*, 2011). Env is considered "partially open" when bound by the b12 bNAb, which is engaged through an overlapping epitope, causing a slight rotation and displacement of gp120 monomers (Liu *et al.*, 2008).

The Membrane Proximal External Region (MPER) participates in viral fusion and cell entry, located on the transmembrane region of gp41, and described as an α-helix, with hydrophobic and aromatic residues pointed into the membrane, and charged/polar residues pointing away (Lee, Ozorowski and Ward, 2016). A few, very potent and broad MPER antibodies have been isolated over time from different donors. The 10E8 bNAb is one of the broadest reported thus far, capable of successful neutralization of over 97% of viral strains (Huang *et al.*, 2012). Binding studies and crystal structure of 10E8 in complex with the MPER epitope, indicate a unique mode of recognition of a structurally conserved epitope, which comprises of highly conserved hydrophobic residues in gp41, two Tryptophan residues at position 672 and 676, Phenylalanine 673 and Arginine or Lysine 683, located right before the transmembrane region (Huang *et al.*, 2012). The linear and highly conserved nature of this epitope makes the MPER an attractive target for vaccine development.

The V3-glycan "supersite" comprises of a high-mannose patch surrounding the glycan at position 332 (Asn332), located under the conserved base of the V3 loop and adjacent to the coreceptor binding site of the gp120 region, characterized by a GDIR peptide motif (Walker *et al.*, 2011). BNAbs targeting the V3 region (PGT121–123, PGT125–131, PGT135, 10-1074 and 2G12) are characterized by an extended CDR-H3 with a nonpolar tip allowing them to access cryptic epitopes and display modest breadth and potency and dependence on N332 and N301 glycans (Walker *et al.*, 2011; Mouquet *et al.*, 2012; Longo *et al.*, 2016). Structural studies show that the antibody light-chain binds to conserved regions of the gp120 epitope and the variable sequence is targeted by the heavy chain of a bNAb (Mouquet *et al.*, 2012).

The gp120/gp41 interface epitope is located between the gp41 and gp120 complex within a space of a single protomer and includes glycans from both subunits of a second protomer (Blattner *et al.*, 2014). This epitope exists in cleaved and native-like forms of a trimer and is recognized by handful of bNAbs (PGT151–PGT158, 35O22 and 8ANC195) (Blattner *et al.*, 2014). PGT151 like antibodies recognize and stabilize

a glycan-dependent epitope on cleaved Env in a pre-fusion state and 8ANC195 anchors it in partially open conformation (Zhang *et al.*, 2016).

1.10. BNAbs in clinical developments

A number of bNAbs are presently in clinical trials to determine their therapeutic use in passive immunization, as briefly summarized in Table 1.2. The most clinically advanced is VRC01, a bNAb directed against the CD4bs, and although VRC01 is not the most potent antibody in comparison to bNAbs targeting glycan epitopes, it is very broad and able to neutralize 91% of pseudoviruses (Wu *et al.*, 2010). Positive data from a safety and efficacy trial (VRC602) enabled further initiation of multiple phase 2 studies across eleven countries (Stephenson and Barouch, 2016; Salazar *et al.*, 2017). Currently, VRC01 is being tested in AMP trials (NCT02716675 and NCT02568215), as intravenous infusions to determine the necessary levels to achieve protection and prevent HIV-1 acquisition, as well as to characterize any "breakthrough infections" (Liu *et al.*, 2016). Another CD4bs bNAb being currently tested in clinical trials is 3BNC117, which after meeting safety and efficacy requirements of phase 1, progressed to phase 2a (Stephenson and Barouch, 2016). A dose escalation study demonstrated that 3BNC117 is capable of heightening the humoral immunity against HIV and exerting strong selective pressure on the virus latent reservoir during analytical treatment interruption, reducing viral load (Salazar *et al.*, 2017). In addition to monotherapy, 3BNC117 is also being tested in combinatorial therapy in conjunction with another bNAb, 10–1074, which targets the V3 glycan supersite, and when used in combination, it showed no enhancement of 3BNC117 activity in non-human primate studies (Stephenson and Barouch, 2016; Salazar *et al.*, 2017). Another V3 specific bNAb being tested for safety and efficacy is PGT121, which is able to neutralize 70% of tested global viruses with potency a log higher than that of VRC01 (Stephenson and Barouch, 2016). Passive administration of PGT121 bNAb showed protection against simian-human immunodeficiency virus (SHIV) challenge in NHP and suppression of virus replication when used alone or in combination with other bNAbs (Longo et al., 2016). In addition, the cocktail of PGDM1400 +PGT121 neutralized 98% of global strains and is currently being tested in clinical trial (NCT03205917) to evaluate the safety, tolerability and efficacy of the PGDM1400 in combination with PGT121 for HIV prevention and therapy (Stephenson and Barouch, 2016; NIH, 2017). PGDM1400

bNAb targets the V1V2 glycan and neutralizes 83% of tested global viruses with potency a log greater than PGT121, and two logs higher than VRC01 (Stephenson and Barouch, 2016). Clinical trials are projected to begin in the near future.

Table 1.2 Biotherapeutics presently in clinical trials for the prevention of HIV infection, modified from Salazar (Salazar et al., 2017).

1.11. The Variable regions 1 and 2 (V1V2) of the HIV-1 Env.

The V1V2 site is one of the five major "sites of vulnerability" of the gp120 spike, located at the trimer apex protected by dense glycan shield and high sequence diversity from antibody neutralization (Kwong *et al.*, 2011). In the prefusion state, V1V2 shields the V3 loop and the coreceptor binding sites, exposing them upon CD4 binding which causes trimer rearrangement (Julien *et al.*, 2013). Although V1V2 sequence is one the most diverse among the variable regions of the Env, a large number of bNAbs such as PG9, PG16, CH01-04 and PGT141–145 (PGDM141-145) and CAP256-VRC26.25, are able to recognize it (Gorman *et al.*, 2016). Although antibodies directed against the same cluster of epitopes often show diverse modes of recognition, they also share a number of similarities (Gorman *et al.*, 2016). Structural analysis of V1V2 bNAbs revealed an anionic and protruding CDR-H3 described as a "hammer-head", and

sulfated tyrosines, often containing a shared YYD motif (Doria-Rose *et al.*, 2014; Gorman *et al.*, 2016). Apex bNAbs penetrate the dense glycan shield, binding the positively charged C strand of V1V2 with a single antibody arm, that recognizes the conserved lysine-rich region on V2 (Gorman *et al.*, 2016). Epitope binding is strongly dependent on the recognition of the N-linked glycan (N160) and Lys169, mutating glutamic acid (E) to lysine (K) at position 168-169, or 171 on the viral epitope drastically affects bNAb sensitivity, most likely by creating charge repulsion between the positively charged C strand and negatively charged CDR-H3 of the bNAb (Doria-Rose *et al.*, 2014). Although PG9/PG16 and CAP256-VRC26 antibodies are isolated from different VH-germline gene families, they share 99% sequence identity at the amino acid level and the usage of a conserved D-gene encoded YYD-motif to interact with the V2-epitope (Andrabi *et al.*, 2015). Both PG9 and PG16, were derived from B-cell cultures isolated from HIV-1 infected individuals, targeting a quaternary epitope located on V2/V3 loop of gp120 with high potency and breadth, particularly against non-clade B isolates (Walker *et al.*, 2009). Antibodies CH01-04 belong to the same clonal lineage and were isolated from an individual of African origin, chronically infected with a HIV-1 strain from clade A (Bonsignori *et al.*, 2011). CH01-04 epitope specificity is similar to that of PG9/PG16 targeting a conformational epitope located in the V2 loop, and neutralized between 36-45% pseudotyped viruses compared to over 70% neutralized by PG9/PG16 (Walker *et al.*, 2009; Bonsignori *et al.*, 2011). PGDM1400 is one of the thirteen PGT145 antibody family members isolated from an African donor, with a strong preference for native Env trimer and is characterized by broad and remarkably potent neutralization capacity, exceeding 83% coverage against a large multiclade virus panel (Sok *et al.*, 2014). Antibodies from the V1/V2-targeting families are among the exceptionally potent anti-HIV-1 bNAbs to date and are very attractive for vaccine development.

1.11. CAP256-VRC26.25 bNAb

CAP256-VRC26.25 also called CAP256.25 is a novel bNAb isolated from an HIV-1 subtype C infected individual in the CAPRISA cohort with broadly neutralizing plasma activity (E.S. Gray *et al.*, 2011; Doria-Rose *et al.*, 2014, 2016). The CAP256.25 bNAb neutralizes 70% of clade C viruses and 57% of all other clades, often with great potency, with a median IC_{50} of 0.001µg/mL as shown on Figure 1.5 (Doria-Rose *et al.*,

2016). CAP256.25 binds a quaternary epitope at the V1V2 apex of the trimer, with a stoichiometry of one per trimer and potential interaction with more than one protomer and the best antibody out of the 33 family members (Gorman *et al.*, 2016). Residues in V2 associated with sensitivity or resistance have been identified, including at positions 160, 166, 167 and 169 (Doria-Rose *et al.*, 2016). The heavy chain of CAP256.25 possesses an unusually long CDR-H3 (36 amino acids) which enables penetration of the glycan shield. Increased structural stability of the CDR-H3 in conjunction with a flexibility at its base, contributes to enhanced neutralization breadth and potency of CAP256.25 (Doria-Rose *et al.*, 2016).

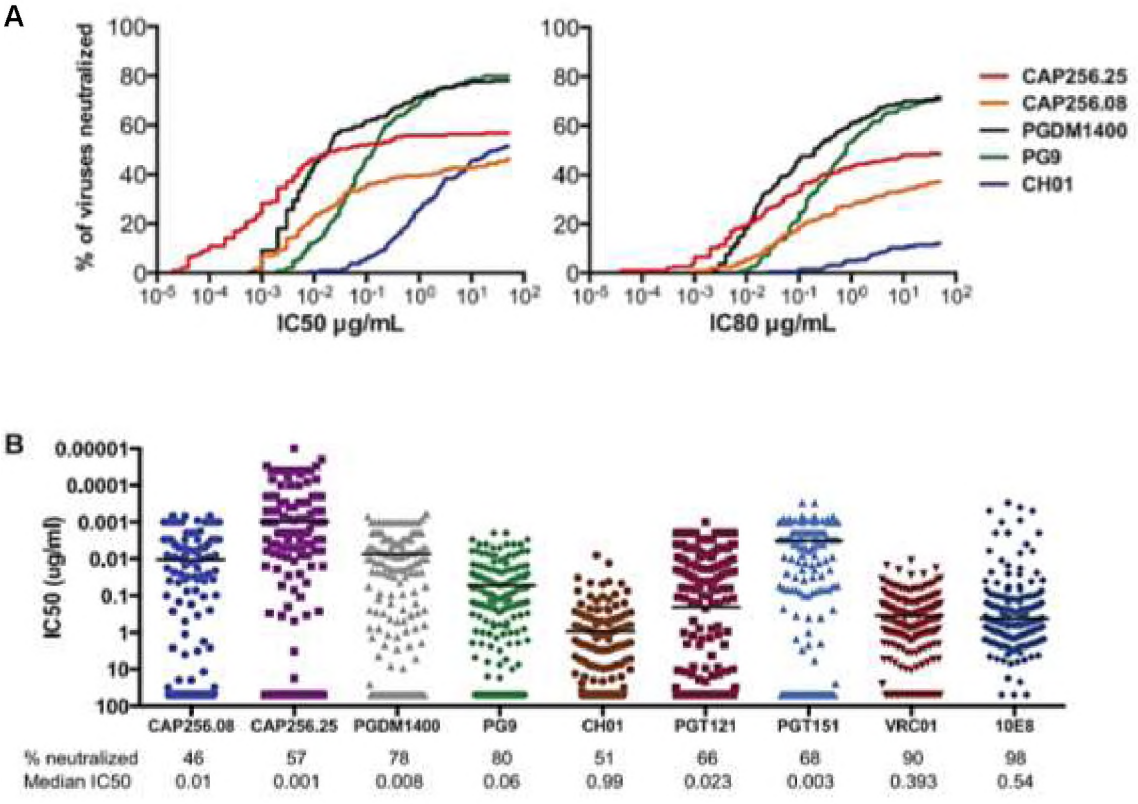

Figure 1.5 Neutralization breadth and potency of CAP256.25. (A) Neutralization breadth-potency curves for selected V1V2 antibodies, showed as the percentage of virus neutralized at IC_{50} or IC_{80}. **(B)** Neutralization of different epitopes by selected bNAbs, each dot indicates the IC_{50} value for a single virus as median value of neutralized viruses (Doria-Rose *et al.*, 2016).

Although CAP256.25 has demonstrated broad and potent HIV-1 neutralization, it failed to neutralize several commonly used SHIVs (SF162P3 and BaLP4), hence, a novel SHIV-325c, containing a clade C Env was constructed to further test its neutralization activity (Julg, Tartaglia, *et al.*, 2017). Sensitivity of SHIV-325c against the V2 antibodies (PG9, CAP256.25, and PGDM1400) was determined using a panel of 14 bNAbs; as a

control several other bNAbs, with specificity toward different HIV epitopes were also used. CAP256.25 antibody was modified to contain the LS mutation in its Fc region, which prolongs the in vivo half-life from 4.4 to 8.8 days. SHIV-325c challenge of rhesus macaques showed full protection even at the lowest dose (0.08 mg/kg), while all control animals became infected (Figure 1.6) (Julg, Tartaglia, *et al.*, 2017).

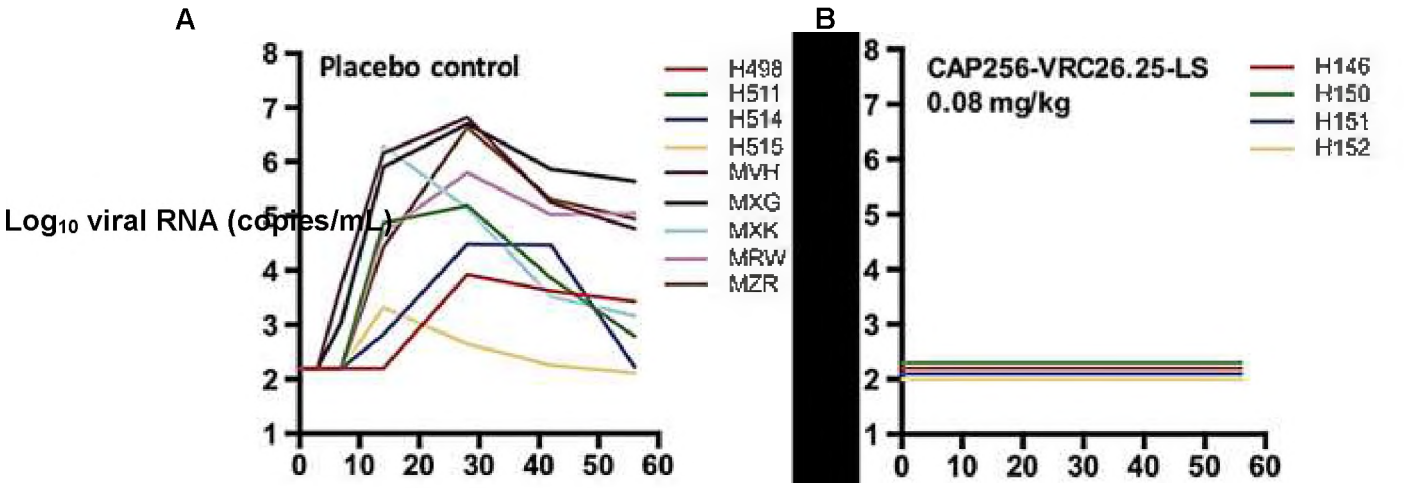

Figure 1.6 Efficacy of CAP256.25 neutralization in SHIV- 325c challenge in NHP. (A) Plasma viral RNA levels for animals which received saline control **(B)** CAP256-VRC26.25-LS dosed at 0.08 mg/kg (Julg, Tartaglia, *et al.*, 2017).

Multiple studies have demonstrated synergistic improvement in breadth and potency of bNAbs when used in combination. A mathematical model was developed to determine how many bNAbs and in which combinations are optimal to achieve long term benefits in a preventative or therapeutic context (Wagh *et al.*, 2016). Predicted bNAb neutralizing activity was calculated for fifteen bNAbs targeting four distinct epitope regions (CD4bs, MPER, V2 and V3 glycan) in over 1,600 possible double, triple, and quadruple combinations (Wagh *et al.*, 2016). Combinations of two bNAbs 10-1074 (V3) or VRC07-523 (CD4bs) tested in conjunction with CAP256.25 (V2), provided increased breadth and potency when compared to each bNAb tested separately (Wagh *et al.*, 2016). The best improvement in breadth and potency was achieved when combining all three bNAbs: CAP256.25, 10-1074, alongside the VRC07-523, resulting in neutralization of 99.5% of clade C viruses at a potency of 0.0083 µg/mL (Wagh *et al.*, 2016). Adding a fourth bNAb to target an additional epitope did not improve coverage or potency of the combination (Wagh *et al.*, 2016). The above

findings indicate that the therapeutic index of bNAbs can be significantly increased by using various combinations, which not only maximizes breadth and potency, but also minimizes the possibility for viral escape by concurrent targeting of diverse epitopes (Wagh *et al.*, 2016).

High potency and breadth against clade C viruses combined with high efficacy at a very low dose, makes CAP256.25 antibody a very attractive candidate for clinical development for the prevention of HIV infections in the parts of the world where subtype C predominates (Wagh *et al.*, 2016; Julg, Tartaglia, *et al.*, 2017).

1.12. Single domain antibody fragments

In 1993 a novel antibody structure, devoid of a light chain, yet fully functional was discovered in the *Camelidae* family (camels, llamas and other dromedaries) (Muyldermans *et al.*, 1994). Heavy chain antibodies (HCAbs) consist of a single antigen binding domain denoted VHH (Nanobody, sdAb), and two constant domains (CH2 and CH3) as illustrated on Figure 1.7.

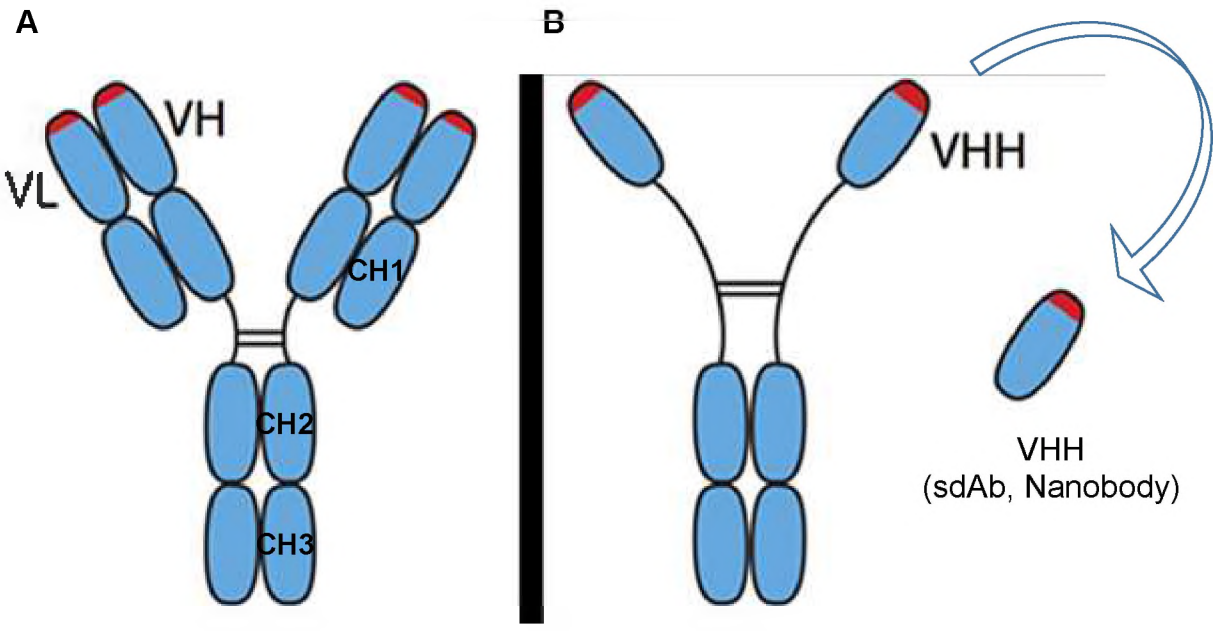

Figure 1.7 Illustrative comparison of conventional and the heavy chain antibody **(A)** Conventional IgG antibody. **(B)** Camelid heavy-chain antibody with the variable domain (VHH) indicated by an arrow (Eden *et al.*, 2018).

VHH structure comprises of conserved hydrophilic amino acid residues in the second framework region and long surface exposed loops which are homologous to human VH3 genes (Muyldermans, 2001, 2013; Forsman *et al.*, 2008; Siontorou, 2013).The mechanism of VHH binding to human lysozyme was delineated by crystallography showing penetration by the super-long CDR-H3, suggesting that sdAb are able to access residues often unavailable to conventional antibodies (Figure 1.8) (Desmyter *et al.*, 1996; Arbabi-Ghahroudi, 2017).

Figure 1.8 Crystal structure of a camel VHH in complex with lysozyme (PDB: 1MEL). VHH is represented as a ribbon with CDR-H3 loop in red; Lysozyme is illustrated using mesh surface.

The lack of a variable light chain means that the VHH paratope is assembled tightly over a small surface providing sdAb with the opportunity to engage with novel epitopes that are inaccessible to traditional heavy and light chain pairs, such as viral surface canyons (Chen and Dimitrov, 2009; Chen *et al.*, 2010). The discovery of camelid heavy chain antibodies opened up new opportunities for the development of single domain antibodies, and incorporating their unique features into engineered human sdAb. The generation of antibodies for therapeutic and prophylactic applications in large quantities can be very challenging, hence exploration of small antibody derivatives as an equivalent choice is worth exploring (Wesolowski *et al.*, 2009). Single domain antibody derivatives have several advantages over canonical antibodies, including

small size, hydrophilic character and good solubility allowing high yield production in *E.coli* (Wesolowski *et al.*, 2009).

Since the paratope of camel sdAb is restricted to a single domain, each residue has an important function in antigen binding and structural stability of the antibody fragment (Conrath *et al.*, 2005). To counterbalance the absence of a light chain, sdAb contain four well defined amino substitutions (tetrad) in the framework region 2 (Val**37**Phe, Gly**44**Glu, Leu**45**Arg and Trp**47**Gly) that are considered to be important for the solubility (Muyldermans *et al.*, 1994; Conrath *et al.*, 2005). In a canonical variable heavy (VH) domain, "tetrad" residues are highly hydrophobic in nature and responsible for stabilizing the variable light (VL) domain, whereas in sdAbs, the tetrad is solvent-exposed and prevents the association with a possible VL domain (Muyldermans *et al.*, 1994). Another important feature of camelid sdAb is a significantly longer CDR-H3 loop folding over the former VL side which favours the solubility and a high affinity of sdAb for its antigen (Desmyter *et al.*, 1996). Based on the crystallographic data, Gly47 plays an important structural role in CDR-H3 conformation, improving positioning of the long CDR-H3 into a space normally occupied by the LC, as opposed to an enhancement of solubility (Conrath *et al.*, 2005).

M36 is the first and only described, fully engineered sdAb directed against HIV-1, and specific for a CD4 induced (CD4i) epitope located on gp120 glycoprotein (Wan *et al.*, 2013). It was constructed as a chimera by grafting of CDR-H2 from the VH4-34 germline, the CDR-H3 from VH3-23, in addition to a combination of sequences from five other human Fab libraries (Chen, Zhu, Feng, Xiao, *et al.*, 2008). Further rounds of panning against the large phage-display libraries, combined with reverse mutation to germline sequences (germlining) and in *silico* modelling improved the biochemical properties of m36 while preserving neutralizing activity against HIV-1 (Chen, Zhu, Feng, Xiao, *et al.*, 2008; Chen *et al.*, 2015). M36 sdAb is broadly cross-reactive against the primary isolates with potency on average 2–3 fold higher than that of m9, which is an *in vitro* matured derivative of the X5 antibody, which binds the same epitope as m36 (Zhang *et al.*, 2004). Both m36 and m9 show better neutralizing activity compared to first generation HIV-1 mAbs when tested against large viral panels (Figure 1.9 A, B). In addition m36 was also more potent than gp41-derived peptide C34 (Figure 1.9 C), an on entry inhibitor, comparable to T20 peptide (DP178, brand name Fuzeon) (Zhang *et al.*, 2004, 2010; Chen, Zhu, Feng and Dimitrov, 2008). Since sdAbs are able to

engage occluded epitopes, which are often unattainable to molecules of larger size, they could potentially enable the evolution of a novel class of potent HIV inhibitors (Chen, Zhu, Feng and Dimitrov, 2008).

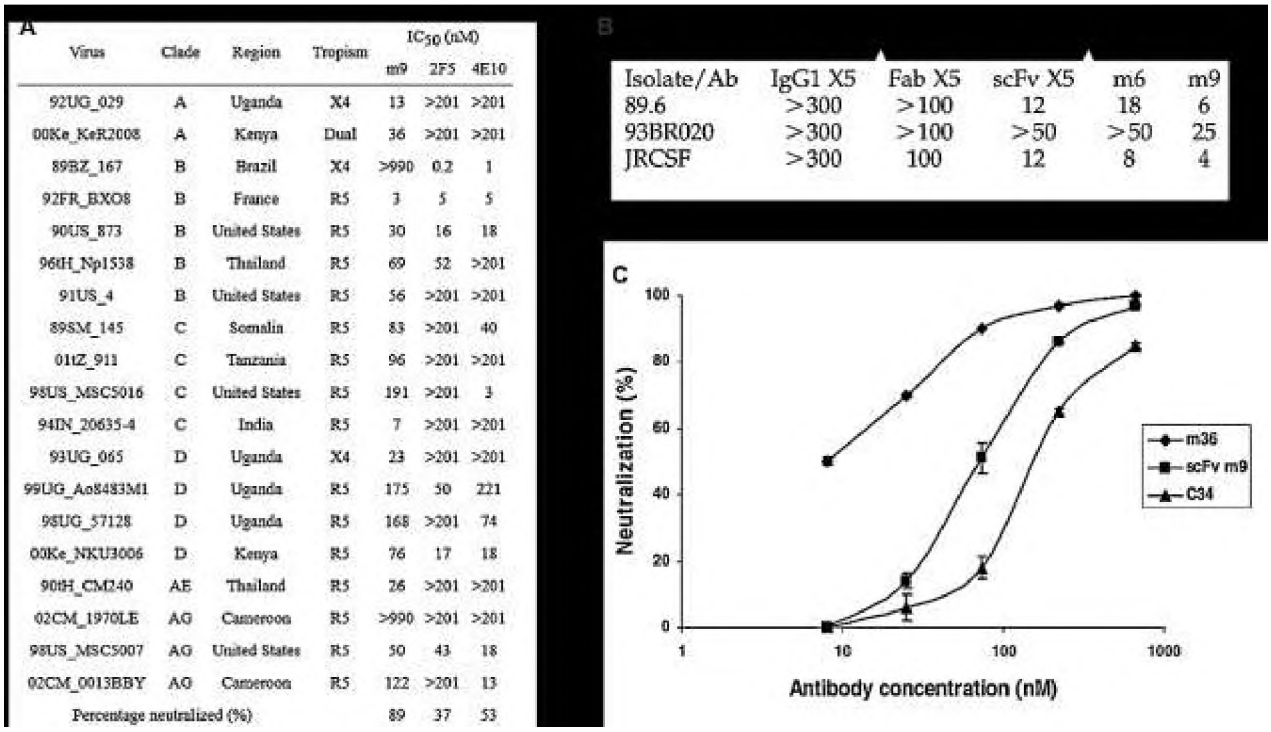

A

Virus	Clade	Region	Tropism	IC_{50} (nM) m9	2F5	4E10
92UG_029	A	Uganda	X4	13	>201	>201
00Ke_KeR2008	A	Kenya	Dual	36	>201	>201
89BZ_167	B	Brazil	X4	>990	0.2	1
92FR_BX08	B	France	R5	3	5	5
90US_873	B	United States	R5	30	16	18
96tH_Np1538	B	Thailand	R5	69	52	>201
91US_4	B	United States	R5	56	>201	>201
89SM_145	C	Somalia	R5	83	>201	40
01tZ_911	C	Tanzania	R5	96	>201	>201
98US_MSC5016	C	United States	R5	191	>201	3
94IN_20635-4	C	India	R5	7	>201	>201
93UG_065	D	Uganda	X4	23	>201	>201
99UG_Ao8483M1	D	Uganda	R5	175	50	221
98UG_57128	D	Uganda	R5	168	>201	74
00Ke_NKU3006	D	Kenya	R5	76	17	18
90tH_CM240	AE	Thailand	R5	26	>201	>201
02CM_1970LE	AG	Cameroon	R5	>990	>201	>201
98US_MSC5007	AG	United States	R5	50	43	18
02CM_0013BBY	AG	Cameroon	R5	122	>201	13
Percentage neutralized (%)				89	37	53

B

Isolate/Ab	IgG1 X5	Fab X5	scFv X5	m6	m9
89.6	>300	>100	12	18	6
93BR020	>300	>100	>50	>50	25
JRCSF	>300	100	12	8	4

C

Figure 1.9 Neutralizing activity of m9 and m36 sdAb against selected HIV-1 isolates. (A) Neutralization activity of m9 against HIV-1 primary isolates in comparison with 2F5 and 4E10 (Zhang *et al.*, 2010). **(B)** Neutralizing activity (IC_{90}; µg/mL) of m9 derivatives tested against selected HIV-1 strains measured by a PBMC-based assay (Zhang *et al.*, 2004). **(C)** Dose-dependent inhibition of Bal virus by m36, m9, and C34 peptide (Chen, Zhu, Feng and Dimitrov, 2008).

1.13. Study Objectives

The study aimed to generate a sdAb of CAP256.25 and assess its breadth and potency relative to the parental molecule. The rationale for focusing on CAP256.25 is that this mAb belongs to the VH3 gene family and contains a highly charged and protruding CDR-H3, binding to its epitope mainly through its heavy chain (Doria-Rose *et al.*, 2014). In addition, CAP256.25 contains an additional set of Cysteine (C) residues in the H1 and H3 loops, which form an interloop disulfide bond found in many naturally occurring camel sdAbs (Muyldermans, 2013).

Several factors can affect the function of an antibody, such as epitope-paratope structure complementarity, spatial distribution of the epitope, geometry and rigidity

between binding sites (Burton, 2001). The crystal structure of the antigen-binding CDR-H3 of CAP256.25 was solved to 2Å (Gorman *et al.*, 2016) which was used to guide engineering of this antibody as a sdAb. Once all key residues were identified, the CAP256.25 underwent a series of molecular manipulations through mutagenesis, prior to being cloned and tested for neutralization potency. Our findings could provide further understanding of the mechanisms of CAP256.25 neutralization of HIV-1 (i.e. the role of the heavy chain) and aid in the development of sdAb as a novel class inhibitor of HIV-1 entry.

Chapter 2 : Material and Methods

2.1. CAP256-VRC26 and m36 sdAb gene selection

The CAP256-VRC26.25 antibody (abbreviated CAP256.25) was selected as the best candidate for single domain antibody engineering due to over 80% shared homology with the dromedary IGVHH3 germline. This germline is the most frequently used in the seven single domains subfamilies, and accounting for 75% of all isolated dromedary antigen-specific single domains (Goldman *et al.*, 2017). CAP256.25 antibody belongs to the VH3-30 germline, the most thermodynamically stable human variable heavy (IGVH) gene. Favourable features of CAP256.25 also include an extended CDR-H3 loop, capable of protruding deeply into cryptic epitopes of viruses. M36 is a chimeric human single domain antibody fragment comprised of the CDR-H2 and adjacent frameworks (FRs) homologous to the VH4-34 germline and the remaining sdAb sequence homologous to the VH3-23 germline. M36 has shown high efficacy in neutralization assays and will be used as a positive control for the study (Chen *et al.*, 2015).

2.2. Bioinformatics tools and software

Several bioinformatics tools and software packages were used throughout this study to identify, analyse and model proteins of interest as described below. UCSF Chimera software (https://www.cgl.ucsf.edu/chimera/) was used to visualise, analyse and manipulate the molecular structure of human Fab CAP256.25 (PDB ID: 5DT1). The first step of modelling involved removal of the CAP256.25 light chain (LC) and mutating heavy chain FR2 residues involved in controlling the structural stability of the VH/VL interface. Selections were made based on previously published data on numerous humanization efforts for *Camelidae* VHH, including substitution of the hydrophobic patch in FR2 with hydrophilic amino acids (tetrad residues 37, 44, 45, and 47). The conserved VHH tetrad is known to participate in the interactions between light and heavy chain domains and is considered critical for the solubility, stability and expression of engineered single domains (sdAbs). A total of four CAP256.25 sdAb variants were generated, CAP256.25_mut0 or umutated variable heavy (VH) domain, CAP256.25 _mut4 sdAb which comprises of substitutions limited to tetrad residues.

CAP256.25 _mut8 sdAb with four additional substitutions (Val11, His35, Tyr91 and Met108) made in the solvent exposed part of the molecule, and CAP256.25_mut9 containing an additional single residue substitution of Lys to Ala94 at the base of CDR-H3.

M36 and CAP256.25 sdAb genes (WT, mut_4 and mut_8) were synthesized by GenScript (https://www.genscript.com), and the addition of a single amino acid substitution (mut_9) was done by site directed mutagenesis. Sequencher (https://www.genecodes.com/) software was used for DNA sequence analysis. All plasmids used in the study were sequenced using vector primer (Table 2.1) to confirm gene insertion, the presence of desired mutations or potential PCR errors. Sequences were aligned, edited and visualised using AliView software (http://www.ormbunkar.se/aliview/). Primers and annotated plasmid maps used in study were generated using SnapGene (http://www.snapgene.com/) and Genome Compiler (http://www.genomecompiler.com) software.

2.3. Oligonucleotide primer design

Oligonucleotide primers were designed using SnapGene and Genome Compiler software using the following criteria for optimal design and primer performance:

- Sequencing primer: length between 18 to 30 nucleotides with melting temperature (Tm) between 65°C and 75°C,
- Tm of the oligonucleotide primers were set within 5°C of each other.
- Mutagenesis oligonucleotides contained the mismatched region in the middle of the primer sequence with Tm between 78-82°C.
- Primer GC content was set between 40 and 60%, with the GC clamp at the 3' end of each primer to encourage annealing to the template.

Primer synthesis was performed by Inqaba Biotech (http://www.inqababiotec.co.za/) and the sequence is shown in Table 2.1. An online oligonucleotide properties calculator was used to ensure the absence of oligonucleotide sequences resulting in potential primer-dimers or hairpins instead of annealing to the desired DNA sequences (http://biotools.nubic.northwestern.edu/OligoCalc.html).

Table 2.1 Sequencing primer used to confirm insertion of the CAP256.25 sdAb gene into the CMVR vector.

Primer name	Sequence (5'-3')	Number of bases
p8400-CMV-F	GCTGACAGACTAACAGACTGTTC	23

2.4. Sanger sequencing

Plasmids were amplified by polymerase chain reaction (PCR) utilizing the BigDye® Terminator Cycle Sequencing Kit (Applied Biosystems, USA) for Sanger DNA sequencing, which relies on the enzymatic DNA synthesis in the presence of chain-terminating inhibitors. Briefly, 50-300 ng of plasmid template was mixed with 5x BigDye reaction buffer, 10 µM sequencing primer and molecular biology grade water (Sigma, USA) to a final reaction volume of 20 µl (Table 2.2A). All reagents and reactions were kept on ice and protected from light throughout the set up. Samples were mixed by pipetting and briefly centrifuged in a microcentrifuge at room temperature and placed on ice before being transferred to PCR thermo cycler. Thermal cycling was performed in accordance to the conditions listed in Table 2.2B. A complete list of reagents, their respective catalogue numbers and supplier information can be found in Appendix A.

Table 2.2 Parameters for Sanger sequencing of sdAb plasmids.

Component Standard	Reaction (20µl)
BigDye™ Terminator 3.1 Ready Reaction Mix	8 µl
BigDye™ 5X Sequencing Buffer	4 µl
Forward primer (10 µM)	2 µl
Plasmid template	50-300 ng
Deionized water (RNase/DNase-free)	up to 20µl final reaction volume

Parameter	Step/Stage				
	Incubate	25 cycles			Hold
		Denature	Anneal	Extend	
Ramp rate	-	1°C/second			
Temperature	96°C	96°C	50°C	60°C	4°C
Time (minute : second)	01:00	00:10	00:05	04:00	Until ready to purify.

Notes: Sequencing reaction protocol and Sanger sequencing thermal cycling conditions (Fisher Scientific, 2016).

Upon completion the reactions were cleaned by Ethanol/Sodium Acetate precipitation. Briefly, 125 µl of 100% ethanol (EtOH) and 5 µl 3 M sodium acetate was added to each well and mixed with the PCR reaction by pipetting, followed by centrifugation at 2,500 x g for 30 min. Tubes were then inverted and blotted on paper towel to remove EtOH and centrifuged upside down at 150 x g for <1 min to remove excess EtOH. DNA pellet was washed with 20 µl of ice cold 70% ethanol (stored at –20°C) and centrifuged at 2,500x g for 15 min. Tubes were inverted to remove residual EtOH and allowed to dry at 60°C for 3 minutes in the thermo cycler. Samples were then submitted for sequencing to the NICD sequencing facility.

2.5. Enzymatic digest of plasmid DNA with restriction endonucleases

The inserts coding for sdAbs were enzymatically released from the pUC57 plasmid for the purpose of sub-cloning the sdAb genes into a CMVR expression vector. Endonuclease restriction sites were incorporated upstream and downstream of the sdAb genes to allow a double digest. Plasmids were digested with *Xba I* and *Bam HI* using Fermentas Fastdigest® (Thermo Fisher, USA) enzymes according to the manufacturer's instructions. Briefly, all reactions were assembled on ice, in a 20 µl volume compromising 1-3 µg of plasmid DNA, 2 µl of 10x buffer, 2 µl of enzyme and a sterile molecular grade water for the final volume to be equal to 20 µl. The samples were then incubated for 60 minutes at 37ºC in thermocycler. Digested DNA was subsequently visualised using 1- 1.5% agarose gel and purified as described in the methods section below.

2.6. Agarose gel electrophoresis of DNA

DNA fragments were separated by gel electrophoresis in according to their molecular weight alongside a 10 µl DNA ladder. Briefly, a 20-40 µl DNA aliquot was supplemented with 6x loading buffer and loaded on a 1-1.5% agarose gel. The gel was electrophoresed at 70V in 1x TAE running buffer supplemented with 2 µl Ethidium Bromide (Bio-Rad, USA) to visualise DNA bands. The DNA fragments of correct size were visualized on UV box and isolated using a sterile blade and purified with QIAquick Gel Extraction Kit according to manufacturer's instructions (Qiagen, USA). First, the gel fraction containing the DNA fragment was dissolved in QB buffer at 55°C for 10 minutes with occasional inversion before being transferred to the QIAquick spin

column. High-salt concentrations of the QB buffer enabled the DNA to selectively bind silica membrane while all impurities such as residual salt, agarose, loading dye and ethidium bromide were washed away with ethanol based PE Buffer. QIAGEN columns were mounted on the QIAvac 24 Plus vacuum manifold, samples were drawn through columns with pressure less than 400 mbar. Residual PE buffer was removed with an additional 1 minute centrifugation step at 10,000x *g*. Pure DNA was eluted with a 30 µl of RNase/DNase free sterile water and quantified using a NanoDrop ND-1000 spectrophotometer (Thermo Fisher, USA). DNA concentration was measured at 260 nanometres (nm) and proteins at 280 nm, the difference in the absorbance ($A_{260/280}$) was used to determine the purity of purified samples.

2.7. Ligation of sdAb fragments into CMVR vector

Purified sdAb DNA genes were covalently linked with a CMVR plasmid vector backbone using Roche Rapid Ligation kit (Roche, USA). Ligation reaction was carried out in accordance with the manufacturer instructions with 3:1 molar ratio of insert DNA to vector backbone, and insert concentration not exceeding 150 ng and 80 ng of vector. First, the DNA concentration was adjusted with 5x DNA Dilution Buffer to total volume of 10 µl, mixed by pipetting before adding 2x Ligation Buffer and T4DNA Ligase to a final volume of reaction equal to 20 µl. The ligation reaction was mixed by pipetting and incubated for 15-30 minutes at room temperature before transformation into *E.coli* JM109 chemically competent cells (Promega, USA). All ligation reactions included a control reaction of backbone plasmid without the insert to determine the efficiency of the sdAb ligation reaction.

2.8. Bacterial transformation

Chemically competent *E.coli* JM109 strain (Zymo Research, USA) was used for CMVR plasmid propagation and gene transformations following the manufacturer's protocol. Briefly, 50 µl aliquots of chemically competent *E.coli* cells were thawed out on ice for 5 minutes, and supplemented with 1-5 µl of plasmid DNA, gently mixed and incubated on ice for additional 5 minutes, followed by addition of 150 µl of S.O.C media. After 1 hour incubation with agitation of 150 rpm at 37°C in a shaking incubator, 30 µl aliquots of transformants were streaked on LB agar plates containing selection antibiotic (50

µg/mL of Kanamycin, Sigma-Aldrich). Plates were grown overnight at 37°C. The next morning individual colonies were selected and propagated in 3 mL liquid LB media containing selection antibiotic and cultured overnight.

2.9. Plasmid DNA purification

Plasmid DNA was purified using QIAprep Miniprep or Maxiprep Kit (Qiagen, USA) in accordance to the manufacturer's protocol. Briefly, a recombinant *E.coli* colony was isolated and used to inoculate the 3-5 mL of LB liquid media containing Kanamycin antibiotic and grown overnight. The next day, culture was pelleted by centrifugation at 6,800x g for 3 minutes, the broth media was drained and pellets were resuspended completely in 250 µl of buffer P1 by vortexing. When all cell clumps were resuspended, 250 µl of lysis buffer P2 was added and mixture was gently inverted a few times to prevent DNA shearing. After 5 min incubation mixture was neutralized with 350 µl of buffer N3. After lysate clearing, the sample was transferred to QIAprep silica membrane. QIAGEN columns were mounted on the QIAvac 24 Plus vacuum manifold, samples were washed with 750 µl of PE buffer drawn through the columns with pressure less than 400 mbar. Residual PE buffer was removed with an additional 1 minute centrifugation step at 10,000x *g*, and pure DNA was eluted with 30 µl of RNase/DNase free sterile water.

2.10. Site-Directed Mutagenesis

CAP256.25_mut9 sdAb was generated by mutagenesis using the QuikChange Lightning Site-Directed Mutagenesis Kit (Agilent, USA) and CAP256.25_mut8 as a template. Briefly, 100 ng CAP256.25_mut8 plasmid template was mixed with 125 ng of forward (F) and reverse (R) of each mutagenesis primer (sequences are listed in Table 2.3A). Oligonucleotide primers were complementary to the plasmid template except for a single nucleotide mismatch to introduce a change in a codon sequence to generate a mutated plasmid containing the desired mutation at specific location. *PfuUltra-HF* DNA polymerase was used to extend the PCR reaction for 18 cycles according to the program listed in Table 2.3B below. After the reaction was finished, it was treated with *Dpn I* endonuclease, which targets and destroys methylated parental

DNA template. Plasmid DNA was transformed into *E.coli* competent cells as described in the section above, and grown overnight on agar plates containing Kanamycin antibiotic for selection. The next day individual colonies were selected and cultured overnight. Plasmid was extracted as described previously, sequence confirmed and the vector DNA containing the desired mutation was purified on larger scale.

Table 2.3 Parameters used for QuikChange Lightning Site-Directed Mutagenesis primer design and cycling reaction.

Segment	Number of Cycles	Temperature	Time
1	1	95°C	2 minutes
2	18	95°C	20 seconds
		60°C	10 seconds
		68°C	2.5 minutes
3	1	68°C	5 minutes

Notes: Design of mutagenesis primers used to introduce K94A mutation into CAP256.25 sdAb_mut8, targeted codon is indicated in bold and bases undergoing mutagenesis underlined. PCR program with extension set for 30 seconds/kb of plasmid length (Agilent, 2015).

2.11. Expression of single domain antibodies

Once all sdAbs variants were successfully cloned into the expression vector and sequences reconfirmed, plasmid DNA was purified and used to transfect the HEK FreeStyle 293F expression cell line. Recombinant proteins were obtained by a two-step purification as shown in Figure 2.1.

Figure 2.1 Overview of biochemical processes involved in expression an

2.11.1. Growth and maintenance of FreeStyle HEK 293F cells

The Invitrogen FreeStyle™ 293 Expression System (Invitrogen, USA) was used for all the transfections of 293F human embryonic kidney (HEK) cells in a serum-free medium (Invitrogen, 2010). HEK 293F cells were routinely propagated in suspension culture at 37°C in a humidified CO_2 incubator equipped with a platform shaker set which was at constant gyration at 150 rpm. HEK 293F cells were maintained at a density of around 5 x 10^5 cells/mL and not exceeding 20% of the total culture flask volume for a minimum of three to five passages prior to transfections to maximize their growth and viability. FreeStyle 293 Expression medium was changed every couple of days keeping the cell cultures at appropriate density and at a viability of a minimum of 97%.

2.11.2. Large scale transfection of HEK 293F cells

Large scale (0.8-1.6L) transfection of sdAb was performed multiple times over the course of the study. Transfection was performed directly in FreeStyle 293 Expression medium. On the day before transfection, the master cell suspension was split into an appropriate number of flasks at a 1 x 10^6 cells/mL density and cultured overnight. The next day cells were counted with a haemocytometer and transfected with plasmid DNA when they reached 2 x 10^6 cells/mL density. The transfection protocol required the plasmid DNA stock to be diluted to a final concentration of 0.5 µg DNA/µl in pre warmed OPTIMEM Medium. PEI Max transfection reagent (Polysciences, USA) was made as a stock solution at a concentration of 1 mg/mL (0.1g of PEI Max was dissolved in 900 µl sterile water) and pH was adjusted to 7.0 with 1 N Sodium Hydroxide (NaOH), PEI stock solution was sterile filtered using a 0.22 µM syringe filter membrane. PEI Max stock solution was added to pre-warmed OPTIMEM media and incubated at room temperature (RT) for 5 minutes, at the same time, previously diluted plasmid DNA was mixed with OPTIMEM in a syringe and filtered into PEI-OPTIMEM mixture. Plasmid DNA and PEI Max was allowed to complex for 20 minutes at RT before being pipetted drop wise into cells whilst continuously shaking the culture flask. Cells were incubated for an additional 20 minutes with PEI-DNA complex before being transferred to a shaking incubator. Transfected cultures were incubated for 6 days and harvested by centrifugation (4500x *g* for 30 minutes) and further clarified by filtration through a 0.22 µm membrane.

2.12. Purification of single domain antibodies

Nickel (Ni-NTA) resin was used to purify recombinant proteins from the supernatant, in this step the sdAb is captured using its 6His-tag that binds to the nickel-sepharose. Second step involved the use of an AKTAprime Plus chromatographic system to resolve proteins according to their size, separating desired monomer from contaminates and aggregates.

2.12.1. Immobilized metal affinity chromatography (IMAC)

The immobilized metal ion affinity chromatography (IMAC) method was used at the initial purification step of all recombinant proteins expressed in the HEK 293F cell line. During IMAC purification recombinant fusion proteins tagged with six tandem histidine (6His) residues selectively bind high affinity Ni-NTA agarose resin, while the majority of other proteins present in the expression media did not bind to the resin, or bound very weakly. Weakly binding proteins were washed off with low molarity imidazole, whereas high molarity imidazole buffer was used to elute the desired proteins. Imidazole competes for binding to the metal-charged resin with the His-tag and thus is used for elution of the recombinant protein from the column. Briefly, Ni-NTA agarose was gently resuspended in its bottle by inversion, followed by of transfer of 3-5 mL of slurry into a 10 mL purification column. After the resin was allowed to settle, it was washed with 55 mL of sterile PBS and allowed to flow through the matrix by gravity. After column equilibration, clarified supernatant was loaded with 0.5 mL/min flow rate. After all the supernatant had passed through the Ni-NTA column, resin was washed with 55 mL of 30 mM imidazole, prior to elution with 20 mL of 400 mM imidazole and 5 mL of PBS to wash residual protein. Supernatant was collected, diluted with PBS and sterile filtered using 0.22 µm filter and concentrated to 0.5 mL final volume. All purification steps were conducted at 4°C to prevent protein degradation. SdAb samples were further purified by Fast Protein Liquid Chromatography (FPLC).

2.12.2. Fast Protein Liquid Chromatography (FPLC) purification

After IMAC purification was completed, all samples were concentrated and buffer exchanged into PBS to about 500 µl final volume using a Pierce protein concentrator

unit with a 5,000 molecular weight (MW) cut off (Thermo Scientific, USA). The second purification step utilized size exclusion chromatography (SEC) to further separate multiple components on the basis of differences in their size. A HiLoad Superdex 75 prep grade pre-packed column designed for high-resolution preparative gel filtration chromatography was used. The column was first equilibrated in PBS containing 150 mM sodium chloride (NaCl) to minimize pH-dependent ionic interactions with the matrix. The volume of expected elution for sdAb was determined by using Low Molecular Standards (GE, USA as shown on Figure 2.2.). Before each purification the column was calibrated with one column volume (CV) of sterile filtered running buffer (PBS/150mM NaCl). Sample (0.5-0.8 mL) was injected into the column and allowed to fractionate over time, 2.6 mL fractions were collected and pooled together before sterile filtration and concentration. At the end of each experiment an extended wash with the running buffer was performed to remove residual impurities and to prime the HiLoad Superdex 75 column for a new purification.

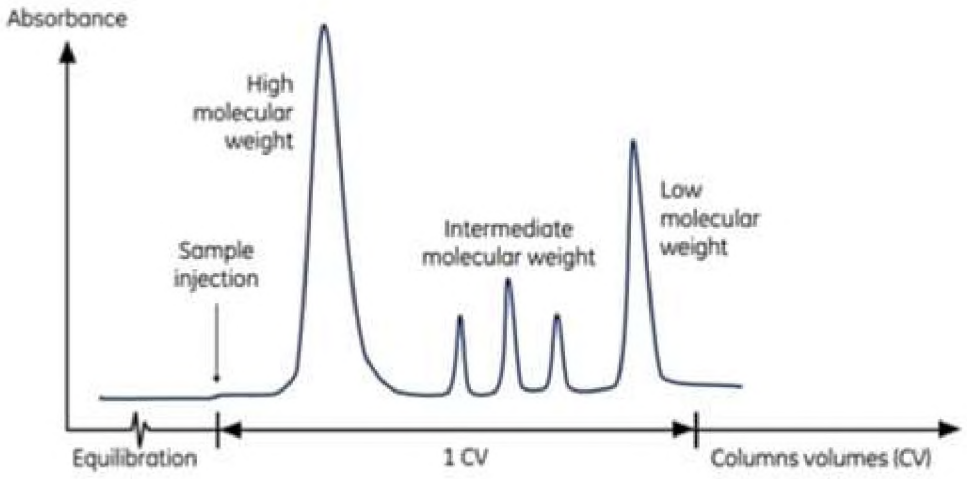

Figure 2.2 Size Exclusion Chromatography purification sample distribution. The contents of a protein are differentiated according to their molecular weight (GE Healthcare Life Sciences, 2017).

2.13. SDS-PAGE Gel Electrophoresis

SDS-PAGE (Sodium Dodecyl Sulfate PolyAcrylamide Gel Electrophoresis) also known as Laemmli protein electrophoresis is a routine biochemical technique to separate molecules by their charge across an applied electrical field. SDS-PAGE involves

multiple steps such as casting one resolving and stacking gel, sample preparation and electrophoresis followed by staining and de-staining of the gel.

2.13.1. Resolving gel preparation

Two glass plates (1mm) were thoroughly cleaned with 70% ethanol and clamped onto the caster using a plastic clamp. The caster was then inverted to drain excess ethanol and allow plates to dry completely while the resolving gel was being prepared. 10 mL of 15% resolving gel was prepared according to the recipe in Table 2.4A and gel solution was poured between the plates assembled with spacers. To maintain an even and horizontal resolving gel surface, 1 mL of isopropanol was layered over the surface. The gel was allowed to set for about 20-30 minutes at room temperature before the stacking gel solution was prepared.

2.13.2. Stacking gel preparation

Stacking gel was prepared as a 10 mL volume and 5% concentration according to the recipe in Table 2.4B. The layer of isopropanol was discarded by inversion and the stacking gel solution was poured above the resolving gel until it overflowed. Plates were gently tapped on sides ensuring no air bubbles were trapped and a comb was inserted into the gel. The gel was allowed to set for about 30 min at ambient temperature.

Table 2.4 Tris-Glycine 15% resolving gel and 5% stacking gel recipe.

15% Resolving Gel	Volume (mL)
40% acrylamide	5.0
1.5 M Tris-HCl, pH 8.8	2.6
Milli-Q water	2.2
10% SDS	0.100
10% APS	0.100
TEMED	0.010

5% Stacking Gel	Volume (mL)
40% acrylamide	1.34
0.5 M Tris-HCl, pH 6.8	2.6
Milli-Q water	5.86
10% SDS	0.100
10% APS	0.100
TEMED	0.010

Notes: SDS- PAGE gel was electrophoresed using 1x Tris-Glycine running buffer.

2.13.3. Sample preparation

SDS-PAGE protein electrophoresis was conducted under denaturing conditions with the SDS detergent, which denatures and binds to proteins making them uniformly negatively charged. A reducing agent (Invitrogen, USA) or 0.1M DTT was added to break down protein-protein disulphide bonds, and water was added as needed for the total reaction volume to be equal to 20 µl (Table 2.5). The reaction mixture was boiled at 95°C for 5 min, transferred to ice and centrifuged at 10,000x *g* for 5 min before being loaded onto the gel. The SDS-PAGE gel was electrophoresed at 110 Volts in SDS-PAGE Tris-Glycine running Buffer using the Bio-Rad Vertical Electrophoresis Apparatus (http://www.bio-rad.com/en-us/category/vertical-apparatus). After electrophoresis, the gel was gently separated from glass plates and stained overnight in TaKaRa Coomassie Brilliant Blue (CBB) Protein Safe Stain (Clontech, USA). The next day the staining solution was removed and the gel was placed on a rocking platform and de-stained with distilled water to remove excess stain for about 4 hours until blue bands were visible on a clear background.

Table 2.5 SDS-PAGE sample preparation.

Reagent	Reaction (20µl)
Sample (neat or diluted in H_2O)	14 µl
NuPAGE™ LDS Sample Buffer (4X)	5 µl
NuPAGE™ Sample Reducing Agent (10X)	1 µl
Water (Sigma)	If needed

Notes: SdAb samples purified by IMAC and SEC columns were resolved on 15% Tris-Glycine gel. The CAP256.25 sdAb_mut and mut8 were always assayed neat and m36 was diluted appropriately with sterile water.

2.14. Western blot analysis

Western blot was used to detect purified sdAb proteins and to assess protein purity and level of protein expression post IMAC and SEC purification. Following the separation by SDS-PAGE, the gel was superimposed over a PVDF or nitrocellulose membrane and proteins were transferred using TransBlot® Turbo™ Transfer System for 30min. After the transfer process was completed, the blotting membrane was blocked overnight at 4°C with 0.5% skim milk dissolved in TBS buffer, to prevent any

nonspecific reactions from occurring. The following day the membrane was repeatedly washed in TBS buffer and incubated for 1 hour with anti-His-Alkaline phosphatase (AP) diluted 1:2000 in TBS buffer. After this incubation, the membrane was washed multiple times and developed using AP substrate (Sigma, USA).

2.15. Preparation and analysis of cytosolic fractions

To determine if CAP256.25 sdAb variants were retained inside the cells instead of being secreted into the culture medium, we isolated and analysed crude fractions of cell cultures used for the protein expression. Cells were washed with PBS buffer and then disrupted by vigorous pipetting in ice cold RIPA buffer for 30 minutes on ice to disrupt the outer cell membrane and solubilize intracellular proteins. Following lysis with RIPA buffer, Laemmli sample buffer was added to the homogenized sample, prior being boiled and assayed on the Western blot as described above.

2.16. Growth and maintenance of JC53 cells

JC53 cells also known as TZM-bl cells were used in neutralization. They were routinely cultivated in an incubator at 37°C with a 5% CO_2 and 95% humidity. Cells were passaged every 2-3 days and subcultured when they reached confluency of 95%. Briefly, spent culture medium was aspirated using a sterile Pasteur pipette, the monolayer was washed with 5 mL of sterile PBS (Gibco, USA), then treated with 3 mL of 1xTrypsin–EDTA solution for 30 seconds at RT. Trypsin was removed and the flask was further incubated for 1-2 minutes at 37°C to facilitate monolayer displacement. The trypsin was neutralized with 7-10 mL of DMEM media (Gibco, USA) supplemented with 10% Foetal Calf Serum (Thermo Fisher, USA), 1x Gentamycin antibiotic (Sigma, USA) and 2.5% HEPES (Gibco, USA). The Trypan Blue reagent (Sigma, USA) was added to an aliquot of cell suspension at 1:1 ratio, the mixture was counted using an automatic cell counter (Bio-Rad, USA) to accurately determine number of cells per mL.

2.17. TZM-bl viral neutralization assay

Function and potency of sdAb antibodies was compared against the parental CAP256.25 mAb using the TZM-bl viral neutralization assay. This assay measures the reduction in luciferase gene expression in JC53 cells after a single round of infection with Env pseudotyped viruses in the presence of antibody compared to a virus control. Neutralization breadth and potency of the sdAb constructs was determined using a 12-virus clade C and global panel of HIV-1 Env-pseudoviruses available in the HIV Virology Laboratories at the NICD. Firstly, 25 µl of the pseudotyped virions were incubated with 25 µl of serially diluted sdAb starting at 10 µg/mL for sdAb or at 1 µg/mL for an IgG control. After 1 hour of incubation at 37°C, 20 µl of JC53 cells at density of 10,000 cells per well were added to the virus-antibody complex and co-cultured for 48 hours at 37°C. Following the required incubation period 100 µl of supernatant was removed and volume was replaced with 100 µl of luciferase substrate. After a 2 minute incubation in the dark, luciferase was vigorously mixed by pipetting with cells and the suspension was transferred to a flat black bottom plate and the RLU (Relative Lights Units) were measured on a SpectraMax Microplate Luminometer (Molecular Devices). Data was processed using Excel software to generate a titration curve to determine IC_{50}, the concentration of antibody at which 50% of the virus is neutralized.

Chapter 3 : Results

3.1. Rationale for selection of CAP256.25 for expression as a single domain antibody

Human antibody molecules always occur as paired entities and consist of two heavy and two light chains. In contrast dromedary species are able to express fully functional unpaired heavy chain antibodies which account for 75% of antibodies in the *Camelidae* immune system (Hamers-Casterman *et al.*, 1993). The discovery of dromedary antibodies paved the way for the development of single domain antibodies (sdAb) by incorporating their unique features into human heavy chain frameworks. We have selected the CAP256.25 antibody as a suitable candidate to engineer as a sdAb derivative because of its unique structural characteristics. Firstly binding to the HIV Env epitope with a single Fab arm, more specifically CDR-H3, which interacts with C strand of V1V2 (Figure 3.1), and N-glycans from residues 160 and 156 as implicated by the paratope mapping studies and negative stain electron microscopy (EM) (Doria-Rose *et al.*, 2016; Gorman *et al.*, 2016).

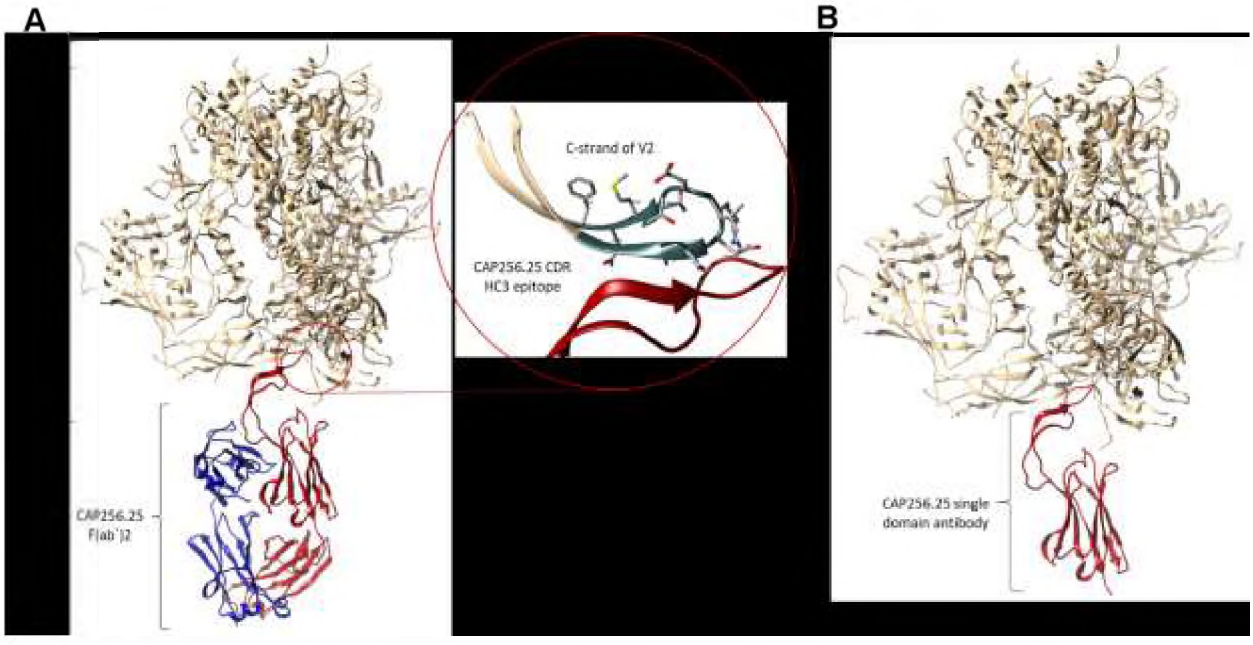

Figure 3.1 Ribbon representation of CAP256.25 bound to BG505 SOSIP.664 Env trimer (PDB ID: 5DT1). (A) F(ab')2 portion of CAP256.25 with the light chain indicated in blue and the heavy chain in red respectively. The inset illustrates CAP256.25 CDR-

H3 interaction with the V1/V2 region of HIV gp120. **(B)** Single domain (sdAb) derivative of CAP256.25 antibody.

The CAP256.25 epitope is formed by multiple protomers producing a conformational epitope, and includes dependence on an N-linked glycan at residue 160 along with the C strand of V1V2 (Gorman *et al.*, 2016; Hicar *et al.*, 2016). CAP256.25 accesses the basic region of the epitope through an extended CDR-H3, efficiently penetrating the dense glycan shield and engaging with a conserved glycan at N160 (Andrabi *et al.*, 2017). In addition to dependence on N160, a single change of Lysine at position 169, abrogates neutralization by CAP256.25-VRC26 antibody creating an escape mutation for the virus (Doria-Rose *et al.*, 2014). Polymorphisms at position 169 are prevalent in clade B and C and can be found in 80% of resistant clade B strains, which explains that while CAP256.25 neutralized over 70% of global strains, its activity against clade B strains was significantly diminished (Doria-Rose *et al.*, 2016). The second factor favouring CAP256.25 sdAb is a shared sequence homology between CAP256.25 and the Camelidae IGVHH3 family as described below.

3.2. Sequence homology comparison

To rationally design CAP256.25 sdAb derivatives, we did structural comparisons between previously isolated VHHs, such as A12 and based the design of a sdAb derivative on shared sequence homology with the dromedary IGVHH3 (3-1) family. CAP256.25 antibody belongs to the IGVH3-30 germline, which shares over 84% sequence homology with the dromedary subfamily three. Homology assessment was based on sequences derived from *Lama glama* or *Camelus ferus* and compared to the corresponding human gene family (Klarenbeek *et al.*, 2015; Goldman *et al.*, 2017). A12 is a VHH generated by llama immunization, followed by sequential bio-panning with gp120 from clades A, B, and C, and with specificity to the CD4bs (McCoy *et al.*, 2012). To establish homology between llama VHH antibodies and human heavy chains, the amino acid sequence of dromedary IGVHH3 was aligned with A12 and CAP256.25 antibody sequences (Table 3.1, a comprehensive read out for all sdAb sequences is included in the supplementary section A). In addition, we used m36 for sequence comparison (a chimeric human single domain antibody fragment). Although, there are many conserved sequence hallmarks in VHH domains relative to canonical human

IGHV domains, the most important occur at four positions known as the “tetrad” in the second framework region (Riechmann and Muyldermans, 1999). Tetrad residues are encoded by IGVHH germline genes of *Camelidae* and not a consequence of somatic hypermutations (Nguyen, Desmyter and Muyldermans, 2001). Tetrad residues are highly hydrophobic in canonical VHs as opposed to dromedary VHHs, thus the rationale for substitution of human tetrad with *Camelidae* is to minimize the hydrophobic interactions of the VH/VL interface, which are a major factor contributing to the instability of autonomous single domains (Gil and Schrum, 2013).

domains used and generated (mut0 sdAb, llama IGVHH3 germline, A12 sdAb and m36 sdAb.

3.3. Generation of CAP256.25_mut4 sdAb

The first step in "camelization" of CAP256.25_mut0 (the umutated parental CAP256.25 sdAb) involved replacement of the tetrad of exposed hydrophobic side chains in FR2 (positions Phe37, Glu44, Arg45, and Phe/Gly47) with hydrophilic residues to improve the solubility of engineered human single domains (Barthelemy *et al.*, 2008). Since the crystal structure of m36 sdAb is not available, we used the A12 VHH structure to model tetrad residue substitutions in CAP256.25 sdAb, as shown in Figure 3.2A.

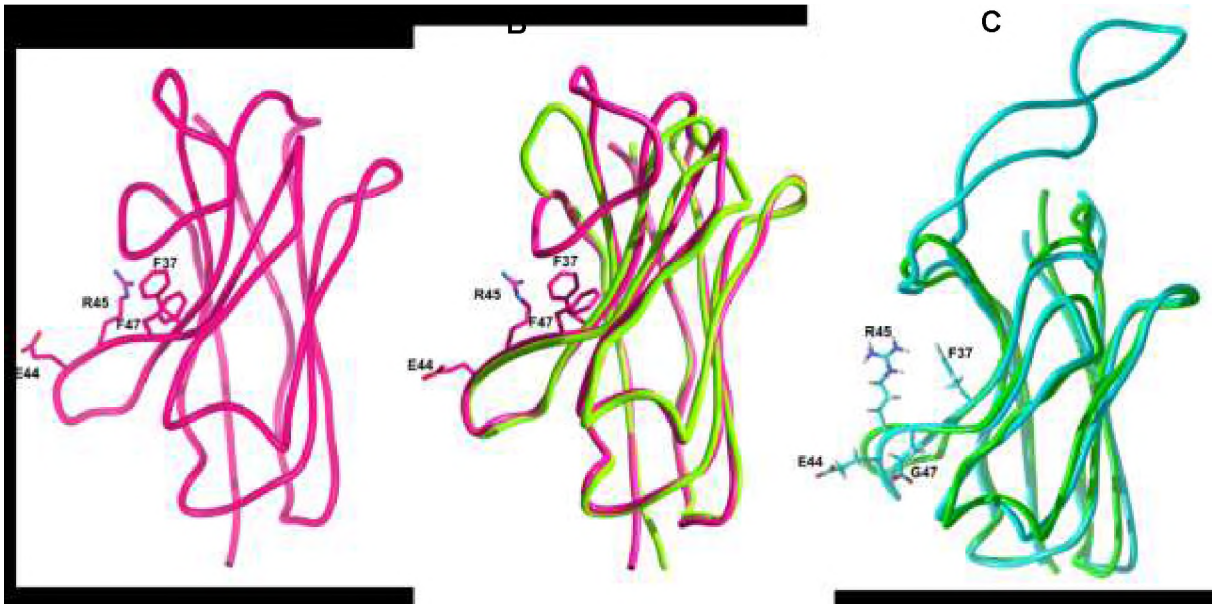

Figure 3.2 Structural characteristics of single domain antibodies used as a guide to model CAP256.25 sdAb. (A) Ribbon representation of llama derived A12 sdAb (PDB ID: 3r0m). **(B)** Homology between CD4-binding site of A12 sdAb (pink) and murine homolog of CD4-inducible m36 sdAb (green). **(C)** Structural homology between m36 sdAb and V2-specific human derived CAP256.25 parental antibody (cyan). Tetrad residues are indicated as atoms for all models.

VHH A12 belongs to gene family IGVHH3 typified by a KEREF motif. In addition several other motifs are found at positions 43-47 in IGVHH FR2 regions, such as KEREL, KQREL, KQREF or KEREG. Using UCSF Chimera software we assessed the structural impact of these different motifs on the CAP256.25 parental antibody. The overall rationale for introducing changes to CAP256.25_mut0 sdAb was to maximize the hydrophilicity of the former light chain interface either by the substitution or by occlusion of hydrophobic elements. The criteria for choosing the single best combination of substitutions involved avoiding structural deformations of the parental

molecule while successfully minimizing the hydrophobic patch in the former VL/VH interface. First, we substituted Glycine (G) at position 44 with Glutamic Acid (E) and Leucine (L) at position 45 with Arginine (R), both mutations were consistent with the conserved tetrad found in the more soluble camelid VHHs. Hydrophilicity was further increased by substitution of Tryptophan (W) at position 47 with a much smaller Glycine residue, which was structurally a better fit than Phenylalanine (F). The fourth change involved replacement of Valine (V) at position 37 with a Glycine residue, which is a more hydrophobic residue. This particular change influences the secondary and tertiary structure of VHH and it involves interactions between Phenylalanine 37, Tyrosine 91, Tryptophan 103, and the soluble portion of Arginine 45 which all together nucleate the hydrophobic core of VHH (Rouet, Lowe and Christ, 2014). Newly generated CAP256.25 sdAb, containing a KEREG motif in FR2 was renamed CAP256.25_mut4 sdAb, the homology modelling of which is shown in Figure 3.3.

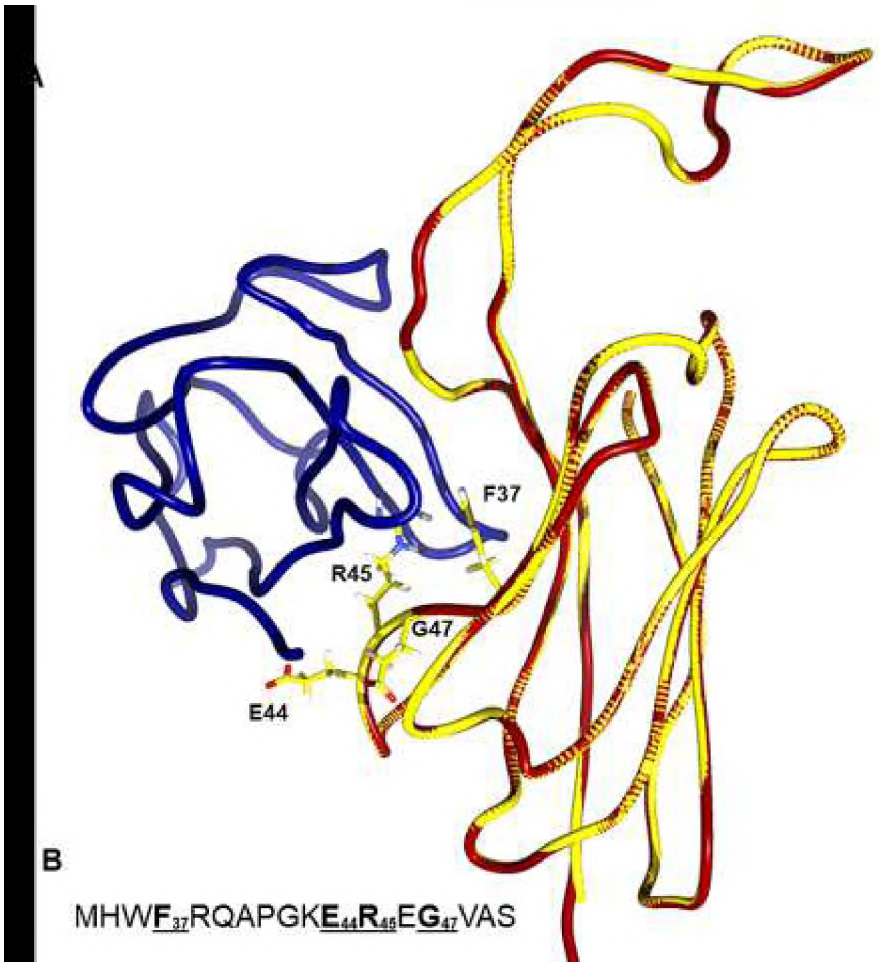

Figure 3.3 Structural characteristics of CAP256.25_mut4 sdAb. **(A)** Ribbon representation of CAP256.25_mut0 sdAb (red) superimposed over CAP256.25_mut4 sdAb (yellow). Tetrad residues indicated as atoms, former light chain in blue. **(B)** Framework 2 sequence with underlined tetrad residues.

3.4. Generation of CAP256.25_mut8 sdAb

After the introduction of four mutations in FR2 to stabilize the former VH/VL interface we analysed additional substitutions in the solvent exposed part of CAP256.25_mut4 sdAb to further improve its stability and solubility. In the majority of human canonical antibodies, position 11 (FR1) is occupied by Valine and functions as a ball-socket connection between VH and CH1. In contrast *Camelidae* VHH position 11 is occupied by a conserved Serine. CAP256.25_mut0 contains two consecutive Valine residues and mutating the surface exposed and non-polar Valine 11 to polar Serine results in enhanced solubility of the sdAb. Position 35 (FR2) is located on the surface exposed VH/VL interface, actively supporting the antibody structure and has been implicated in the stabilization of the hydrophobic core. Substituting the positively charged Histidine with non-polar Glycine resulted in enhanced favourable interactions with Phenylalanine at position 37, which is also a critical residue in the conserved tetrad motif. Gly35 gently pushes Phe37 into the cavity of the former VH/VL interface resulting in an increase of surface hydrophilicity. Another substitution closely interacting with and stabilizing Phe37 was a second Phenylalanine at position 91 in FR3, which is probably involved in aromatic ring stacking with adjacent Phe37. Substitution of polar Tyr91 to non-polar Phenylalanine further stabilized CAP256 sdAb_mut4 structure. Glutamine is found to be conserved in position 108 (FR4) in all VHHs, while the corresponding position in canonical IGVH is occupied predominantly by a polar residue, such as Threonine or Methionine (J. J. Gray *et al.*, 2011). Introduction of the more polar Glutamine seems to result in a more favourable molecule structure. In summary, a total of four additional mutations were introduced into CAP256.25_mut4 sdAb backbone, resulting in the generation of CAP256.25_mut8 sdAb. Sequence comparison of all three sdAb is shown in Table 3.2.

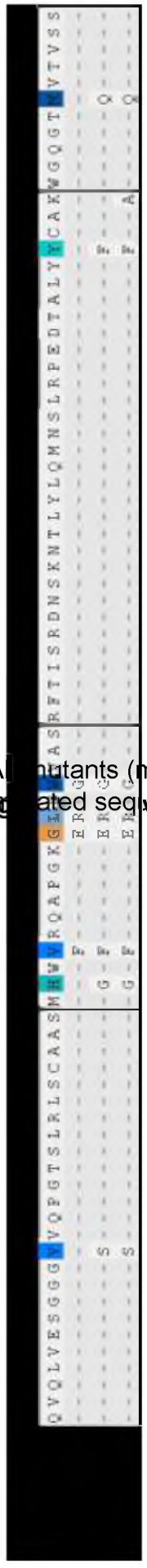

of two CAP256.25 sdA[illegible]nutants (mut4, mut8 and mut9) containing four and eight substitutions
ag of CAP256.25 sing[illegible]ated sequence denoted mut0 **va[illegible]ated in the study.**

3.5. CAP256.25_mut9 sdAb

The final step in camelization involved analysing the CAP256.25_mut8 sdAb energy landscape to gain insight into how introduced mutations might have affected the sdAb and determine if there are any additional changes beneficial to CAP256.25_mut8 sdAb. Proper protein folding is critical for maintaining structural stability of every molecule, when the energy is not distributed evenly through the core it creates "sites of high local frustration". To determine if the energy landscape of the CAP256.25_mut8 sdAb was compromised through the molecular engineering we used the frustratometer tool. The frustratometer algorithm models and quantifies the location of frustration manifested in the molecule. Sites of high frustration include key residues involved in antigen binding, such as the CDR-H3 or energetically unfavourable sites, which compromise core stability and cause potential aggregation. One of the residues identified was Lysine at position 94, located at the base of CDR-H3 and adjacent to a Cysteine residue, which is involved in disulphide bond formation with CDR-H1. A major difference between VHH and monoclonal human antibodies is the inter- or intraloop disulfide bridge linking CDR-H1 and CDR-H3, which structurally stabilizes VHH domains and is mostly absent in canonical antibodies. Interestingly the CAP256.25 antibody possesses two Cysteine residues participating in the formation of a disulfide bond. Sequence analysis revealed that over 75% of VHH domains contain double Alanine residues (CAA) next to Cysteine at the base of CDR-H3. CAP256.25 contains a CAK motif, which when substituted with Alanine resulted in a much less frustrated molecule. Homology modelling and mutational transitions of this newly generated molecule named CAP256.25_mut9 are illustrated in Figure 3.4A and the corresponding sequence in Figure 3.4B.

A

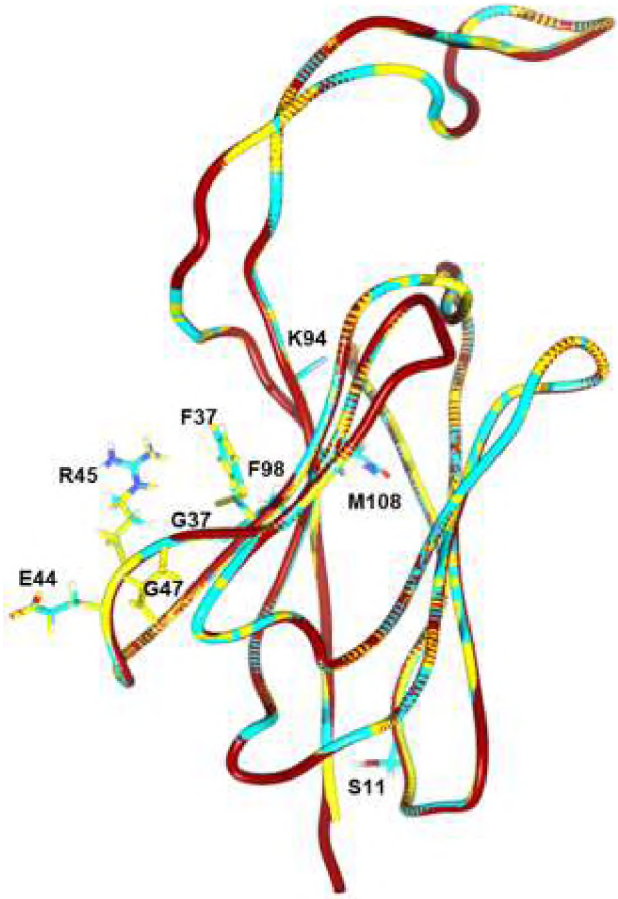

B

CA**A**$_{94}$DLREDECEEWWSDYYDFGKQLFCAKSRGGLVIADNV

Figure 3.4 Structural characteristics of CAP256.25_mut9 sdAb modelled in *sillico*. (A) Ribbon representation of CAP256.25 sdAb_mut0 (red) superimposed over CAP256.25 sdAb_mut4 (yellow) and CAP256.25 sdAb_mut9 (cyan). Mutated residues are indicated as atoms. **(B)** K94A mutation in CDR-H3 sequence is underlined.

3.6. Hydrophobicity of surface exposed framework residues

The Kyte-Doolittle scale was used to assess the level of hydrophobicity of the CAP256.25 derivatives by measuring the interactions of surface exposed residues with water. It is thermodynamically favourable for molecules to minimize the interaction with nonpolar hydrophobic moieties reducing aggregation of nonpolar residues to accumulate in a cage-like network of water surrounding all hydrophobic amino acids. All three CAP256.25 sdAb derivatives were modelled using UCSF Chimera software to determine changes in hydrophobicity of CAP256.25 sdAb fragments using Kyte-Doolittle hydropathy scale, an important determinant of protein folding. The amino acid side chain (R-group) determines whether the residue is hydrophobic or hydrophilic. In general hydrophobic amino acids and hydrophobic side chains make up the core of

the molecule as they are not soluble in water (Supratim Choudhuri, 2014). Hydrophobicity of the molecule is central to understanding the mechanism of protein folding and stability, thus playing an important role in protein structure prediction (Gromiha and Pongor, 2010). Hydrophobicity of an amino acid is measured by assigning specific values and thus creating a hydropathy scale, which calculates the overall hydrophobicity of a molecule (Supratim Choudhuri, 2014). The Kyte-Doolittle hydrophobicity plot, was used to determine changes in hydrophobicity of the CAP26.25_mut9 sdAb variant in relation to the CAP256.25_mut0 sdAb. It assigns scores to all amino acids, colour coding hydrophilic residues in blue and hydrophobic in orange. The increase in hydrophilicity or blue colour across all CAP256.25 sdAb fragments is shown in Figure 3.5

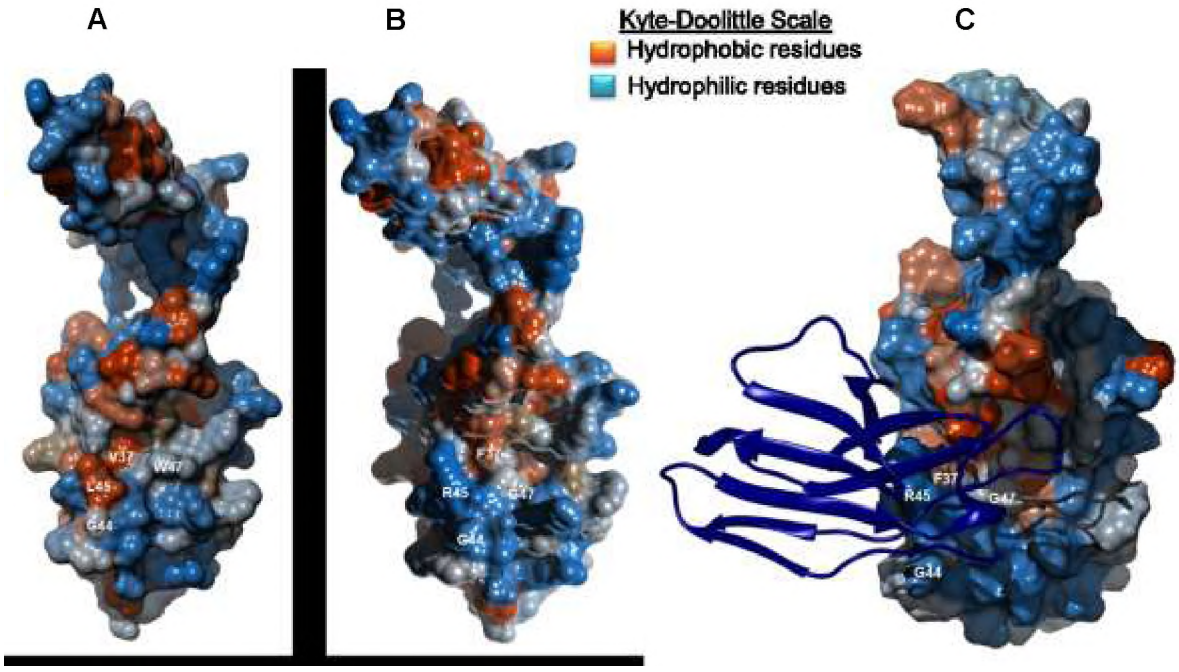

Figure 3.5 Kyte-Doolittle scale indicating hydrophobic amino acids of CAP256.25 sdAb variants. (A) CAP256.25_mut0 sdAb **(B)** CAP256.25 sdAb_mut 4 sdAb **(C)** CAP256.25_mut8 sdAb with superimposed former LC (blue), structure is rotated slightly to the left.

3.7. Generation of sdAb derivatives expression plasmids

Single domain genes of CAP256.25_mut4, mut8 and m36 were generated by GenScript and sub-cloned from the parental pUC57 vector into CMVR, a mammalian expression vector (aidsreagent.org), using *XbaI*, multiple cloning site (MCS) position 1374 and *BamHI* (MCS position 2801) restriction endonucleases (Thermo, USA). CAP256.25_mut9 was generated by the site-directed mutagenesis as described in section 2.10. The size of the gene fragments was confirmed by agarose gel electrophoresis, and products corresponding to the expected sizes, 435bp for m36 sdAb and 528bp for CAP256.25 sdAb (mut4 and mut8) (Figure 3.6), were excised from the gel and purified. For complete sequences please refer to Supplementary section B, and an annotated vector map is illustrated in Figure 3.6. The CAP256.25 and m36 sdAb genes were inserted into the CMVR vector and confirmed by sequencing with CMV-F primer. Sequencing showed the sdAb constructs were in the correct orientation and free of errors.

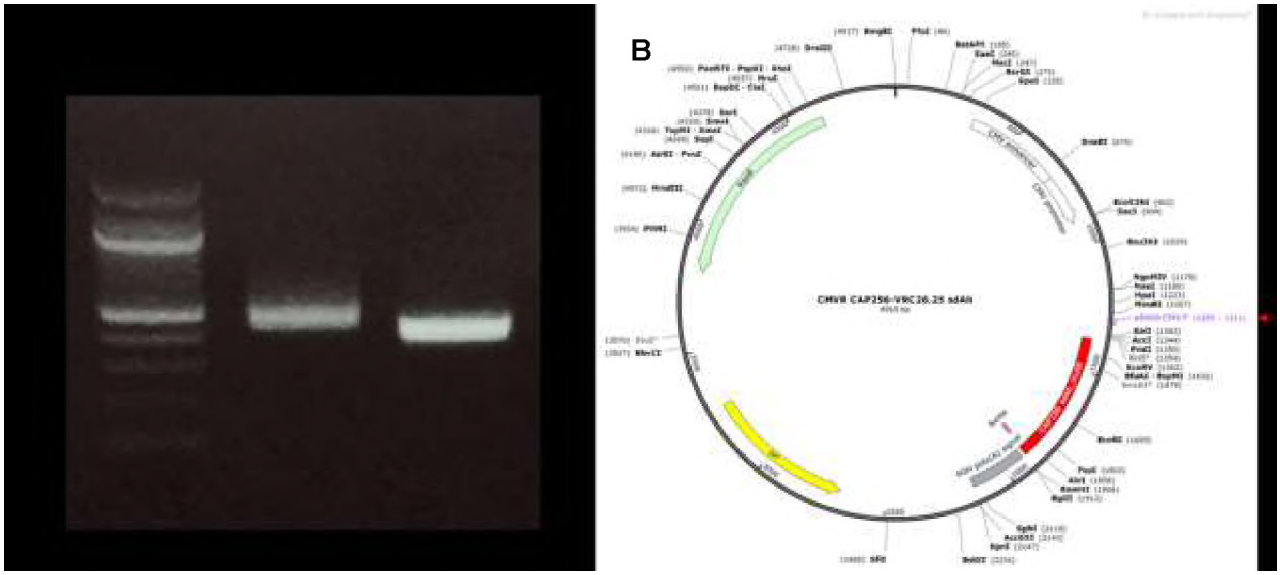

Figure 3.6 Agarose gel electrophoresis of sdAb DNA after enzymatic release from pUC57 plasmid. DNA Molecular Weight Marker XIV (Roche) was used to determine size of sdAb fragments after enzymatic digest, in lane two and three are the bands corresponding to CAP256.25 sdAb_mut8 and m36 sdAb **(B)** Annotated map of CMVR vector containing CAP256.25 sdAb gene, p8400-CMV-F priming site indicated with arrow

3.8. Expression and purification of single domain proteins.

In the initial step recombinant proteins were purified from the supernatant using a Ni-NTA resin in which the sdAb is captured using its 6HIS tag that binds to the nickel-sepharose. As eluted protein often contains mixtures of monomeric and oligomeric species, depending on overall protein stability, hydrophilicity and interactions with the hydrophobic column matrix (Barthelemy *et al.*, 2008) the second step involved the use of an AKTA prime Plus chromatographic system to resolve proteins according to their size, separating desired monomer from contaminates and aggregates. Analysis of the SEC chromatograph indicated strong differences in purification profiles between m36 sdAb and CAP256.25 sdAb variants, as shown in Figure 3.7 and Western blot results in Figure 3.10. Purification profile of the CAP256.25_mut4 was similar to that of the CAP256.25_mut8 sdAb (data not shown). High molecular weights (HMW) aggregates were observed for all sdAb variants, with significantly lower amounts seen in the m36 sdAb preparations. The CAP256.25 sdAb variants also contained lower molecular weight (LMW) peaks, suggesting a lack of overall stability of the CAP256.25 sdAb constructs.

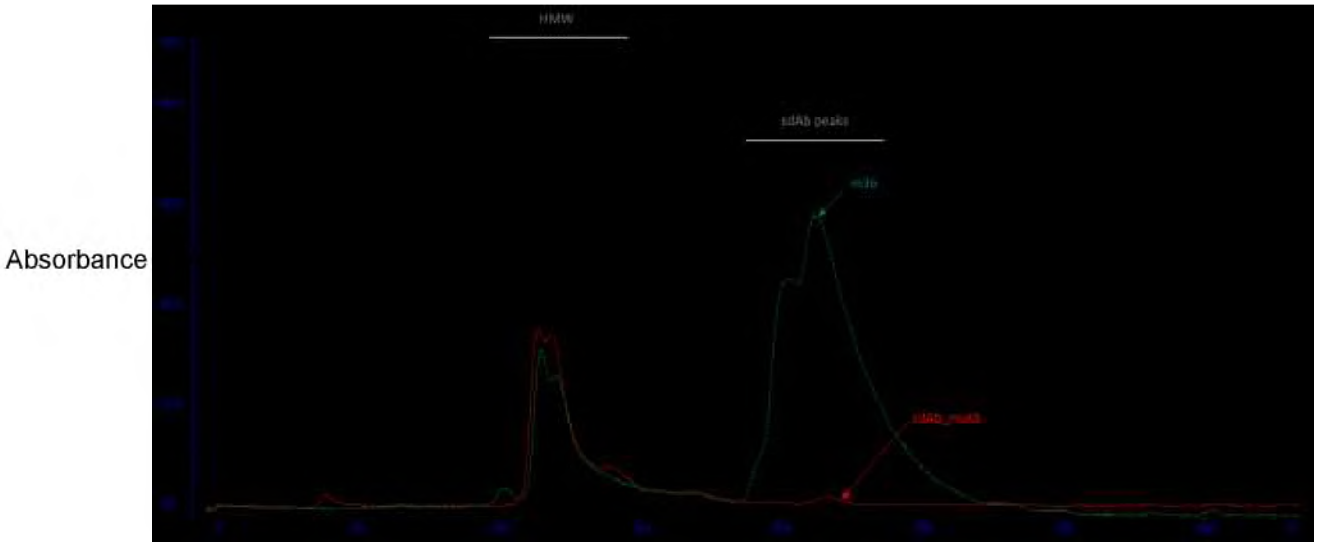

Figure 3.7 Chromatographic separation of m36 sdAb, CAP256.25_mut8 and CAP256.25_mut9 sdAb. M36 sdAb trace is shown in green color, CAP256.25_mut8 sdAb in red and CAP256.25_mut9 sdAb in black.

Significant differences were also noted in production levels between m36 sdAb and CAP256.25 sdAb derivatives. The m36 sdAb cultures consistently yielded high levels

of purified protein, averaging around 1.2 mg total per 0.8L culture, while CAP256.25 sdAbs variants expressed at drastically lower levels, yielding 0.01 mg/mL for both CAP256.25_mut4 and CAP256.25_mut8 sdAb for the same culture volume. CAP256.25_mut0 was expressed three times, however, expression levels were not sufficient to pursue further. To increase production levels, we used the FreeStyle HEK293F Expi cell line, derived from the 293 cell line and engineered to grow at higher density thus producing high yields of recombinant human proteins. Using 293F Expi cell line, m36 sdAb expression was increased to 2.24 mg per 0.2 L culture a factor of eight, but no change in yield was observed for CAP256.25_mut 8 sdAb. However, an increase in production levels by a factor of six was observed for CAP256.25_mut9 variant in direct comparison to CAP256.25_mut8 sdAb expression, using 293F Expi cell line. Direct comparison of expression levels between different CAP256.25 sdAb variants is shown in the Table 3.3.

Table 3.3 Summary of the expression and purification of single domain antibodies.

Transfection date	Expression Cell Line	Single domain antibodies	Culture Volume (L)	Concentration (mg/mL)	Total Yield (mg)
2016-11-08	293F	m36	0.8	2.80	1.12
2017-10-17	293F Expi	m36 (day 4)	0.2	2.80	1.12
		m36 (day 7)		1.60	2.24
2016-10-24	293F	CAP256.25_mut0	0.8	Below Detection Level	NA
2016-12-12		CAP256.25_mut4		0.10	0.01
2016-10-24		CAP256.25_mut8	1.6	0.11	0.02
2017-01-06		CAP256.25_mut8 (prep1)	0.8	0.20	0.02
		CAP256.25_mut8 (prep2)		0.19	0.02
2017-10-17	293F Expi	CAP256.25_mut8	1.6	0.14	0.02
2017-11-09					
2017-11-09		CAP256.25_mut9 (K94A)	1.6	0.40	0.16

Notes: Expression and purification of sdAbs is summarized according to production cell line, culture volume and usable protein yield after FPLC (SEC) purification.

3.9. Visualisation of purified proteins by Western blot

Purity of single domain antibodies was examined using SDS-PAGE and Western blot. This confirmed significant differences in expression levels and degree of purity

between m36 sdAb and CAP256.25 sdAb variants. M36 sdAb showed high levels of purity post Ni-NTA column and SEC, with a clearly defined single band at the expected molecular weight (~12kDa) as shown in Figure 3.8A. In contrast, the CAP256.25 sdAb variants contained high levels of impurities after Ni-NTA purification clearly visible on SDS-PAGE gel indicating possible lack of stability, given that production and purification proceses were identical to m36 sdAb. Although CAP256.25 variants expresssed poorly, a protein band coresponding to ~12 kDa was visible on the SDS-PAGE gel (Figure 3.8B). Based on band intensity and purification results, CAP256.25_mut8 sdAb appeared to be expressed at higher levels compared to CAP256.25_mut4. However, these were not visible on Western blot suggesting either that this was not the correct protein or that sdAbs were being expressed at exceptionally low levels that could not be detected. Possible reasons for a lack of CAP256.25 expression include improper folding of a single domain due to insufficient solublity, structural deformations or VL/VH interface stickiness. Since we were able to express, purify and visualise m36 sdAb on both SDS-PAGE and by Western blot, but CAP256.25_mut8 with a much lower degree of sucess, we decided to investigate if 6His-tag in CAP25.25_mut8 sdAb was being occluded or if the bulk of properly folded protein was being retained inside the cells.

A

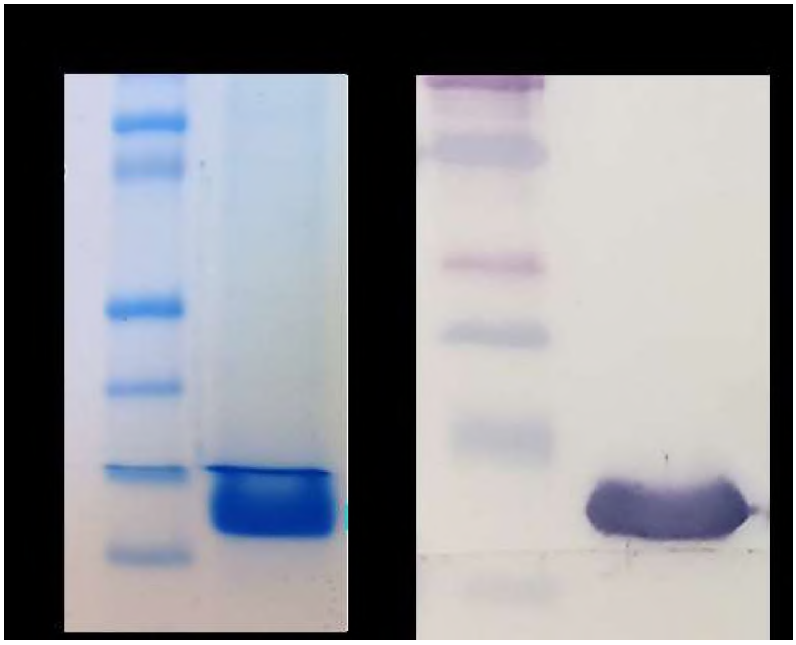

B

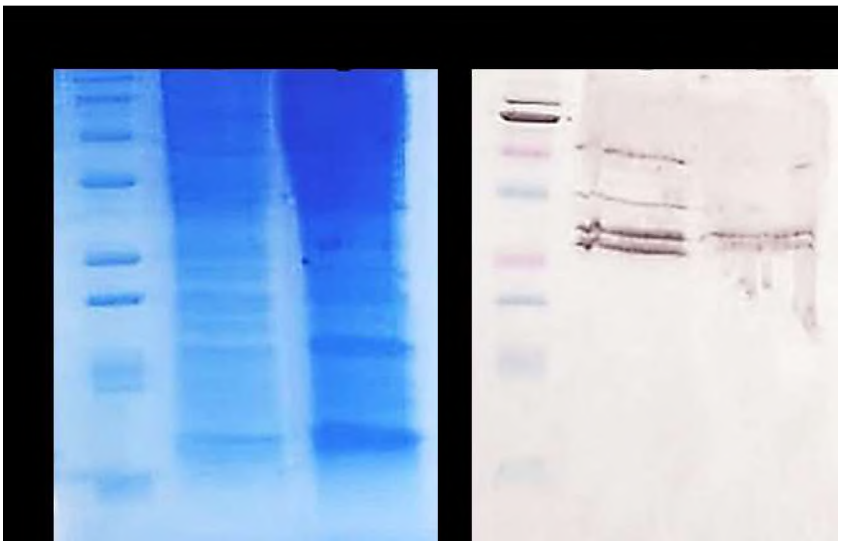

Figure 3.8 Purified single domain antibodies visualised on SDS-PAGE alongside the Western blot containing the same samples after Size Exclusion Chromatography (A) m36 sdAb **(B)** CAP256.25_mut4 and CAP256.25 sdAb_mut8 sdAb.

3.10. Reduction of purified sdAb proteins with urea

Due to the very limited availability of material, first we decided to investigate if high molecular weight bands were as a result of CAP256.25_mut8 sdAb not being sufficiently reduced under standard conditions. Standard reducing conditions of the Laemmli buffer contain 10% SDS detergent and 1M DTT reducing agent. We increased denaturing conditions by addition of increasing concentrations of urea, as shown on Figure 3.9A. CAP256.25_mut8 sdAb sample was reduced to three distinct sets of bands at aproximately 12, 25 and 40kD indicating potential stickiness of sdAb and the presence of monomeric, dimeric and trimeric species. In contrast m36 sdAb was reduced as before to a monomeric species indicated by a single band on the gel of expected size. Western blot analysis reconfirmed the presence of monomeric species for m36 sdAb, but despite loading the maximum amount of sample for CAP256.25_mut8 sdAb, the protein was still not visible on the Western blot membrane (Figure 3.9B). This indicated that suffcient level of CAP256.25 sdAb was not present in the supernatant to be detected by this method.

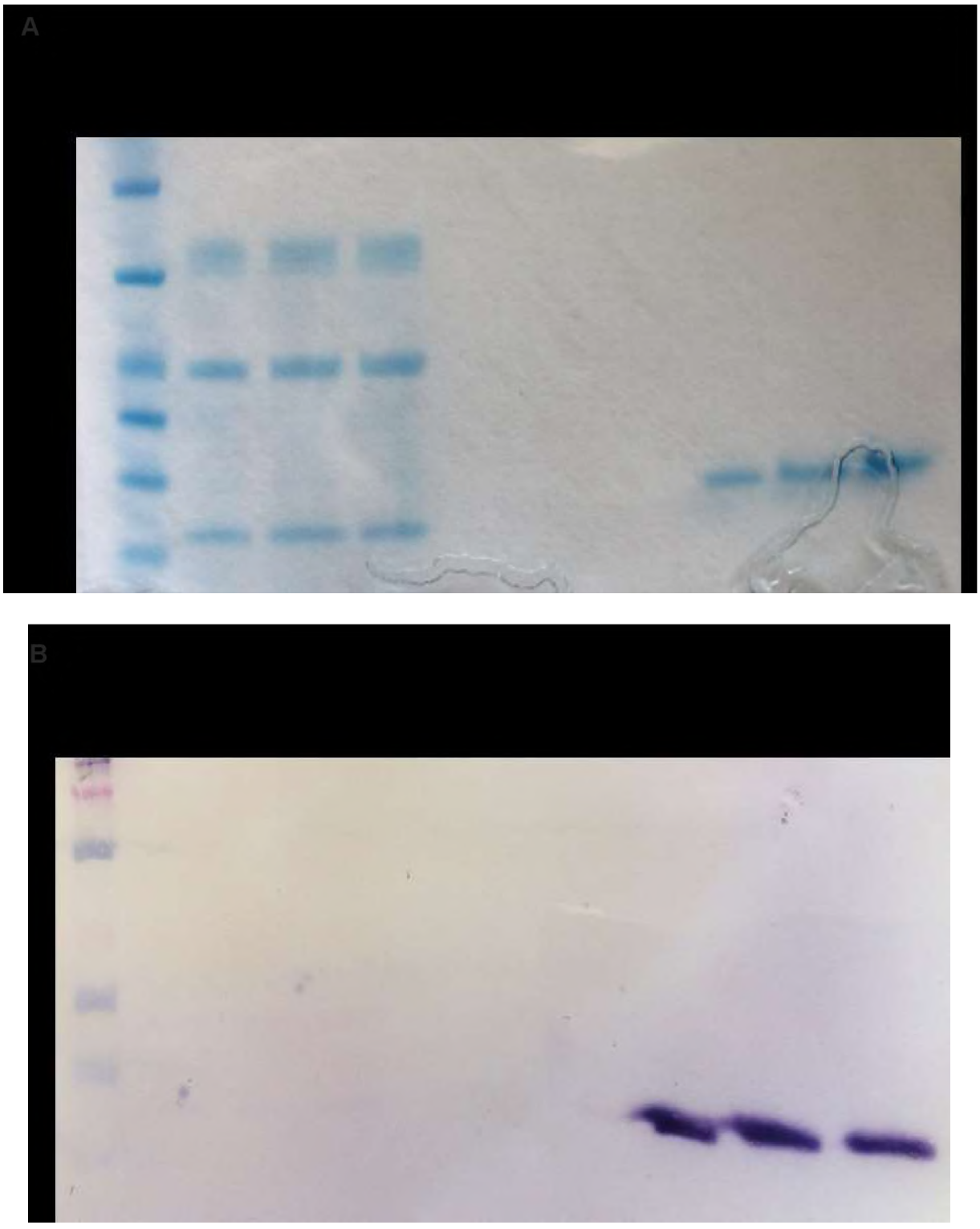

Figure 3.9 Biochemical analysis of single domain antibodies denatured with DTT and urea. (A) SDS-PAGE (**B)** Western Blot of CAP256.25_mut8 sdAb and m36 sdAb in the presence of DTT and 2 concentrations of Urea. Lanes between two sets of samples were left blank intentionally to avoid potential cross contamination.

3.11. Preparation and analysis of cytosolic fractions

To determine if the bulk of the CAP256.25 sdAb protein was retained inside the cell instead of being secreted into the culture medium, we isolated and analysed cellular fractions derived from cultures previously transfected with single domains. Whole cells were lysed in RIPA buffer, extracted and visualized by Western blot as shown in Figure 3.10. As previously, purification of proteins secreted into the supernatant, produced a big range of bands corresponding to various sizes of protein, prominent after IMAC purification but not SEC (Figure 3.10). Lane 1 contains the HMW fraction from SEC purification and some of the bands (25-37 kDa) do correspond to those in lane 2 (IMAC) and lane 3 (SEC). Bands of approximately 12 kDa were present in IMAC sample, but not post SEC, suggesting that CAP256.25_sdAb aggregates, while m36 sdAb is not affected by downstream processing. The absence of CAP256.25_mut8 sdAb protein in the two different preparations of cytosolic fractions suggests that proteins were not expressed or trapped inside the cell. The maximum amount of protein was loaded on the gel to visualise all possible protein fractions.

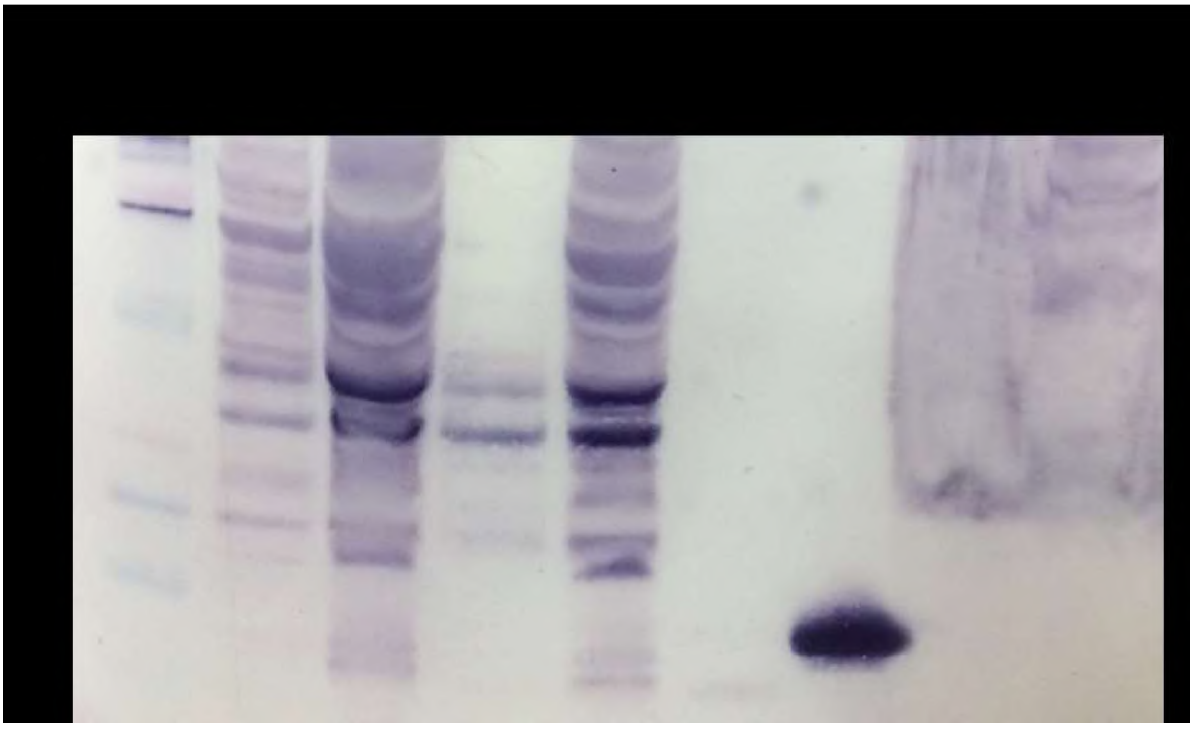

Figure 3.10 Western blot analysis of CAP256.25 sdAb expression in purified supernatant and cytosolic fraction extract. CAP256.25_mut8 sdAb HMW and protein fractions purified by IMAC and SEC from two separate purification experiments (prep 1 and 2) alongside m36_sdAb purified by SEC and included as a control. Cytosolic fractions of CAP256.25_mut8 sdAb transfections.

3.12. Neutralization activity of CAP256.25 sdAbs

CAP256.25 is one of the most potent antibodies in its class, neutralizing 57% of global viruses with a median IC_{50} of 0.001 µg/mL (Doria-Rose *et al.*, 2016). Due to challenges in production and purification of CAP256.25 sdAb variants we had limited quantities of protein available to test for activity. On average we were able to purify about 0.02 mg total in a volume not exceeding 100 µl for CAP256.25_mut8, but given the high potency of the parental antibody we proceeded with the neutralization assay. We chose a small panel of eight clade C viruses comprised of pseudoviruses most sensitive to neutralization by the CAP256.25 parental antibody (Figure 3.11).

CAP256_mut4 sdAb was only tested once against CAP256 SU (superinfecting) virus, which is hypersensitive to neutralization by CAP256.25 bNAb (Figure 3.11A). However, since CAP256.25_mut4 sdAb showed no activity against the SU virus and the antibody was limiting, it was not pursued any further. The CAP256.25_mut8 variant was able to neutralize the most sensitive virus, CAP256SU and CAP256SU wk34_80, albeit with loss in potency (Figure 3.11A). CAP256.25_mut8 also neutralized three additional viruses (ConC, CAP210 and ZM53) with significant loss of potency and showed no neutralization of three viruses (PV.04, Du422 and ZM194). In summary, CAP256.25_mut8 sdAb was able to neutralize five out of eight viruses, which are known to be neutralized by parental antibody. The CAP256.25 IgG antibody neutralization is dependent on a Lysine (K) 169 located in the V2 loop, single amino acid substitution from Lysine to Glutamic acid (E) abrogates neutralization by this antibody. Hence, a CAP256 SU K169E isolate was used to confirm that CAP256.25_mut8 sdAb had the same epitope specificity as the parental IgG. Both, CAP256.25 IgG and its sdAb derivative showed no activity against CAP256 SU K169E or Murine Leukaemia Virus (MLV). MLV was included in all neutralization assays as a negative control for toxicity, no toxicity was observed for any of the sdAb derivatives expressed in HEK293F cells (Figure 3.11B). We did, however, observe toxicity when HEK293F Expi cells were used for sdAb expression. CAP256.25_mut9 sdAb was only expressed in HEK293F Expi cells and therefore, its activity could not be determined.

A

B

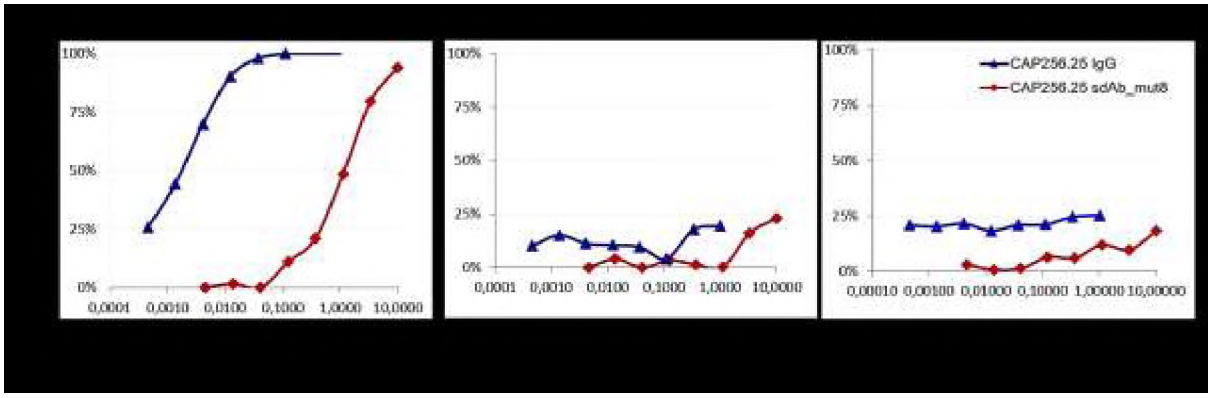

Figure 3.11 Breadth and potency of CAP256.25_mut8 sdAb. (A) IC_{50} values in µg/mL against the panel of heterologous pseudoviruses, IC_{50} values between 0.1 and 1.0 µg/mL are coloured red; 1 to 10 µg/mL, yellow; and above 10 µg/mL, blue. **(B)** Neutralization of CAP256.25_mut8 sdAb against the sensitive SU and K169E pseudoviruses.

We also tested m36 sdAb neutralization against 24 heterologous pseudoviruses from two different panels: clade C and global panel, as shown in Figure 3.12A. As expected m36 showed the best breadth and potency against viruses from clades B, C, BC, and no activity against clades A, AC, AE or G. The m36 sdAb showed very good activity against clade C viruses, neutralizing nine out of twelve viruses with potency of between 0.1 and 1.0 µg/mL, and three isolates with potency between 1 and 10 µg/mL. As expected m36 sdAb showed activity against CAP256 SU K169E isolate similar to that of CAP256 SU, which was expected, since m36 sdAb specificity is directed against CD4bs and not the V1V2 epitope (Figure 3.12B). Murine Leukaemia Virus (MLV) was

included in all neutralization assays as a negative control for potential toxicity, and no toxicity was observed for m36 sdAb.

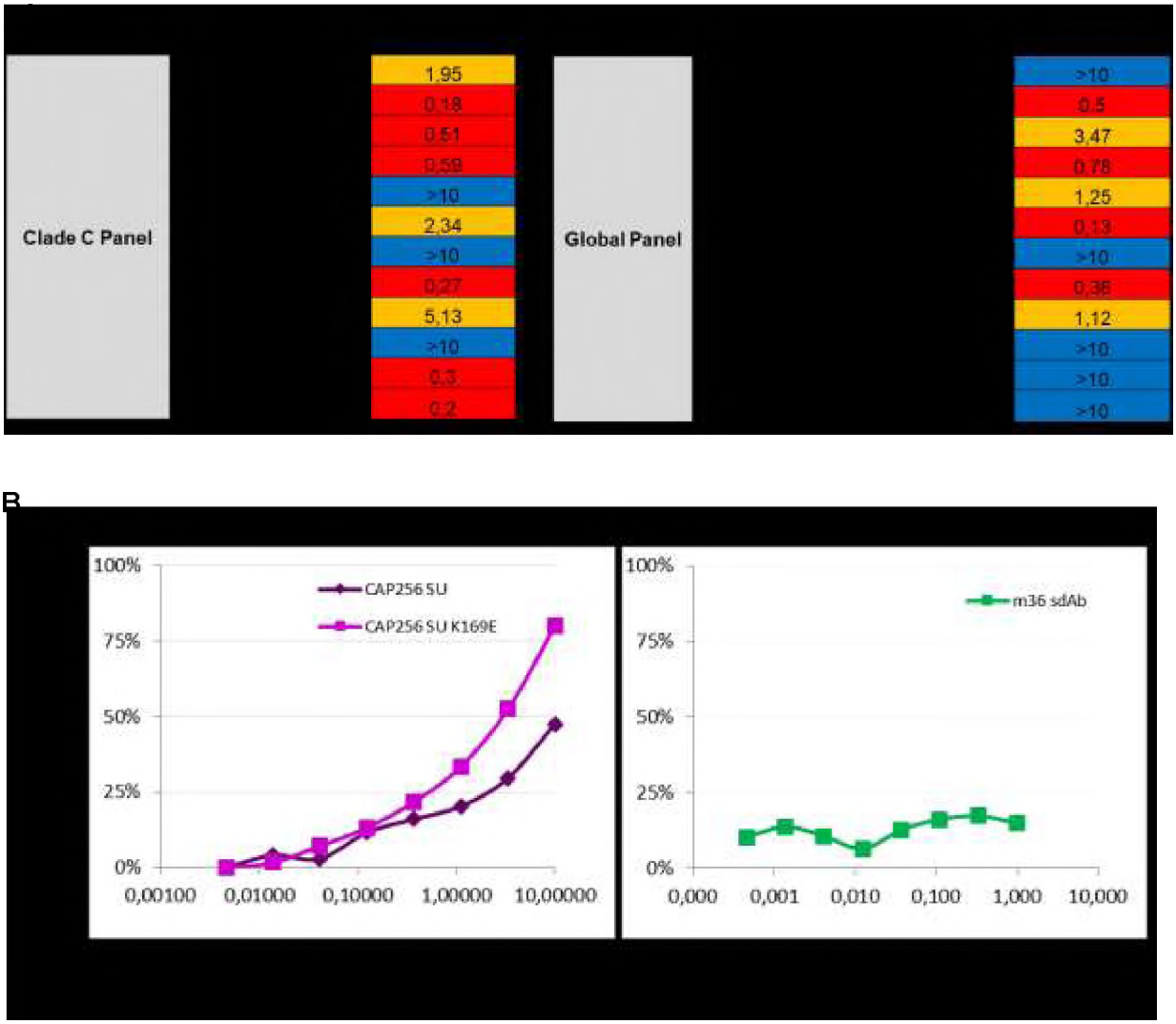

Figure 3.12 Breadth and potency of m36 sdAb. (A) Neutralization of m36 sdAb against the clade C and global panel. IC_{50} values in µg/mL against the HIV strains indicated in the left-hand column on TZM-bl cells, IC_{50} values between 0.1 and 1.0 µg/mL are coloured red; 1 to 10 µg/mL, yellow; and above 10 µg/mL, blue. **(B)** Neutralization of CAP256 SU, CAP256 SU K169E pseudoviruses and MLV control.

Chapter 4 : Discussion

In the 1900s Paul Ehrlich proposed antibodies as “magic bullets” capable of identifying and destroying foreign antigens, and ever since we have sought to tap into their biotherapeutic potential. Antibodies are comprised of two identical antigen binding arms (Fab) and a single Fc tail, which is involved in effector functions. Since then, antibodies and their derivatives established themselves as essential tools used in research and therapy. To date, there are over 70 therapeutic mAbs currently licensed for use in immunotherapy for many different indications, however, only three antibodies are licensed for infectious diseases: palivizumab for the prevention of respiratory syncytial virus (RSV) and two mAbs (raxibacumab and obiltoxaximab) for prophylaxis and treatment of anthrax (Sparrow *et al.*, 2017; Wu, Jiang and Ying, 2017).

Until very recently antibodies have not been actively pursued for HIV-1 therapy due to low breadth and potency demonstrated by the first generation bNAbs, however recent advancements in B-cell isolation technologies have allowed discoveries of many novel very broad and more potent bNAbs, some of which are already in clinical development (Morris and Mkhize, 2017). Although antibodies are hailed as “magic bullets” in immunotherapy, there are serious drawbacks associated with their development. Factors contributing to the limited development of therapeutic antibodies are the cost of manufacturing, which is directly linked to their large size (150 kDa) and biochemical properties. Although, the production costs of antibodies in recent years have been reduced to about 100 US dollars per gram, this is still significant especially when several grams are required for an individual treatment dose (Sparrow *et al.*, 2017). In addition, immunotherapy targeting a single site of HIV-1 is of concern, as the rapidly mutating pathogen is able to escape even from the broadest antibodies (Moore, Williamson and Morris, 2015). However, this can be overcome by combining few individual bNAbs into a cocktail to increase coverage against a broad range of viruses (Wagh *et al.*, 2016). The field of passive immunization for HIV is rapidly gaining traction with the increased availability of more broad and potent mAbs and the initiation of a large efficacy trial for HIV prevention. The first antibodies to be tested in clinical efficacy trial is VRC01 bNAb, which is able to neutralize 90% of HIV strains circulating in general population (Wu *et al.*, 2010; Morris and Mkhize, 2017). VRC01

demonstrated safety and efficacy during clinical trials and has paved the way for clinical development of much broader and more potent "second generation" bNAbs, such as VRC07-523, PGDM1400 and CAP256-VRC26.25. The VRC07-523 bNAb is a close relative of VRC01, while both PGDM1400 and CAP256-VRC26.25 are directed against the trimer apex (Morris and Mkhize, 2017). Increased breadth and potency have been observed in bi- and tri- specific constructs, in which antigen binding domains directed against distinct epitopes are combined into a single molecule (Morris and Mkhize, 2017). Multiple engineering efforts are ongoing to increase the therapeutic index of antibodies, such as fusions or smaller and more efficient derivatives, which are comprised of only the antigen-binding moiety, such as a single domain unit termed sdAb, VHH or Nanobody®. Engineered antibody fragments are also more advantageous over classical antibodies against occluded epitopes such as CD4i, where, size-dependent neutralization has been demonstrated using small antibody fragments (Chen and Dimitrov, 2009; Wu, Jiang and Ying, 2017).

Single domain antibodies are small monomeric units (12-15 kDa), which exhibit high solubility, affinity and specificity to a target antigen (Saerens, 2010). The simplicity and unique biochemical properties of the VHH domains have also attracted interest in developing them into novel biologics for multiple therapeutic indications. One of the first sdAb biotherapeutics is Caplacizumab which is expected to be approved by FDA in 2018. Currently, there are eight sdAb products in clinical development, and over twenty six in various stages of development, including a couple against HIV-1 (Revets, 2013; Steeland, Vandenbroucke and Libert, 2016; Wu, Jiang and Ying, 2017). A phase I clinical trial (ALX- 0651) was conducted in 2012, evaluating the safety and tolerability of anti-CXCR4 and anti-CD4 bi-specific sdAb (Catelijne Stortelers, 2015). Bi-specific molecule combines two functional antagonists, one specific for anti-CXCR4 (281F12) epitope, and anti-CD4 (3F11) sdAb, inhibiting gp120-CD4 interaction (Catelijne Stortelers, 2015). The newly formatted CXCR4-CD4 bi-specific demonstrated synergistic improvement, resulting in up to 320-fold enhancement over monovalent sdAbs, while, using two sdAbs as combinatorial cocktail resulted in only 2-fold enhancement (Catelijne Stortelers, 2015). Another sdAb in development is Nb190, the first intracellular inhibitor targeting Rev protein and preventing Rev-Rev multimerization, effectively inhibiting HIV-1 viral replication of different HIV viruses (Vercruysse *et al.*, 2013). The m36 sdAb targets the CD4i epitope and is one of the

best characterized antibody fragments thus far; it is also the most potent and broad sdAbs to date and is used in this study as a positive control. M36 sdAb has been developed in multiple proof of concept studies into various sdAb formats, such as bi-specific, bi-specific multivalent, Fc fusions (Ying *et al.*, 2013; Chen *et al.*, 2014; Sun *et al.*, 2014). In addition there is an ongoing effort to express m36 and other VHH antibodies isolated by llama immunization to display on the surface of recombinant *Lactobacillus* to block HIV at the site of transmission (Marcobal *et al.*, 2016). Single domain antibodies are generated by immunization of dromedaries (llama, alpaca or camel) and screening of immune libraries against the antigen of interest, followed by a few rounds of phage panning before optimal clones are selected (Vanlandschoot *et al.*, 2011). Single domain derivatives of conventional mAbs are generated through a process of "camelization", which involves substitution of key human residues with those found in camelid sdAb, which helps to improve solubility and decrease aggregation associated with engineered heavy chain antibodies (Carter and Merchant, 1997). However, when key residues in VHH framework 2 were reversely engineered to match those found in classical mAbs, generated variants often display poor solubility, rendering them "sticky" and prone to aggregation (Bannas, Hambach and Koch-Nolte, 2017).

We utilized in *silico* modelling tools to generate single domain derivative of CAP256.25 bNAb, which was camelized based on published data and structural characteristics of the molecule. The CAP256.25 antibody was chosen as the best candidate for this proof of concept study, because of several unique characteristics including: interaction with epitope mainly by an extended CDR-H3, sequence homology to IGVHH3 camel family and exceptional potency demonstrated in multiple studies. Structural data suggested that interaction of CAP256.25 bNAb with its viral epitope is primarily through the heavy chain (as shown in Figure 3.1). First, we generated a single domain derivative CAP256.25_mut0 from the parental antibody, which we tried to express multiple times using HEK 293F mammalian cell line, however, we were never able to purify sufficient amount of protein because of the extremely low expression levels. The second derivative we generated, was CAP256_mut4 sdAb, containing four substitutions in the former VH/VL interface (Figure 3.3). VHH tetrad substitutions at position 37 and 45 are critical to compensate for the loss of binding by the light chain domain, and substitution of residues 44 and 45 to increase overall solubility.

Substitution at position 35 produces a cavity which buries the side chain of residue 47, which in turn nucleates a small hydrophobic core, further decreasing hydrophobicity of the former LC interface, it also interacts with hydrophobic residues 91 and 103, found at the base CDR-H3 loop. Although, we were able to detect and purify CAP256.25_mut4 sdAb, this variant did not exhibit any neutralization activity, possibly caused by the high hydrophobicity of the molecule. Four additional mutations located in surface exposed parts of the molecule were introduced to generate the CAP256.25_mut8, further decreasing its hydrophobicity. CAP256.25_mut8 sdAb was able to neutralize five sensitive viruses from a clade C panel, albeit at the significantly lower levels than the parental antibody. Lastly, one more substitution was introduced at the base of H3, predicted to decrease hotspot of molecular frustration, termed CAP256.25_mut9 sdAb. Although, we have seen a significant increase in expression levels, by a factor of eight, the impact of K94A mutation on neutralization could not be determined because of the toxicity associated with expression in HEK293F Expi cells. Increasing the solubility landscape of CAP256.25_mut8 sdAb has proven to be beneficial for expression and activity of the molecule in comparison to WT or CAP256.25_mut4 sdAb. CAP256.25_mut9 expressed at significantly higher levels compared to the mut8 sdAb, suggestive of beneficial substitution, however, since it showed low levels of toxicity, its activity is unknown.

Low expression yields from all four CAP256.25 sdAb derivatives suggest that sdAbs have compromised thermodynamic stability resulting in aggregation and stickiness. There was some indication of the benefits of more extensive camelization as CAP256.25_mut8 showed the best expression and neutralization compared to less mutated CAP256.25_mut4 sdAb. To further optimize expression levels without additional molecular manipulations of sdAbs, we switched from the HEK293F cell line, which is widely used for the expression of recombinant proteins to HEK293F Expi, a higher density production cell line. Although yields were significantly higher in HEK293F Expi cells, purified proteins exhibited low levels of toxicity against MLV (data not shown).

Conventional antibodies are produced using mammalian cell lines because of their dependence on post-translational modifications (PTM), such as glycosylation or serine and tyrosine phosphorylation. These are key mechanisms for maintaining protein

function and activity, which are not present in bacterial expression systems (Walsh, Garneau-Tsodikova and Gatto, 2005). Antibody derivatives such as monovalent antibody fragment (Fab), Fab dimer or sdAb fragments can be easily produced at high levels using microbial hosts such as *E.coli* or yeast (*P.pastoris*, *S.cerevisiae*), as they lack an Fc tail, whose function depends on PTM (Vanlandschoot *et al.*, 2011; Liu and Huang, 2018). The most popular method for sdAb production is periplasmic expression in *E.coli,* however, CAP256.25 bNAb binding and neutralization depends on tyrosine sulfation, which a part of a eukaryotic PTM and therefore, we decided not to utilize a bacterial expression system during this study.

The degree of structural frustration manifested in CAP256.25_mut8 sdAb was identified using Frustratometer software. One of the identified hotspots was Lysine 94, located at the base of CDR-H3. Sequence homology comparison between dromedary IGVHH3 germline and human VH germline revealed a conserved Alanine present in *Camelidae* species, while CAP256.25 bNAb contained Lysine. To test if the substitution had an effect on CAP256.25_mut8 sdAb stability, we generated CAP256.25_mut9 sdAb, comprised of a single change from Lysine to Alanine at position 94. The single substitution resulted in increased protein yield, suggesting this substitution was beneficial, however, functionality could not been determined.

Overall, we made a total of nine substitutions generating three sdAb variants that were all tested for neutralizing activity. CAP256.25_mut4 comprised of VHH tetrad substitutions, showed low levels of expression, but had no neutralization capabilities. CAP256.25_mut8 sdAb, neutralized HIV-1 isolates, although with diminished potency in comparison to the parental antibody. It is of interest that even though we were unable to detect the CAP256.25_mut8 sdAb on the Western blot, we were able to measure its activity in the neutralization assay. It is possible that the detection antibody used for the Western blot was not sensitive enough to detect CAP256.25 sdAb His-tag. Another possibility is that the 6-His tag on the sdAb is being occluded or not properly recognized by the anti-His detection antibody used in Western blot or simply that neutralization is a far more sensitive assay than the Western blot. The CAP256.25_mut9 sdAb, showed an eight fold improvement in expression levels over CAP256.25_mut8 sdAb, however we could not test for activity because of the observed toxicity. Based on expression levels and neutralization profiles, we conclude

that the tetrad substitutions alone were not sufficient for generation of functional human sdAb derivative and that while all 9 substitutions improved expression we could not determine their impact on neutralization.

Published data indicates that sdAb behaviour is strongly influenced by a number of factors, first being the thermodynamic instability (tendency to misfold and/or aggregate) often resulting from insufficient number of substitutions at specific positions. A second factor is the colloidal instability, defined as propensity for multimerization by properly folded monomers, which then tend to precipitate (Soler, de Marco and Fortuna, 2016). Usable protein yield depends on many factors, one being the colloidal interactions in addition to the degree of sdAb solubility. Despite multiple engineering attempts to identify sequence hotspots responsible for aggregation of the single domains and utilization of various structural models, none has been successful so far (Barthelemy *et al.*, 2008). Our data supports those findings, as more substitutions led to better expression of CAP256.25_mut8 over mut4 sdAb, while biochemical data (Western blot and SEC chromatograph) indicated multimerization of sdAbs. The protruding CDR-H3 of VHH domains plays a critical role in increasing surface interactions with the target antigen and compensating for the missing VL domain. It further stabilized hydrophobic interactions with framework residues by folding over them, resulting in slightly skewed target engagement (Bannas, Hambach and Koch-Nolte, 2017). The CDR-H3 of CAP256.25 antibody projects away from the Fab, engaging the viral spike from a different angle and any changes made to the angle of projection resulted in diminished neutralization potency of CAP256.25 bNAb (Doria-Rose *et al.*, 2016). The CDR-H3 sequence and angle of projection plays an important role in stability and solubility of single domains, however, this places significant constraints on the types of CDR-H3 structure that could improve biochemical properties of engineered single domain antibodies (Barthelemy *et al.*, 2008).

Multiple factors contributed to the high level of solubility and stability of the m36 sdAb. The first is the large size and quality of the library used for panning, which was further validated by successful isolation of large number and high affinity VHHs against diverse viral and cancer immunogens. Second is the very high degree of engineering and optimization involved in generation of final m36 sdAb format (Chen, Zhu, Feng,

Xiao, *et al.*, 2008). M36 sdAb was panned against two naïve Fab libraries derived from cord blood, two naïve Fab libraries derived from adults, and an immune Fab library derived from HIV-1 infected patients, followed by panning against diverse selection of heavy chains from five human antibody Fab libraries (Chen, Zhu, Feng, Xiao, *et al.*, 2008). Next, the diversity of CDR sequences was optimized by testing of 143 randomly selected clones, with different CDR-H2 origins (6 out of 7 groups of VHH germline) and various CDR-H3 lengths, followed by substitution of solvent exposed framework residues (Chen, Zhu, Feng, Xiao, *et al.*, 2008). Meanwhile, CAP256.25 sdAb contains only nine substitutions, all derived from in *silico* modelling rather than phage libraries, with all mutations involving only solvent exposed residues in various frameworks and none involving CDR optimization, which influences stability of single domain antibodies.

In addition to camelization efforts, attempts have been made to engineer sdAbs by CDR grafting, albeit with limited success. While camelization involves transferring conserved residues from the VHH to a human framework, grafting involves transfer of the entire antigen specificity regions from donor onto the scaffold (Saerens *et al.*, 2005). Despite the efforts in VHH engineering, a universal VHH scaffold is not yet available. Although, cAbBCII10 from VHH framework family 2 was identified as a potential candidate, based on the high levels of stability and expression (5 mg/L in *E. coli*), the complexity of donor loop structures made grafting highly unpredictable, resulting in generation of molecules with impaired antigen binding capabilities and distorted frameworks, leading to an overall loss of structural stability and aggregation propensity (Saerens, 2010; Soler, de Marco and Fortuna, 2016; Goldman *et al.*, 2017). Based on sequence homology between CAP256.25 antibody and camel IGVHH3, we decided to derive sdAb through the camelization method rather than CDR grafting.

In retrospect, it appears that multiple factors contributed to the poor expression of CAP256.25 single domain antibody derivatives, limiting a full assessment of their functional activity. However available data suggest that the neutralization capacity of CAP25.25 sdAb was also significantly affected by the process of camelization. Taken together, these results demonstrate that conformational stability and protein yield are influenced by various factors including folding efficiency, solubility, degree and type of interactions between CDR and framework residues, aggregation hotspots and

sequences disparities. These factors individually or together, could have contributed to the dramatic deterioration of biophysical properties seen in engineered CAP256.25 sdAbs. Computational approaches used to engineer recombinant protein, can predict which residues result in improved biophysical behaviour of protein constructs, however, they are unable to predict protein yields. To our knowledge, CAP256.25_mut8 sdAb is the first antibody fragment derived in *silico* with specificity to V2 loop of HIV-1 spike. While the neutralization potency of sdAb was severely impacted by the engineering effort its IC_{50} activity against sensitive strains was equal to VRC01 bNAb, which is currently being tested in clinical trials.

Immunotherapy targeting a single epitope on the viral spike is of concern for a rapidly mutating pathogen, enabling viral escape even from the broadest antibodies and selection of resistance in an antibody-treated population resulting in a decreased therapeutic index. The discovery and characterization of bNAbs over the last decade has generated numerous inhibitors that can potently neutralize many HIV-1 isolates. It is possible that immunizing dromedaries with a new generation of HIV-1 trimers, isolated from individuals with exceptional bNAb responses, may increase the odds of isolating broadly neutralizing and potent VHHs. In addition, engineered multivalent sdAbs exhibit significantly better neutralizing in comparison to their monovalent equivalents, generated inhibitors can be then used to design multivalent and bi-specific antibodies, targeting multiple epitopes and resulting in increased breadth and neutralization potency (Forsman *et al.*, 2008). The unique properties of VHH, combined with high levels of stability and expression significantly decrease production costs, which makes them ideal candidates for the development of microbicides. Overcoming the limitation of engineered inhibitors could be of value, potentially providing sustainable, effective, and universal protection from HIV-1. In conclusion, this proof-of-concept study provides a glimpse into many factors affecting the overall stability and solubility of single antibody domains derived from human antibody with the guidance of the *Camelidae* immune system.

References

Agilent (2015) 'QuikChange Lightning Site-Directed Mutagenesis Kit Instruction Manual LIMITED PRODUCT WARRANTY QuikChange Lightning Site-Directed Mutagenesis Kit'. Available at: https://www.agilent.com/cs/library/usermanuals/Public/210518.pdf (Accessed: 22 March 2018).

AMP Study (2015). Available at: http://www.hvtn.org/en/science/HVTN-studies/AMPstudy.html.

Andrabi, R. *et al.* (2015) 'Identification of Common Features in Prototype Broadly Neutralizing Antibodies to HIV Envelope V2 Apex to Facilitate Vaccine Design.', *Immunity*. NIH Public Access, 43(5), pp. 959–73. doi: 10.1016/j.immuni.2015.10.014.

Andrabi, R. *et al.* (2017) 'Glycans Function as Anchors for Antibodies and Help Drive HIV Broadly Neutralizing Antibody Development', *Immunity*. Elsevier Inc., pp. 1–14. doi: 10.1016/j.immuni.2017.08.006.

Arbabi-Ghahroudi, M. (2017) 'Camelid Single-Domain Antibodies: Historical Perspective and Future Outlook', *Frontiers in Immunology*, 8(November), pp. 1–8. doi: 10.3389/fimmu.2017.01589.

Balazs, A. B. *et al.* (2012) 'Antibody-based protection against HIV infection by vectored immunoprophylaxis', *Nature*. Nature Publishing Group, 481(7379), pp. 81–84. doi: 10.1038/nature10660.

Balazs, A. B. *et al.* (2014) 'Vectored immunoprophylaxis protects humanized mice from mucosal HIV transmission', *Nature Medicine*. Nature Publishing Group, 20(3), pp. 296–300. doi: 10.1038/nm.3471.

Bannas, P., Hambach, J. and Koch-Nolte, F. (2017) 'Nanobodies and nanobody-based human heavy chain antibodies as antitumor therapeutics', *Frontiers in Immunology*, 8(NOV), pp. 1–13. doi: 10.3389/fimmu.2017.01603.

Barré-Sinoussi, F. *et al.* (1983) 'Isolation of a T-lymphotropic retrovirus from a patient at risk for acquired immune deficiency syndrome (AIDS).', *Science (New York, N.Y.)*, 220(4599), pp. 868–71. Available at: http://www.ncbi.nlm.nih.gov/pubmed/6189183.

Bartesaghi, A. *et al.* (2013) 'Prefusion structure of trimeric HIV-1 envelope glycoprotein determined by cryo-electron microscopy', *Nature Structural and Molecular Biology*. Nature Publishing Group, 20(12), pp. 1352–1357. doi: 10.1038/nsmb.2711.

Barthelemy, P. A. *et al.* (2008) 'Comprehensive analysis of the factors contributing to the stability and solubility of autonomous human VH domains', *Journal of Biological Chemistry*, 283(6), pp. 3639–3654. doi: 10.1074/jbc.M708536200.

Blattner, C. *et al.* (2014) 'Structural Delineation of a Quaternary, Cleavage-Dependent Epitope at the gp41-gp120 Interface on Intact HIV-1 Env Trimers', *Immunity*. Cell Press, 40(5), pp. 669–680. doi: 10.1016/J.IMMUNI.2014.04.008.

Bonsignori, M. *et al.* (2011) 'Analysis of a clonal lineage of HIV-1 envelope V2/V3

conformational epitope-specific broadly neutralizing antibodies and their inferred unmutated common ancestors.', *Journal of virology*, 85(19), pp. 9998–10009. doi: 10.1128/JVI.05045-11.

Brady et al. (2017) 'Antibody gene transfer with adeno-associated viral vectors as a method for HIV prevention', *Immunological Reviews*, 275(1), pp. 324–333. doi: 10.1111/imr.12478.

Buonaguro, □ L, Tornesello, M. L. and Buonaguro, F. M. (2007) 'Human Immunodeficiency Virus Type 1 Subtype Distribution in the Worldwide Epidemic: Pathogenetic and Therapeutic Implications', *JOURNAL OF VIROLOGY*, 81(19), pp. 10209–10219. doi: 10.1128/JVI.00872-07.

Burrell, C. J., Howard, C. R. and Murphy, F. A. (2017) *Fenner and White's medical virology*. Available at: https://www.sciencedirect.com/science/book/9780123751560.

Burton, D. R. (2001) *Antibodies in viral infection*. Springer.

Burton, D. R. and Mascola, J. R. (2015) 'Antibody responses to envelope glycoproteins in HIV-1 infection', *Nature Immunology*, 16(6), pp. 571–576. doi: 10.1038/ni.3158.

Carter, P. and Merchant, A. M. (1997) 'Engineering antibodies for imaging and therapy', *Current Opinion in Biotechnology*, 8(4), pp. 449–454. doi: 10.1016/S0958-1669(97)80067-5.

Catelijne Stortelers (2015) 'Bispecific Nanobodies with enhanced cell specificity', in *PEGS 2015 Boston*. Available at: http://www.ablynx.com/uploads/data/files/ablynx bispecific nanobodies_pegs conference_150508_final.pdf.

CDC (2011) *CDC*. Available at: https://www.cdc.gov/mmwr/preview/mmwrhtml/su6004a11.htm.

Chakrabarti, L. *et al.* (1987) 'Sequence of simian immunodeficiency virus from macaque and its relationship to other human and simian retroviruses', *Nature*, 328(6130), pp. 543–547. doi: 10.1038/328543a0.

Chen, W., Zhu, Z., Feng, Y., Xiao, X., *et al.* (2008) 'Construction of a large phage-displayed human antibody domain library with a scaffold based on a newly identified highly soluble, stable heavy chain variable domain.', *Journal of molecular biology*. NIH Public Access, 382(3), pp. 779–89. doi: 10.1016/j.jmb.2008.07.054.

Chen, W., Zhu, Z., Feng, Y. and Dimitrov, D. S. (2008) 'Human domain antibodies to conserved sterically restricted regions on gp120 as exceptionally potent cross-reactive HIV-1 neutralizers.', *Proceedings of the National Academy of Sciences of the United States of America*, 105(44), pp. 17121–6. doi: 10.1073/pnas.0805297105.

Chen, W. *et al.* (2010) 'Bifunctional fusion proteins of the human engineered antibody domain m36 with human soluble CD4 are potent inhibitors of diverse HIV-1 isolates', *Antiviral Research*, 88(1), pp. 107–115. doi: 10.1016/j.antiviral.2010.08.004.

Chen, W. *et al.* (2014) 'Exceptionally Potent and Broadly Cross-Reactive, Bispecific Multivalent HIV-1 Inhibitors Based on Single Human CD4 and Antibody Domains', *Journal of Virology*, 88(2), pp. 1125–1139. doi: 10.1128/JVI.02566-13.

Chen, W. *et al.* (2015) 'Germlining of the HIV-1 broadly neutralizing antibody domain m36.', *Antiviral research*. NIH Public Access, 116, pp. 62–6. doi: 10.1016/j.antiviral.2015.02.001.

Chen, W. and Dimitrov, D. S. (2009) 'Human monoclonal antibodies and engineered antibody domains as HIV-1 entry inhibitors.', *Current opinion in HIV and AIDS*, 4(2), pp. 112–7. doi: 10.1097/COH.0b013e328322f95e.

Conrath, K. *et al.* (2005) 'Antigen binding and solubility effects upon the veneering of a camel VHH in framework-2 to mimic a VH', *Journal of Molecular Biology*, 350(1), pp. 112–125. doi: 10.1016/j.jmb.2005.04.050.

D'arc, M. *et al.* (2015) 'Origin of the HIV-1 group O epidemic in western lowland gorillas.', *Proceedings of the National Academy of Sciences of the United States of America*. National Academy of Sciences, 112(11), pp. E1343-52. doi: 10.1073/pnas.1502022112.

Department of Health, R. (2016) 'National Policy on HIV Pre-exposure Prophylaxis (PrEP) and Test and Treat'. Available at: http://www.sahivsoc.org/Files/PREP and TT Policy - Final Draft - 5 May 2016 (HIV news).pdf (Accessed: 3 January 2018).

Desmyter, A. *et al.* (1996) 'Crystal structure of a camel single-domain VH antibody fragment in complex with lysozyme', *Nature Structural & Molecular Biology*. Nature Publishing Group, 3(9), pp. 803–811. doi: 10.1038/nsb0996-803.

Doria-Rose, N. A. *et al.* (2009) 'Frequency and phenotype of human immunodeficiency virus envelope-specific B cells from patients with broadly cross-neutralizing antibodies.', *Journal of virology*, 83(1), pp. 188–99. doi: 10.1128/JVI.01583-08.

Doria-Rose, N. A. *et al.* (2014) 'Developmental pathway for potent V1V2-directed HIV-neutralizing antibodies', *Nature*. Nature Publishing Group, 509(7498), pp. 55–62. doi: 10.1038/nature13036.

Doria-Rose, N. A. *et al.* (2016) 'New Member of the V1V2-Directed CAP256-VRC26 Lineage That Shows Increased Breadth and Exceptional Potency', 90(1), pp. 76–91. doi: 10.1128/JVI.01791-15.Editor.

Eden, T. *et al.* (2018) 'A cDNA immunization strategy to generate nanobodies against membrane proteins in native conformation', *Frontiers in Immunology*, 8(JAN), pp. 1–13. doi: 10.3389/fimmu.2017.01989.

Edlefsen et al. (2013) 'Sieve analysis in HIV-1 vaccine efficacy trials.', *Current opinion in HIV and AIDS*. NIH Public Access, 8(5), pp. 432–6. doi: 10.1097/COH.0b013e328362db2b.

Fisher Scientific, T. (2016) 'For Research Use Only. Not for use in diagnostic procedures. BigDye ™ Terminator v3.1 Cycle Sequencing Kit USER GUIDE', *Thermo Fisher*, 4337454(4337457). Available at: https://tools.thermofisher.com/content/sfs/manuals/cms_081527.pdf (Accessed: 21 March 2018).

Forsman, A. *et al.* (2008) 'Llama Antibody Fragments with Cross-Subtype Human Immunodeficiency Virus Type 1 (HIV-1)-Neutralizing Properties and High Affinity for HIV-1 gp120', *Journal of Virology*, 82(24), pp. 12069–12081. doi:

10.1128/JVI.01379-08.

Gabrielli, E. *et al.* (2009) 'Antibody complementarity-determining regions (CDRs): a bridge between adaptive and innate immunity.', *PloS one*. Public Library of Science, 4(12), p. e8187. doi: 10.1371/journal.pone.0008187.

Gao, F. *et al.* (1992) 'Human infection by genetically diverse SIVSM-related HIV-2 in West Africa', *Nature*, 358(6386), pp. 495–499. doi: 10.1038/358495a0.

Gardner, M. R. *et al.* (2015) 'AAV-expressed eCD4-Ig provides durable protection from multiple SHIV challenges', *Nature*. Nature Publishing Group, 519(7541), pp. 87–91. doi: 10.1038/nature14264.

GE Healthcare Life Sciences (2017) *GE Healthcare Life Sciences*. Available at: https://www.gelifesciences.com/solutions/protein-research/knowledge-center/protein-purification-methods/size-exclusion-chromatography.

Gil, D. and Schrum, A. G. (2013) 'Strategies to stabilize compact folding and minimize aggregation of antibody-based fragments.', *Advances in bioscience and biotechnology (Print)*. NIH Public Access, 4(4a), pp. 73–84. doi: 10.4236/abb.2013.44A011.

Goldman, E. R. *et al.* (2017) 'Enhancing stability of camelid and shark single domain antibodies: An overview', *Frontiers in Immunology*, 8(JUL), pp. 1–11. doi: 10.3389/fimmu.2017.00865.

Gorman, J. *et al.* (2016) 'Structures of HIV-1 Env V1V2 with broadly neutralizing antibodies reveal commonalities that enable vaccine design.', *Nature structural & molecular biology*. Nature Publishing Group, 23(1), pp. 81–90. doi: 10.1038/nsmb.3144.

Graham, B. S. and Ambrosino, D. M. (2015) 'History of passive antibody administration for prevention and treatment of infectious diseases.', *Current opinion in HIV and AIDS*, 10(3), pp. 129–34. doi: 10.1097/COH.0000000000000154.

Gray, E. S. *et al.* (2011) 'The neutralization breadth of HIV-1 develops incrementally over four years and is associated with CD4+ T cell decline and high viral load during acute infection.', *Journal of virology*. American Society for Microbiology (ASM), 85(10), pp. 4828–40. doi: 10.1128/JVI.00198-11.

Gray, E. S. *et al.* (2011) 'The Neutralization Breadth of HIV-1 Develops Incrementally over Four Years and Is Associated with CD4+ T Cell Decline and High Viral Load during Acute Infection', *Journal of Virology*, 85(10), pp. 4828–4840. doi: 10.1128/JVI.00198-11.

Gray, J. J. *et al.* (2011) 'Analysis and Modeling of the Variable Region of Camelid Single Domain Antibodies', *Journal of immunology*, 186(11), pp. 6357–6367. doi: 10.4049/jimmunol.1100116.Analysis.

Gromiha, M. M. and Pongor, S. (2010) *Protein bioinformatics : from sequence to function*, *Protein Bioinformatics*. Academic Press/Elsevier. doi: 10.1016/B978-8-1312-2297-3.50016-3.

Hamers-Casterman, C. *et al.* (1993) 'Naturally occurring antibodies devoid of light chains', *Nature*. Nature Publishing Group, 363(6428), pp. 446–448. doi:

10.1038/363446a0.

Hammer, S. M. *et al.* (2013) 'Efficacy Trial of a DNA/rAd5 HIV-1 Preventive Vaccine', *New England Journal of Medicine*. Massachusetts Medical Society , 369(22), pp. 2083–2092. doi: 10.1056/NEJMoa1310566.

Haynes, B. F. *et al.* (2012) 'Immune-Correlates Analysis of an HIV-1 Vaccine Efficacy Trial', *New England Journal of Medicine*. Massachusetts Medical Society , 366(14), pp. 1275–1286. doi: 10.1056/NEJMoa1113425.

Hicar, M. D. *et al.* (2016) 'Human Antibodies that Recognize Novel Immunodominant Quaternary Epitopes on the HIV-1 Env Protein', *PLOS ONE*. Edited by J. K. Scott. Public Library of Science, 11(7), p. e0158861. doi: 10.1371/journal.pone.0158861.

HIV Sequence Database (2017). Available at: https://www.hiv.lanl.gov/content/sequence/HelpDocs/subtypes-more.html.

HIV strains and types | AVERT (2017). Available at: https://www.avert.org/professionals/hiv-science/types-strains (Accessed: 1 January 2018).

Huang, J. *et al.* (2012) 'Broad and potent neutralization of HIV-1 by a gp41-specific human antibody', *Nature*. Nature Publishing Group, 491(7424), pp. 406–412. doi: 10.1038/nature11544.

Invitrogen (2010) 'FreeStyle ™ 293 Expression System', *Methods*, (October), pp. 1–23.

Janeway CA et al. (2001) *Immunobiology: The Immune System in Health and Disease. 5th edition*. Garland Science. Available at: https://www.ncbi.nlm.nih.gov/books/NBK10775/ (Accessed: 7 June 2018).

Jardine, J. G. *et al.* (2016) 'HIV-1 broadly neutralizing antibody precursor B cells revealed by germline-targeting immunogen', *Science*, 351(6280), pp. 1458–1463. doi: 10.1126/science.aad9195.

Johnson, P. R. *et al.* (2009) 'Vector-mediated gene transfer engenders long-lived neutralizing activity and protection against SIV infection in monkeys', *Nature Medicine*. Nature Publishing Group, 15(8), pp. 901–906. doi: 10.1038/nm.1967.

Johnson, P. R. and Schnepp, B. C. (2014) 'Vector-Mediated In Vivo Antibody Expression', *Microbiology Spectrum*, 2(4), pp. 1–11. doi: 10.1128/microbiolspec.AID-0016-2014.

Julg, B., Tartaglia, L. J., *et al.* (2017) 'Broadly neutralizing antibodies targeting the HIV-1 envelope V2 apex confer protection against a clade C SHIV challenge', pp. 1–12.

Julg, B., Sok, D., *et al.* (2017) 'Protective Efficacy of Broadly Neutralizing Antibodies with Incomplete Neutralization Activity against Simian-Human Immunodeficiency Virus in Rhesus Monkeys.', *Journal of virology*. American Society for Microbiology, 91(20), pp. e01187-17. doi: 10.1128/JVI.01187-17.

Julien, J.-P. *et al.* (2013) 'Crystal structure of a soluble cleaved HIV-1 envelope trimer.', *Science (New York, N.Y.)*. NIH Public Access, 342(6165), pp. 1477–83. doi: 10.1126/science.1245625.

Kapur, S. (ed.) (2012) *Immunosuppression - Role in Health and Diseases*. InTech. doi: 10.5772/1897.

Klarenbeek, A. *et al.* (2015) 'Camelid Ig V genes reveal significant human homology not seen in therapeutic target genes, providing for a powerful therapeutic antibody platform.', *mAbs*. Taylor & Francis, 7(4), pp. 693–706. doi: 10.1080/19420862.2015.1046648.

Kwong, P. D. *et al.* (1998) 'Structure of an HIV gp120 envelope glycoprotein in complex with the CD4 receptor and a neutralizing human antibody.', *Nature*. NIH Public Access, 393(6686), pp. 648–59. doi: 10.1038/31405.

Kwong, P. D. *et al.* (2000) 'Structures of HIV-1 gp120 Envelope Glycoproteins from Laboratory-Adapted and Primary Isolates', *Structure*. Cell Press, 8(12), pp. 1329–1339. doi: 10.1016/S0969-2126(00)00547-5.

Kwong, P. D. *et al.* (2011) 'Structure of HIV-1 gp120 V1/V2 domain with broadly neutralizing antibody PG9.', *Nature*. NIH Public Access, 480(7377), pp. 336–43. doi: 10.1038/nature10696.

Lee, J. H., Ozorowski, G. and Ward, A. B. (2016) 'Cryo-EM structure of a native, fully glycosylated, cleaved HIV-1 envelope trimer', *Science*, 351(6277), pp. 1043–1048. doi: 10.1126/science.aad2450.

De Leys, R. *et al.* (1990) 'Isolation and partial characterization of an unusual human immunodeficiency retrovirus from two persons of west-central African origin.', *Journal of virology*, 64(3), pp. 1207–16. Available at: http://www.ncbi.nlm.nih.gov/pubmed/2304140 (Accessed: 11 December 2017).

Li, Y. *et al.* (2011) 'Mechanism of Neutralization by the Broadly Neutralizing HIV-1 Monoclonal Antibody VRC01', *Journal of Virology*, 85(17), pp. 8954–8967. doi: 10.1128/JVI.00754-11.

Liu, J. *et al.* (2008) 'Molecular architecture of native HIV-1 gp120 trimers', *Nature*, 455(7209), pp. 109–113. doi: 10.1038/nature07159.

Liu, J. *et al.* (2016) 'Antibody-mediated protection against SHIV challenge includes systemic clearance of distal virus', *Science*, 353(6303), pp. 1045–1049. doi: 10.1126/science.aag0491.

Liu, Y. and Huang, H. (2018) 'Expression of single-domain antibody in different systems', *Applied Microbiology and Biotechnology*. Applied Microbiology and Biotechnology, 102(2), pp. 539–551. doi: 10.1007/s00253-017-8644-3.

Longo, N. S. *et al.* (2016) 'Multiple Antibody Lineages in One Donor Target the Glycan-V3 Supersite of the HIV-1 Envelope Glycoprotein and Display a Preference for Quaternary Binding', *Journal of Virology*. Edited by G. Silvestri, 90(23), pp. 10574–10586. doi: 10.1128/JVI.01012-16.

Marcobal, A. *et al.* (2016) 'Expression of Human Immunodeficiency Virus Type 1 Neutralizing Antibody Fragments Using Human Vaginal *Lactobacillus*', *AIDS Research and Human Retroviruses*, 32(10–11), pp. 964–971. doi: 10.1089/aid.2015.0378.

Margolis, D. A. *et al.* (2017) 'Long-acting intramuscular cabotegravir and rilpivirine in

adults with HIV-1 infection (LATTE-2): 96-week results of a randomised, open-label, phase 2b, non-inferiority trial.', *Lancet (London, England)*. Elsevier, 390(10101), pp. 1499–1510. doi: 10.1016/S0140-6736(17)31917-7.

Mascola, J. R. and Haynes, B. F. (2013) 'HIV-1 Neutralizing Antibodies: Understanding Nature's Pathways', *Immunological Reviews*, 254(1), pp. 225–244. doi: 10.1111/imr.12075.

McCoy, L. E. *et al.* (2012) 'Potent and broad neutralization of HIV-1 by a llama antibody elicited by immunization', *The Journal of Experimental Medicine*, 209(6), pp. 1091–1103. doi: 10.1084/jem.20112655.

Medina-Ramírez, M., Sanders, R. W. and Sattentau, Q. J. (2017) 'Stabilized HIV-1 envelope glycoprotein trimers for vaccine use.', *Current opinion in HIV and AIDS*. Wolters Kluwer Health, 12(3), pp. 241–249. doi: 10.1097/COH.0000000000000363.

Moldt, B. *et al.* (2012) 'Highly potent HIV-specific antibody neutralization in vitro translates into effective protection against mucosal SHIV challenge in vivo', *Proceedings of the National Academy of Sciences*, 109(46), pp. 18921–18925. doi: 10.1073/pnas.1214785109.

Moore, P. L., Gray, E. S. and Morris, L. (2009) 'Specificity of the autologous neutralizing antibody response', *Current Opinion in HIV and AIDS*, 4(5), pp. 358–363. doi: 10.1097/COH.0b013e32832ea7e8.

Moore, P. L., Williamson, C. and Morris, L. (2015) 'Virological features associated with the development of broadly neutralizing antibodies to HIV-1.', *Trends in microbiology*. NIH Public Access, 23(4), pp. 204–11. doi: 10.1016/j.tim.2014.12.007.

Morris, L. and Mkhize, N. N. (2017) 'Prospects for passive immunity to prevent HIV infection', *PLOS Medicine*. Public Library of Science, 14(11), p. e1002436. doi: 10.1371/journal.pmed.1002436.

Mouquet, H. *et al.* (2012) 'Complex-type N-glycan recognition by potent broadly neutralizing HIV antibodies.', *Proceedings of the National Academy of Sciences of the United States of America*. National Academy of Sciences, 109(47), pp. E3268-77. doi: 10.1073/pnas.1217207109.

Mueller, C. and Flotte, T. R. (2008) 'Clinical gene therapy using recombinant adeno-associated virus vectors', *Gene Therapy*, 15(11), pp. 858–863. doi: 10.1038/gt.2008.68.

Muyldermans, S. *et al.* (1994) 'Sequence and structure of VH domain from naturally occurring camel heavy chain immunoglobulins lacking light chains.', *Protein engineering*, 7(9), pp. 1129–35. Available at: http://www.ncbi.nlm.nih.gov/pubmed/7831284.

Muyldermans, S. (2001) 'Single domain camel antibodies: Current status', *Reviews in Molecular Biotechnology*, 74(4), pp. 277–302. doi: 10.1016/S1389-0352(01)00021-6.

Muyldermans, S. (2013) 'Nanobodies: Natural Single-Domain Antibodies', *Annual Review of Biochemistry*, 82(1), pp. 775–797. doi: 10.1146/annurev-biochem-063011-092449.

Nel, A. *et al.* (2016) 'Safety and Efficacy of a Dapivirine Vaginal Ring for HIV Prevention in Women', *New England Journal of Medicine*. Massachusetts Medical Society, 375(22), pp. 2133–2143. doi: 10.1056/NEJMoa1602046.

Nguyen, V. K., Desmyter, A. and Muyldermans, S. (2001) 'Functional heavy-chain antibodies in Camelidae.', *Advances in immunology*, 79, pp. 261–96. Available at: http://www.ncbi.nlm.nih.gov/pubmed/11680009.

NIH (2017) *A Clinical Trial of PGDM1400 and PGT121 Monoclonal Antibodies in HIV-infected and HIV-uninfected Adults*. Available at: https://clinicaltrials.gov/ct2/show/NCT03205917.

Pancera, M. *et al.* (2014) 'Structure and immune recognition of trimeric pre-fusion HIV-1 Env', *Nature*. Nature Publishing Group, 514(7523), pp. 455–461. doi: 10.1038/nature13808.

Pantophlet, R. and Burton, D. R. (2006) 'GP120: Target for Neutralizing HIV-1 Antibodies', *Annual Review of Immunology*, 24(1), pp. 739–769. doi: 10.1146/annurev.immunol.24.021605.090557.

Pegu, A. *et al.* (2017) 'Use of broadly neutralizing antibodies for HIV-1 prevention', *Immunological Reviews*, 275(1), pp. 296–312. doi: 10.1111/imr.12511.

Pottage (2017) *ViiV Healthcare announces start of phase III study of long-acting cabotegravir for HIV prevention in women | GSK*. Available at: https://www.gsk.com/en-gb/media/press-releases/viiv-healthcare-announces-start-of-phase-iii-study-of-long-acting-cabotegravir-for-hiv-prevention-in-women/ (Accessed: 10 February 2018).

Rathore, U. *et al.* (2017) 'Glycosylation of the core of the HIV-1 envelope subunit protein gp120 is not required for native trimer formation or viral infectivity', *Journal of Biological Chemistry*, 292(24), pp. 10197–10219. doi: 10.1074/jbc.M117.788919.

Rerks-Ngarm, S. *et al.* (2009) 'Vaccination with ALVAC and AIDSVAX to Prevent HIV-1 Infection in Thailand', *New England Journal of Medicine*, 361(23), pp. 2209–2220. doi: 10.1056/NEJMoa0908492.

Rerks-Ngarm, S. (2009) 'Vaccination with ALVAC and AIDSVAX to Prevent HIV-1 Infection in Thailand', *New England Journal of Medicine*. Massachusetts Medical Society, 361(23), pp. 2209–2220. doi: 10.1056/NEJMoa0908492.

Revets, H. (2013) *Nanobodies®: journey from research to commercial*. Available at: https://eipg.eu/wp-content/uploads/2013/07/eipg-vapi-upip-19-april-2013-hilde-revets.pdf.

Riechmann, L. and Muyldermans, S. (1999) 'Single domain antibodies: comparison of camel VH and camelised human VH domains', *Journal of Immunological Methods*, 231(1–2), pp. 25–38. doi: 10.1016/S0022-1759(99)00138-6.

Rouet, R., Lowe, D. and Christ, D. (2014) 'Stability engineering of the human antibody repertoire', *FEBS Letters*. Federation of European Biochemical Societies, 588(2), pp. 269–277. doi: 10.1016/j.febslet.2013.11.029.

Saerens, D. *et al.* (2005) 'Identification of a universal VHH framework to graft non-canonical antigen-binding loops of camel single-domain antibodies', *Journal of*

Molecular Biology, 352(3), pp. 597–607. doi: 10.1016/j.jmb.2005.07.038.

Saerens, D. (2010) 'Isolation and optimization of camelid single-domain antibodies: Dirk Saerens' work on nanobodies.', *World journal of biological chemistry*. Baishideng Publishing Group Inc, 1(7), pp. 235–8. doi: 10.4331/wjbc.v1.i7.235.

Salazar, G. *et al.* (2017) 'Antibody therapies for the prevention and treatment of viral infections.', *NPJ vaccines*. Nature Publishing Group, 2, p. 19. doi: 10.1038/s41541-017-0019-3.

Sanders, R. W. *et al.* (2002) 'Stabilization of the soluble, cleaved, trimeric form of the envelope glycoprotein complex of human immunodeficiency virus type 1.', *Journal of virology*. American Society for Microbiology, 76(17), pp. 8875–89. doi: 10.1128/JVI.76.17.8875-8889.2002.

Sanders, R. W. *et al.* (2015) 'HIV-1 neutralizing antibodies induced by native-like envelope trimers', *Science*, 349(6244), pp. aac4223-aac4223. doi: 10.1126/science.aac4223.

Saunders, K. O. *et al.* (2015) 'Broadly Neutralizing Human Immunodeficiency Virus Type 1 Antibody Gene Transfer Protects Nonhuman Primates from Mucosal Simian-Human Immunodeficiency Virus Infection.', *Journal of virology*. American Society for Microbiology, 89(16), pp. 8334–45. doi: 10.1128/JVI.00908-15.

Sharp, P. M. and Hahn, B. H. (2010) 'The evolution of HIV-1 and the origin of AIDS.', *Philosophical transactions of the Royal Society of London. Series B, Biological sciences*. The Royal Society, 365(1552), pp. 2487–94. doi: 10.1098/rstb.2010.0031.

Siontorou, C. G. (2013) 'Nanobodies as novel agents for disease diagnosis and therapy', *International Journal of Nanomedicine*, 8, pp. 4215–4227. doi: 10.2147/IJN.S39428.

Sok, D. *et al.* (2014) 'Recombinant HIV envelope trimer selects for quaternary-dependent antibodies targeting the trimer apex', *Proceedings of the National Academy of Sciences*, 111(49), pp. 17624–17629. doi: 10.1073/pnas.1415789111.

Soler, M. A., de Marco, A. and Fortuna, S. (2016) 'Molecular dynamics simulations and docking enable to explore the biophysical factors controlling the yields of engineered nanobodies.', *Scientific reports*. Nature Publishing Group, 6, p. 34869. doi: 10.1038/srep34869.

South Africa | UNAIDS (2017) *South Africa | UNAIDS*. Available at: http://www.unaids.org/en/regionscountries/countries/southafrica.

Sparrow, E. *et al.* (2017) 'Therapeutic antibodies for infectious diseases.', *Bulletin of the World Health Organization*. World Health Organization, 95(3), pp. 235–237. doi: 10.2471/BLT.16.178061.

Stamatatos, L. *et al.* (2009) 'Neutralizing antibodies generated during natural HIV-1 infection: good news for an HIV-1 vaccine?', *Nature medicine*. Nature Publishing Group, 15(8), pp. 866–870. doi: 10.1038/nm.1949.

Statistics South Africa (2017). Available at: http://www.statssa.gov.za/?page_id=1854&PPN=P0302&SCH=7048.

Steeland, S., Vandenbroucke, R. E. and Libert, C. (2016) 'Nanobodies as

therapeutics: big opportunities for small antibodies', *Drug Discovery Today*, 21(7), pp. 1076–1113. doi: 10.1016/j.drudis.2016.04.003.

Stephenson, K. E. and Barouch, D. H. (2016) 'Broadly Neutralizing Antibodies for HIV Eradication', *Current HIV/AIDS Reports*, 13(1), pp. 31–37. doi: 10.1007/s11904-016-0299-7.

Sun, M. *et al.* (2014) 'Rational Design and Characterization of the Novel, Broad and Potent Bispecific HIV-1 Neutralizing Antibody iMabm36', *JAIDS Journal of Acquired Immune Deficiency Syndromes*, 66(5), pp. 473–483. doi: 10.1097/QAI.0000000000000218.

Supratim Choudhuri (2014) *Hydrophobicity, Hydrophilicity, and Antigenicity Prediction, and the Hydropathy Plot*, *Bioinformatics for Beginners*. Available at: https://www.sciencedirect.com/topics/biochemistry-genetics-and-molecular-biology/hydrophilicity-plot.

Taylor, B. S. *et al.* (2008) 'The challenge of HIV-1 subtype diversity.', *The New England journal of medicine*. NIH Public Access, 358(15), pp. 1590–602. doi: 10.1056/NEJMra0706737.

Tomaras, G. D. and Plotkin, S. A. (2017) 'Complex immune correlates of protection in HIV-1 vaccine efficacy trials', *Immunological Reviews*, 275(1), pp. 245–261. doi: 10.1111/imr.12514.

UNAIDS (2016) 'UN AIDS Report 2016', *UNAIDS*. Available at: http://www.unaids.org/sites/default/files/media_asset/global-AIDS-update-2016_en.pdf.

UNAIDS (2017) *UNAIDS Data 2017*, *Joint United Nations Programme on HIV/AIDS*. doi: 978-92-9173-945-5.

Vanlandschoot, P. *et al.* (2011) 'Nanobodies??: New ammunition to battle viruses', *Antiviral Research*, 92(3), pp. 389–407. doi: 10.1016/j.antiviral.2011.09.002.

Vercruysse, T. *et al.* (2013) 'Mapping the Binding Interface between an HIV-1 Inhibiting Intrabody and the Viral Protein Rev', *PLoS ONE*. Edited by Y. Wu. Public Library of Science, 8(4), p. e60259. doi: 10.1371/journal.pone.0060259.

Vidarsson et al. (2014) 'IgG subclasses and allotypes: from structure to effector functions.', *Frontiers in immunology*. Frontiers Media SA, 5, p. 520. doi: 10.3389/fimmu.2014.00520.

Wagh, K. *et al.* (2016) 'Optimal Combinations of Broadly Neutralizing Antibodies for Prevention and Treatment of HIV-1 Clade C Infection', *PLoS Pathogens*, 12(3), pp. 1–27. doi: 10.1371/journal.ppat.1005520.

Walker, L. M. *et al.* (2009) 'Broad and Potent Neutralizing Antibodies from an African Donor Reveal a New HIV-1 Vaccine Target', *Science*, 326(5950), pp. 285–289. doi: 10.1126/science.1178746.

Walker, L. M. *et al.* (2011) 'Broad neutralization coverage of HIV by multiple highly potent antibodies', *Nature*. Nature Publishing Group, 477(7365), pp. 466–470. doi: 10.1038/nature10373.

Walsh, C. T., Garneau-Tsodikova, S. and Gatto, G. J. (2005) 'Protein

posttranslational modifications: The chemistry of proteome diversifications', *Angewandte Chemie - International Edition*, 44(45), pp. 7342–7372. doi: 10.1002/anie.200501023.

Wan, C. *et al.* (2013) 'Epitope Mapping of M36, a Human Antibody Domain with Potent and Broad HIV-1 Inhibitory Activity', *PLoS ONE*, 8(6), pp. 4–11. doi: 10.1371/journal.pone.0066638.

Wesolowski, J. *et al.* (2009) 'Single domain antibodies: Promising experimental and therapeutic tools in infection and immunity', *Medical Microbiology and Immunology*, 198(3), pp. 157–174. doi: 10.1007/s00430-009-0116-7.

WHO (2015) 'WHO | Pre-exposure prophylaxis', *WHO*. World Health Organization. Available at: http://www.who.int/hiv/topics/prep/en/ (Accessed: 3 January 2018).

Wibmer, C. K., Moore, P. L. and Morris, L. (2015) 'HIV broadly neutralizing antibody targets.', *Current opinion in HIV and AIDS*. NIH Public Access, 10(3), pp. 135–43. doi: 10.1097/COH.0000000000000153.

Wu, X. *et al.* (2010) 'Rational design of envelope identifies broadly neutralizing human monoclonal antibodies to HIV-1.', *Science (New York, N.Y.)*, 329(5993), pp. 856–61. doi: 10.1126/science.1187659.

Wu, Y., Jiang, S. and Ying, T. (2017) 'Single-Domain Antibodies As Therapeutics against Human Viral Diseases', *Frontiers in Immunology*. Frontiers, 8, p. 1802. doi: 10.3389/fimmu.2017.01802.

www.clinicaltrials.gov (no date) *www.clinicaltrials.gov*. Available at: https://www.clinicaltrials.gov/ (Accessed: 7 June 2018).

Ying, T. *et al.* (2013) 'Engineered soluble monomeric IgG1 CH3 domain generation, mechanisms of function, and implications for design of biological therapeutics', *Journal of Biological Chemistry*, 288(35), pp. 25154–25164. doi: 10.1074/jbc.M113.484154.

Zhang, M.-Y. *et al.* (2010) 'Potent and broad neutralizing activity of a single chain antibody fragment against cell-free and cell-associated HIV-1.', *mAbs*. Taylor & Francis, 2(3), pp. 266–74. Available at: http://www.ncbi.nlm.nih.gov/pubmed/20305395 (Accessed: 11 February 2018).

Zhang, M. Y. *et al.* (2004) 'Improved breadth and potency of an HIV-1-neutralizing human single-chain antibody by random mutagenesis and sequential antigen panning', *Journal of Molecular Biology*, 335(1), pp. 209–219. doi: 10.1016/j.jmb.2003.09.055.

Zhang, Z. *et al.* (2016) 'Antiviral Therapy by HIV-1 Broadly Neutralizing and Inhibitory Antibodies', *International Journal of Molecular Sciences*. Multidisciplinary Digital Publishing Institute, 17(11), p. 1901. doi: 10.3390/ijms17111901.

Zhou, T. *et al.* (2007) 'Structural definition of a conserved neutralization epitope on HIV-1 gp120', *Nature*, 445(7129), pp. 732–737. doi: 10.1038/nature05580.

Zhou, T. *et al.* (2015) 'Structural Repertoire of HIV-1-Neutralizing Antibodies Targeting the CD4 Supersite in 14 Donors.', *Cell*. NIH Public Access, 161(6), pp. 1280–92. doi: 10.1016/j.cell.2015.05.007.

Zolla-Pazner, S. and Cardozo, T. (2010) 'Structure–function relationships of HIV-1 envelope sequence-variable regions refocus vaccine design', *Nature Reviews Immunology*. Nature Publishing Group, 10(7), pp. 527–535. doi: 10.1038/nri2801.

Appendices

Appendix A: Table of Reagents

Reagent	Catalogue Number	Supplier
QuikChange Lightning Site-Directed Mutagenesis Kit	210518	Agilent
Ethidium bromide	1610433	BioRad
Precision Plus Protein™ WesternC™ Blotting Standards	1610385	
TaKaRa CBB Protein Safe Stain	T9320A	Clonetech
HiLoad 26/600 Superdex 75 pg	28989334	GE
Low Molecular Weight (LMW) Standards	28-4038-41	
Acrylamide/bis-acrylamide, 40% solution	A7168	Sigma Aldrich
DNA Molecular Weight Marker XIV (100 bp ladder)	11721933001	
Gentamycin Sulfate	345814-M	
Kanamycin Sulfate	10106801001	
Rapid DNA Ligation Kit	11635379001	
SDS	L3771-25G	
Trypan Blue solution	T8154	
Water, Molecular Biology Grade	W4502	
Ammonium persulphate	17874	Thermo Fisher
BigDye™ Terminator v3.1 Cycle Sequencing Kit	4337455	
DMEM	11965-084	
FastDigest Xbal Restriction Enzyme	FD0684	
FastDigest Bam HI Restriction Enzyme	ER0051	
Freestyle™ 293 Expression Medium	12338026	
Freestyle™ 293-F cells	R790-07	
HEPES	15630080	
GE Healthcare Hyclone™ Heat Inactivated Fetal Bovine Serum (New Zealand)	SH30406.02HI	
Luria-Bertani (LB) broth	12780029	
Novex™ Sharp Pre-stained Protein Standard	LC5800	
NuPAGE™ Sample Reducing Agent (10X)	NP0004	
NuPAGE™ LDS Sample Buffer (4X)	NP0007	
PBS	10010-001	
Pierce™ Protein Concentrator PES, 5K MWCO	88534	
TEMED	15524010	
Trypsin-EDTA	25200056	
QIAprep Spin Miniprep Kit	27104	Qiagen
HiSpeed Plasmid Maxi Kit	12663	
QIAquick Gel Extraction Kit	28704	
QIAquick PCR Purification Kit	28104	
PEI MAX 40K	24765-1	Polysciences, Inc.
JM109 Mix & Go Competent Cells	T3007	ZymoResearch

Appendix B: List of Sequences

CAP256.25_mut0 sdAb

QVQLVESGGGVVQPGTSLRLSCAASQFRFDGYGMHWVRQAPGKGLEWVASISD
GIKKYHAEKVWGRFTISRDNSKNTLYLQMNSLRPEDTALYYCAKDLREDECEEWW
SDYYDFGKQLPCAKSRGGLVGIADNWGQGTMVTVSSGGHHHHHH

CAP256.25_mut4 sdAb

QVQLVESGGGVVQPGTSLRLSCAASQFRFDGYGMHWFRQAPGKEREGVASISHD
GIKKYHAEKVWGRFTISRDNSKNTLYLQMNSLRPEDTALYYCAKDLREDECEEWW
SDYYDFGKQLPCAKSRGGLVGIADNWGQGTMVTVSSGGHHHHHH

CAP256.25_mut8 sdAb

QVQLVESGGGSVQPGKSLRLSCAASRFSFNRYGMGWFRQAPGKEREGVAAISYD
GTDKYHADKVWGRFTISRDNSKNTLYLQMNSLRAEDTALYCCAKDLREDECEEW
WSDYYDFGKQLPCRKSRGVAGIFDGWGQGTQVTVSSGGHHHHHH

CAP256.25_mut9 sdAb

QLVESGGGSVQPGKSLRLSCAASRFSFNRYGMGWFRQAPGKEREGVAAISYD
GTDKYHADKVWGRFTISRDNSKNTLYLQMNSLRAEDTALYCCAADLREDECEEW
WSDYYDFGKQLPCRKSRGVAGIFDGWGQGTQVTVSSGGHHHHHH

m36 sdAb

QVQLVQSGGGLVQPGGSLRLSCAASAFDFSDYEMSWVRQAPGKGLEWIGEINDS
GNTIYNPSLKSRVTISRDNSKNTLYLQMNTLRAEDTAIYYCAIYGGNSGGEYWGQG
TLVTVSSGGHHHHHH